1445

WHOI
DOCUMENT
COLLECTION

A PREDICTIVE HORIZONTAL-TEMPERATURE-GRADIENT MODEL OF THE UPPER 750 FEET OF THE OCEAN

Derived from towed-thermistor-chain data taken in 17 geographical areas of the Eastern North Pacific

E.L. Smith

Research Report

17 March 1967

NAVY ELECTRONICS LABORATORY, SAN DIEGO, CALIFORNIA 92152

WHOI
DOCUMENT
COLLECTION

NEL/REPORT 1445

TK
7855
.U5
no. 1445

DISTRIBUTION OF THIS DOCUMENT IS UNLIMITED

PROBLEM

In general, investigate oceanographic factors pertinent to the behavior of underwater sound; in particular, study vertical fluctuations in thermocline depth. Specifically, study the thermal structure of the upper 750 feet of the ocean utilizing the towed thermistor chain and thereby gain a predictive understanding of these fluctuations and their distribution in time and space. Finally, incorporate the findings in an improved acoustic model that can be used in critical areas of the ocean.

RESULTS

1. Time-dependent vertical-temperature fluctuations in the thermocline were found to exist in all areas of the ocean examined with the NEL Thermistor Chain.

2. Time-dependent horizontal-temperature gradients were computed from continuous cross sections of the upper 750 feet of the ocean in 17 geographical areas of the eastern North Pacific. The horizontal-gradient field alternates in sign with a regularity that implies a dominant frequency of internal waves or convection cells. The corresponding wavelength is 0.72 nautical mile with a standard deviation of 0.16 mile.

3. The vertical-temperature gradient in the thermocline is generally of the order 10^{-2}°C/ft, but ranges between 10^{-1} and 10^{-3} °C/ft. The corresponding horizontal-temperature gradient is generally of the order 10^{-4}°C/ft, but ranges between 10^{-3} and 10^{-5}°C/ft. The slopes of isothermal surfaces are of the order 10^{-2}. Thus, the vertical and horizontal gradients normally differ by two orders of magnitude. The horizontal gradient in the thermocline can be predicted within useful limits from the measured vertical-temperature gradient by means of the equation

$$\frac{dT}{dx} = 0.0047 \left(\frac{dT}{dz}\right)^{0.71}$$

MBL/WHOI
0 0301 0040511 4

4. A predictive model of the horizontal-temperature gradients for a selected area of the sea was constructed on the basis of the above results and a single bathythermograph lowering.

RECOMMENDATIONS

1. Continue development of the thermistor chain to improve its accuracy, reliability, and versatility.

2. Further develop the digital temperature-depth recording system. Use the digitized data in conjunction with the UNIVAC 1218 shipboard computer for detailed statistical analyses and real-time computations of the vertical- and horizontal-temperature-gradient fields.

3. Finally, continue the study of the vertical- and horizontal-temperature gradients in the sea and compile an atlas of horizontal time-dependent gradients.

ADMINISTRATIVE INFORMATION

Work was performed under SR 004 03 01, Task 580 (NEL L40461) by members of the Marine Environment Division. This report covers the period July 1962 to July 1965 and was approved for publication 17 March 1967.

The author is grateful to O.S. Lee for consultation and assistance throughout this investigation and to D.W. Ternyila for data reduction and analysis. Thanks are also due to E.C. LaFond for the use of previous results and figures, and for comments on the manuscript. Comments on the manuscript by G.H. Curl are acknowledged.

CONTENTS

TABLES

ILLUSTRATIONS

INTRODUCTION

The performance of any system whereby information is transmitted from one place to another, using radiated energy as a carrier, is limited by the characteristics of the transmitting medium. When measurements are made of the intensity of underwater sound in the ocean, the results are often highly variable.

Factors contributing to this variability include divergence or partial convergence caused by refraction, destructive and constructive interference associated with multipath propagation caused by reflections from the surface and bottom of the sea, and diffraction and scattering caused by inhomogeneities of the water medium. When there are present additional inhomogeneities such as suspended particles, thermal cells, regions of turbulence, or temperature variations caused by internal waves, an additional variation in intensity occurs.

Multipath interference arises particularly when a transmission path passes through a gradient. Refraction of sound rays by gradients can produce sonar bearing errors and fluctuations in bearing measurements. Although salinity and pressure gradients contribute to this effects, temperature changes normally have the greatest influence on sound velocity and, hence, are the most important source of multipath interference. Therefore, knowledge of temperature gradients is vitally important in the successful use of sonar by the U. S. Navy. This report covers an investigation of a relation existing between the strengths of vertical- and horizontal-temperature gradients and a dominant frequency of oscillation in the thermocline.

PREVIOUS STUDIES

Information on gross physical features of the ocean including temperature gradients is readily available in oceanographic atlases. These atlases are generally derived in one of two ways: first, from an accumulation of data over many years from independently conducted studies; and, second, from a concentrated

study of a specific area in a short time. A good example of results of a concentrated effort is the NORPAC Atlas (1955).[1] The North Pacific Expedition represented a concerted effort of Japan and the U.S., involving 19 research vessels and 1002 hydrographic stations. Most of the data were taken within one month, showing the intensity of the effort. Coastal stations were about 30 miles apart and oceanic stations were from 50 to 120 miles apart. The distance between hydrographic stations is the determining factor in computing horizontal gradients. Horizontal-temperature gradients derived from such sets of data are termed "average gradients" and represent the average temperature change per nautical mile for a given depth.

Average horizontal-temperature gradients may also be determined from two or more space-separated bathythermograph stations. During underwater acoustic experiments, it is not uncommon to determine the average gradient from the difference of two bathythermograph readings — one taken at the transmitting ship, the other at the receiving ship.

Minute physical features, the temperature in particular, have not been investigated as widely as large-scale features even though horizontal thermal microstructure was observed during World War II when Holter (1944) made measurements from a submerged submarine using a thermopile.[2] He detected 0.02°F differences over horizontal distances of about 30 feet. Other contributors in this area include Urick (1948) who, near Key West, detected gradients similar to those found by Holter and concluded also that gradient increased with depth within the mixed layers.[3] From experimental work in deep water, Sheehy (1950) concluded that acoustic intensity fluctuations were caused by inhomogeneities in the water.[4] Lieberman (1951) detected inhomogeneities of mean size of about two feet (60 cm) and temperature variations of 0.05° Celsius (C).[5] Using Lieberman's results, Mintzer (1953 and 1954) made theoretical predictions of intensity fluctuations produced by temperature microstructure in the sea.[6] Priimak (1961) carried out a statistical analysis during a three-dimensional study of the sea, with investigations of the parameters and statistical characteristics of the fluctuations in temperature and

---

1. Superscript numbers denote references in list at end of this report.

pulsations in current.[7] Sagar (1960) found a diurnal cycle of growth and decay of insolation-produced microstructure in the surface layer in the summer months and showed a direct relationship between the existence of microstructure and acoustic intensity fluctuations.[8] Helle (1964) measured thermal microstructure from a submarine using fast-response thermistors.[9] Murphy (1965) used fast-response thermistors mounted on an unmanned torpedo-like research vehicle and recorded temperature deviations of 0.3°C at 50 meters and 0.02°C at 1500 meters.[10] Horizontal gradients measured near the surface were of the order of 0.1°C/nautical mile and 0.001C/nautical mile at 2000 meters.

From the above discussion it can be seen micro-horizontal thermal gradients describe temperature changes over distances from a few inches to a few yards, while average horizontal gradients describe temperature changes over distances of several miles or even several hundred miles. Here we shall deal with distances between these extremes, being concerned with temperature changes over horizontal distances of about 1 mile.

Horizontal-temperature gradients in this intermediate range (1 nautical mile) were first investigated in July 1964 when the NEL Thermistor Chain was used in collaboration with the Marine Physical Laboratory who were making convergence-zone bearing-accuracy measurements. The thermistor chain recorded continuous temperature cross sections parallel and perpendicular to the sound path between the two MPL participating ships. The temperature profiles were resolved into vertical- and horizontal-temperature-gradient fields, which revealed regions of high-intensity gradient. The horizontal-temperature gradient alternated in sign at nearly equal intervals and was consistently two orders of magnitude smaller than the corresponding vertical gradient (Smith, 1965).[11] Fisher *et al* (1965) reported on bearing fluctuations observed.[12] These results, particularly the periodicity of the horizontal-temperature-gradient field, generated interest in gradient fields in other areas already surveyed with the thermistor chain. The speculation followed that, if other areas displayed a similar periodicity in internal temperature structure and if the two-orders-of-magnitude ratio between the vertical and horizontal gradients held, a predictive acoustic model might be constructed.

OBTAINING THE DATA

Temperature data were selected for analysis from 17 widely separated areas involving several water masses (Sverdrup *et al.*, 1942).[13] The data were taken during eight cruises with the NEL Thermistor Chain and provide the best available representation of the geographic and water-mass variety of temperature structures (fig. 1). The positions of the sample areas, cruise numbers, and dates are shown in table I.

The data were obtained solely from the NEL Thermistor Chain, a massive oceanographic instrument (fig. 2) which has been in operation since 1961. The chain is 900 feet long and capable of measuring and continuously recording the temperature structure to a depth of 830 feet, although the average towing depth is about 750 feet. The chain system consists basically of a hoist, links, storage drum, and electronic temperature recording

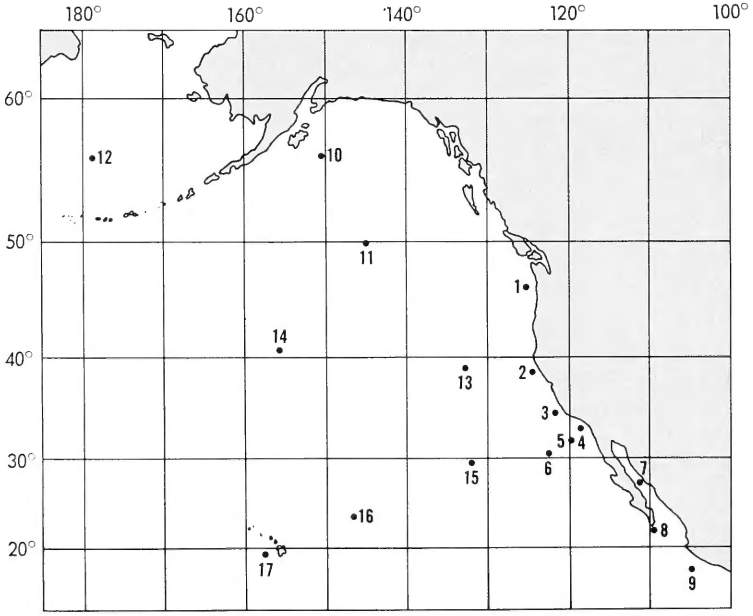

Figure 1. Geographic locations of 17 NEL Thermistor Chain temperature-data sample areas.

TABLE 1. TIME AND POSITION OF EACH SAMPLE AREA

Sample	Time	Date	Cruise	Latitude	Longitude
1	0800	7 August 1962	14	46° 21. 3′N	126° 23. 0′W
2	2000	2 August 1962	14	40° 18. 6′N	124° 57. 6′W
3	1400	27 July 1962	14	34°44. 0′N	121° 34. 5′W
4	0830	18 March 1964	27	33° 20. 4′N	118° 02. 2′W
5	0830	11 February 1965	E-1*	32° 04. 2′N	118° 28. 3′W
6	1500	15 July 1964	29	31° 07. 0′N	120° 56. 7′W
7	1300	30 March 1965	31	27° 34. 6′N	111° 50. 3′W
8	1200	18 March 1965	31	21° 50. 0′N	109° 40. 1′W
9	0100	8 February 1963	18	16° 04. 2′N	100° 10. 0′W
10	1600	10 June 1965	32	56° 08. 8′N	150° 21. 3′W
11	1300	6 June 1965	32	49° 38. 4′N	145° 07. 5′W
12	1230	13 July 1965	32	56° 39. 4′N	176° 51. 1′W
13	1200	31 July 1965	32	37° 54. 8′N	135° 07. 3′W
14	0100	27 July 1965	32	42° 01. 0′N	154° 09. 5′W
15	0100	27 July 1964	29	29° 25. 4′N	132° 19. 2′W
16	1730	31 July 1964	29	26° 17. 9′N	144° 51. 2′W
17	2000	22 August 1964	29	18° 12. 5′N	157° 47. 0′W

*Cruise conducted specifically for equipment modification or maintenance.

equipment. Each link is about a foot long and is faired for hydrodynamic stability while the chain is under tow. Thirty-four thermistors are mounted at 25-foot intervals along the chain. An electrical harness passes through the flat, faired links and conducts the voltage-temperature analog outputs from the thermistor beads to the ship's laboratory. A special computer built into the data system scans each thermistor output every 12 seconds and interpolates between outputs to fix the depths of all whole-degree-Celsius isotherms within the towing depth of the thermistor chain. Towing depth is maintained by a streamlined, 2300-pound

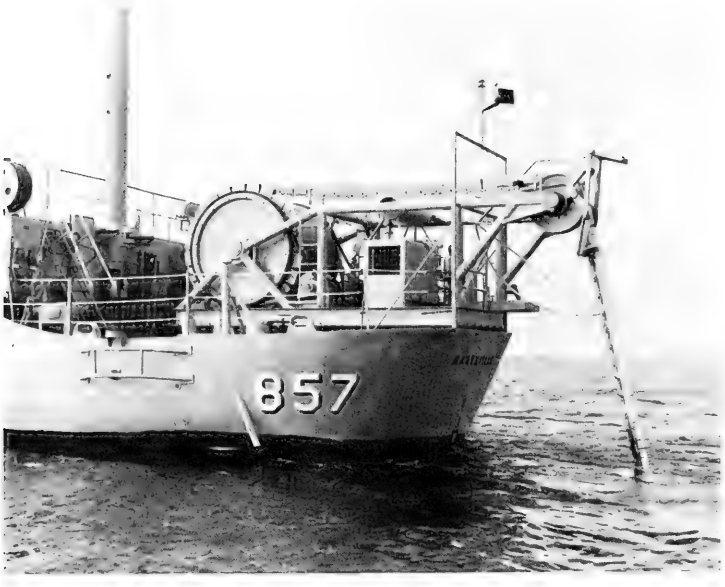

Figure 2. Fantail of USS MARYSVILLE and NEL Thermistor Chain and chain hoist.

depressing weight attached to the bottom of the chain. One link below the deepest temperature sensor and two links above the depressing weight is mounted a Bourdon pressure transducer that provides a measurement of the maximum depth of observation. The interpolated whole-degree-isotherm depths for each 12-second scan are printed in analog form on a 19-inch-wide tape. On more recent cruises the temperature data have been simultaneously punched on paper tape and recorded on magnetic tape in digital form. A single scan of the temperature-depth recordings of the chain is equivalent to one bathythermograph (BT) every 12 seconds, or every 120 feet for the normal towing speed of 6 knots.

GENERAL CHARACTER OF THE DATA

Figure 3 is an example of raw chain data taken off the southern tip of Baja California during the USNEL Boundary Expedition. The thermal structure shown is typical of that region of the ocean and is from Sample Area 8. The record is a two-dimensional picture or cross section of the temperature structure in the upper 750 feet of the ocean. The depth scale is not linear because the catenary-like configuration of the chain under tow results in the thermistors being closer together at the top than at the bottom of the chain. In the analog output record the vertical scale is magnified about 100 times (97 times at normal towing depth of 750 feet) over the horizontal.

Three points need to be made with respect to the validity of these temperature structure data. First, if the vertical fluctuations in isotherm depth are related to internal waves (a periodic phenomenon), a Doppler frequency shift may be introduced into the data measured by moving sensors. The extent of this shift is

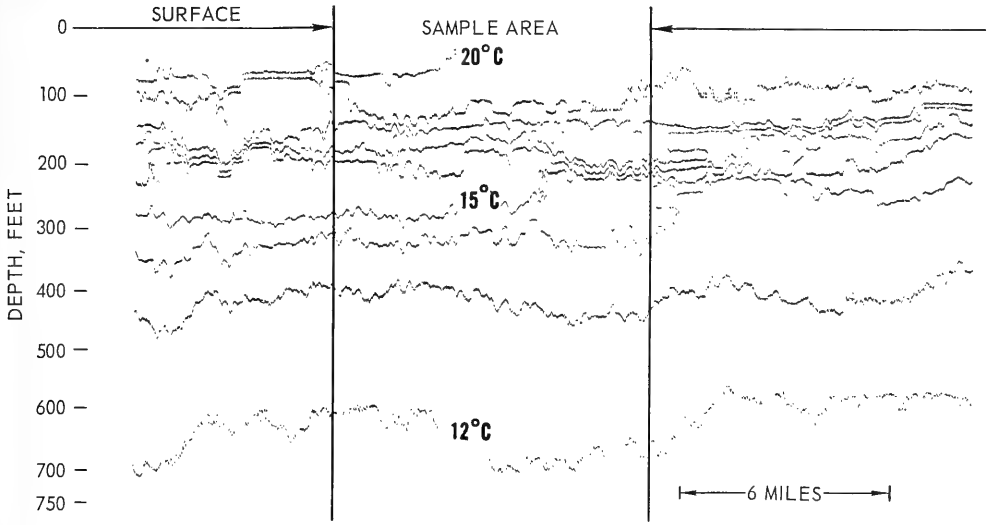

Figure 3. NEL Thermistor Chain data from Sample Area 8, off the southern tip of Baja California. Section set off by vertical lines selected for detailed analysis.

unknown because the direction and velocity of propagation of the internal waves are unknown. However, the shift has no effect on the amplitudes of the vertical variations in isotherm depths. Second, small oscillations of the deep end of the chain are reflected in the depth changes of the isotherms. However, these chain depth changes are very small compared to the vertical-temperature-structure fluctuations which are retained through a low-pass filtering process (discussed later). Third, the isotherm depths for the entire record are not recorded simultaneously, and some change in the thermal structure occurs in the beginning of the data section by the time the end is being recorded. However, the vertical changes in depth of a particular isotherm will be nearly correct in any case.

A broad frequency spectrum exists in the vertical variations of the temperature structure with high frequencies superposed on the lower ones, which is indicative of the complexities of oceanic thermal structure. The sample section selected for analysis is set off by vertical lines in figure 3. To the right of the selected sample area and at a depth of about 200 feet, the 17°C and 14°C isotherms display weak 1°C temperature inversions. Inversions of this nature are not unusual in this area and have been discussed at length in studies of thermal fronts found off the southern end of Baja California (LaFond and LaFond, 1966; Griffiths, 1962).[14, 15] Such inversions were purposely omitted from the selected sample section. The effects of temperature inversions on vertical- and horizontal-temperature gradients are shown in a more descriptive example of the summer temperature structure of the deep Bering Sea, Sample Area 12 (see appendices to this report).

In the thermistor chain data, the vertical excursions of a particular isoltherm increase with depth as the vertical-temperature gradient decreases. In areas where the vertical-temperature gradient increases sharply, the amplitude of the vertical displacement of the isotherms decreases. This inverse relation of the amplitude of vertical displacement to the slope of the vertical-temperature gradient is probably caused by the diference in the vertical stability between the more stable water in the main pycnocline and the less stable water below it.
T. Hesselberg (1918) defined vertical stability by the expression[16]

$$E = \frac{1}{\rho} \frac{d\rho}{dz} \qquad (1)$$

where ρ is density and z is depth. According to this equation, the stability is greatest in the pycnocline where $d\rho/dz$ has the highest value. More energy is required to displace a unit volume of water vertically in an area of high vertical stability than to displace it an equal amount in an area of low vertical stability. Vertical displacements are therefore smaller in the main pycnocline than at other depths for an equal amount of imparted energy. Normally the thermocline and pycnocline are at the same depth, and this same line of reasoning also applies to vertical variations in the thermocline.

The inverse relationship of amplitude of the vertical variations to the vertical-temperature-gradient strength is not unique to this particular sample area but appears to be general throughout the oceans within the penetration depth of the thermistor chain.

Most vertical variations of isothermal surfaces (fig. 3) are highly phase-coherent through the entire recorded cross section; this is probably due to single-mode internal waves or a series of convection cells. Other variations are less coherent and probably represent multimode internal waves or turbulence. Periodic, exponential, or random motion may cause these features. The intent here, however, is not to discuss at length the mechanisms by which variations are generated, but to call attention to the magnitudes of the horizontal gradients resulting from them. Repeated tows over the same track in various areas, and in different directions as well, indicate that vertical motions in the temperature structure are always present and that they change with time. The horizontal-temperature gradients (discussed in a later section) are therefore time-dependent.

Close inspection of the record revealed changes of 1 to 4 feet in isotherm depth for each 12-second scan. To eliminate any aliasing of the data by spurious high-frequency components, the data were low-pass-filtered. The section between the heavy vertical lines in figure 3 will be used for describing the filtering process and the data reduction methods.

SMOOTHED TEMPERATURE STRUCTURES

The simplification of the data by low-pass filtering assumes that the vertical variations of the higher frequencies have considerably lower amplitude than those of lower frequencies, and therefore should have less effect on the refraction of underwater sound.

The low-pass filtering was accomplished by running weighted averages of the depth of each isotherm over 2-minute intervals using half-minute increments. The high-frequency cutoff of the filter is π radians per minute or 10π radians per nautical mile. The band pass is 0 to 0.5 cycle per minute.

The depths of the frequency-smoothed isotherms were replotted on an expanded horizontal scale, and 0.2°C isotherms were added by linear interpolation between the whole-degree isotherms.

Figure 4 displays the smoothed, low-pass-filtered temperature structure from Sample Area 8. The horizontal scale is shown as time but may be interpreted as distance with 10 minutes equivalent to 1 nautical mile at the normal towing speed of 6 knots. The vertical scale is 60 times that of the horizontal. These scale factors also hold for the smoothed structures of the other 16 sample areas, shown in Appendix A.

Three isotherms, the 15°, 16°, and 17°C, converge to form an area of relatively steep temperature gradients at about 200 feet.

This will be designated Area A. The addition of 0.2°C isotherms between 12°C and 15°C made the phase coherence of the vertical variations more obvious. The 20°C isotherm comes to the surface at about time 1236, and the temperature structure between 12°C and 15°C diverges about this same time. Even in a simplified form the temperature structure remains complex.

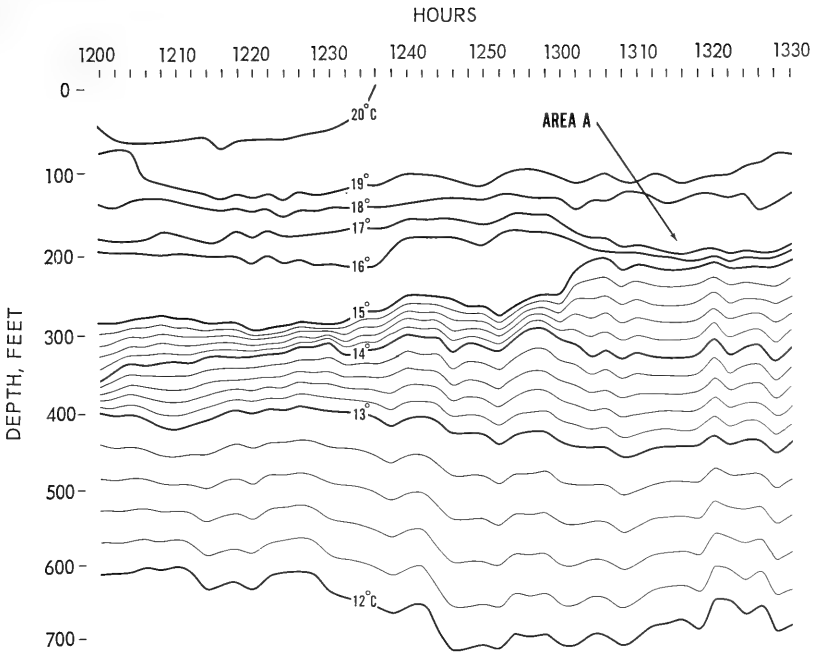

Figure 4. Examples of low-pass-filtered NEL Thermistor Chain data; 0.2°C isotherms added by linear interpolation between whole-degree isotherms.

GRADIENT FIELDS

The following graphic method of differentiation was used to find the vertical- and horizontal-temperature gradient fields. First, the graph of the smoothed temperature structure was overlaid with an exact copy, but the copy was displaced vertically by

20 (Δz) feet. (Several depth intervals were tried but 20 feet yielded the greatest detail for the minimum interval.) This displacement of one smoothed temperature chart over the other caused isotherms of one to intersect isotherms of the other. Next, at points of isotherm intersection the temperature values of one chart were subtracted from the values of the other. This yielded the change in temperature (ΔT) at particular depths and times for Δz. Finally, the resulting vertical-temperature-gradient field of computed values of $\Delta T/\Delta z$ was contoured at selected gradient-strength intervals.

Figure 5 shows the contoured vertical-temperature-gradient field obtained by this differentiation process from the smoothed structure of Sample Area 8 (fig. 4). The vertical and horizontal scales for the gradient field correspond in both depth and time to the smoothed structure from which it was derived. The contoured values in figure 5 have been multiplied by 100 for convenience of presentation. The vertical-temperature-gradient field is all negative, because temperature decreases with respect to depth for the entire field. The vertical-temperature-gradient fields for the other 16 sample areas are contained in Appendix B.

The same method of differentiation was used to obtain the horizontal-gradient field. Here the horizontal differential increment, Δx, was 1000 feet. (Several values were tried, but 1000 feet provided the greatest detail for the smallest interval.) This provided the change in temperature (ΔT) for the horizontal distance increment (Δx). The resulting horizontal-temperature-gradient field of computed values of $\Delta T/\Delta x$ was contoured at selected gradient-strength intervals. The contoured horizontal-temperature-gradient field obtained by differentiation from the smoothed structure of Sample Area 8 is shown in figure 6. The vertical and horizontal scales for the gradient field correspond in both depth and time to the smoothed structure from which it was derived. The contoured gradient strengths in figure 6 have been multiplied by 10^{+4} for convenience of presentation. The actual values of the gradient strengths are in degrees Celsius per foot times 10^{-4}.

Assuming wave motion, the zero-horizontal-gradient contours that are vertical denote phase multiples of $N\pi/2$ (for N odd) in a lateral direction. The zero contours that are horizontal denote the location of nodes in the modal distribution in the vertical

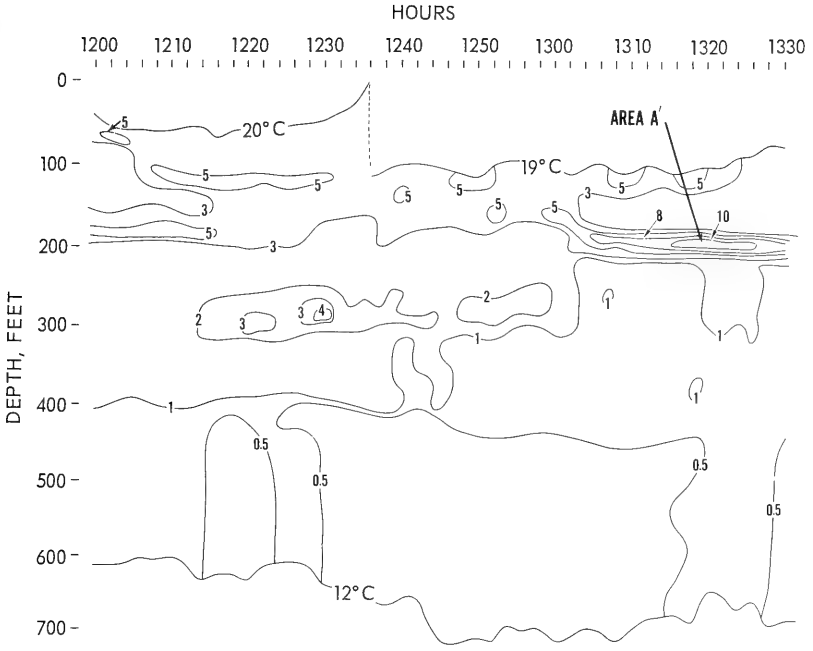

Figure 5. Example of vertical-temperature-gradient field in °C/ft × 10^{-2}. Entire field is negative gradient.

direction. For this reason, the horizontal portions of zero contours are dashed.

The horizontal-gradient field alternates in sign. The gradient values in shaded areas are negative and those in the unshaded areas are positive (fig. 6). The gradient sign is affixed on the basis of encounter, as experienced in time and distance through the temperature structure at a given depth. The horizontal-temperature-gradient fields for the other 16 sample areas are contained in Appendix C.

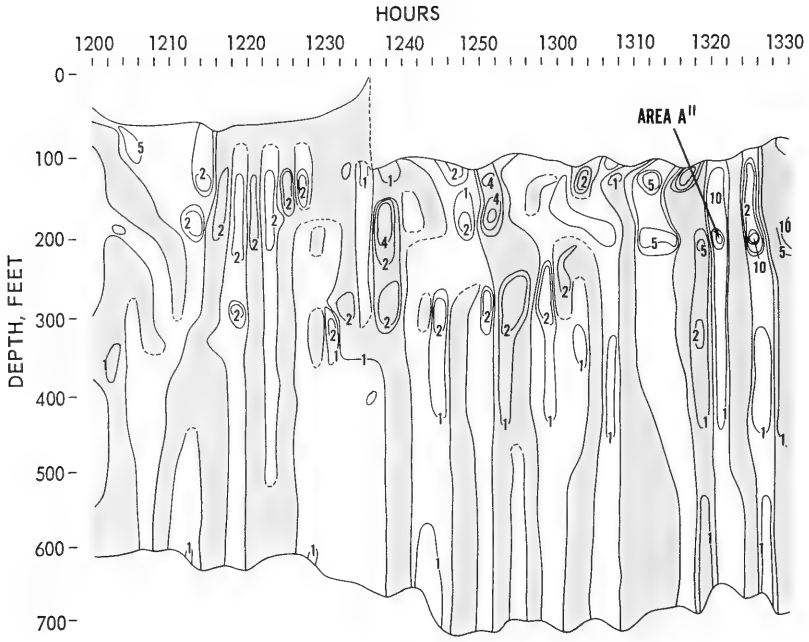

Figure 6. Example of horizontal-temperature-gradient field in °C/ft × 10^{-4}. Shaded areas denote negative gradient.

GRADIENT-STRENGTH MAGNITUDES

The vertical-temperature-gradient field for Sample Area 8 (fig. 5) displays a gradient-strength range of three orders of magnitude in degrees Celsius per foot. The gradient strength for the field, in general, is 10^{-2} °C/ft. In Area A' the vertical gradient increases one order of magnitude to 10^{-1} °C/ft. Area A' corresponds to the previously mentioned Area A of figure 4. It was described as an area of converging isotherms and, hence, of relatively-high-intensity vertical-temperature gradient. At depths greater than 410 feet, the vertical gradient decreases one order of magnitude to 10^{-3} °C/ft.

The horizontal-temperature-gradient field for Sample Area 8 (fig. 6) also displays a gradient-strength range of several orders of magnitude. The contoured gradient strength for the field, in general, is 10^{-4} °C/ft, and gradient-sign changes occur at zero contours. In area A'' the horizontal gradient increases one order of magnitude to 10^{-3} °C/ft. Area A'' corresponds to Areas A and A' of figures 4 and 5, respectively. Below 420 feet the horizontal gradient decreases one order of magnitude to 10^{-5} °C/ft. The horizontal-temperature gradient is zero in the region of gradient-sign changes. The horizontal-gradient strengths referred to are the maximum obtained at a specific depth.

Comparing the vertical and horizontal gradients shows that they differ in strength by two orders of magnitude. When the vertical and horizontal gradients change orders of magnitude, they appear to do so simultaneously.

On the basis of results obtained with the Russian thermistor chain, Lyamin (1965) [17] wrote: "When the temperature fluctuations are compared with the magnitudes of the vertical temperature gradient, they are seen to be proportional to each other. This relationship is noted in all cases without exception and indicates that the temperature fluctuations recorded by horizontally displaced transducers are the result of the vertical displacement of the water layers."

The interrelationship of the magnitudes of horizontal- and vertical-temperature-gradient strengths holds throughout all 17 sample areas with but a single exception. In Sample Area 9 it was found that, in regions of very sharp thermocline (high vertical-gradient values) where the vertical variations in the temperature

structure are small, the magnitude of the horizontal gradient is nearly zero. The smoothed temperature structure of Sample Area 9 exhibits some localized areas essentially free from vertical fluctuations of the isothermal surfaces. Examination of the vertical- and horizontal-gradient fields for Sample Area 9 shows that, when the vertical-temperature gradient is about 2×10^{-1} °C/ft, the corresponding horizontal-temperature gradient is of the order 10^{-6} °C/ft and decreases to zero. Therefore in regions of strong vertical-temperature gradient (high vertical stability), vertical fluctuations in the temperature structure are small and time-dependent horizontal-temperature gradients nearly disappear.

The regularity with which the horizontal-temperature gradient differs from the vertical-temperature gradient suggests that the slope of the isothermal surfaces is the regulating factor. The vertical- and horizontal-gradient interrelationship may be written as the identity

$$\delta T/\delta x = (\delta T/\delta z)\ (dz/dx) \tag{2}$$

where $\delta T/\delta x$ is the horizontal-temperature gradient in °C/ft, $\delta T/\delta z$ is the vertical-temperature gradient in °C/ft, and dz/dx is the slope of the isothermal surface. The ratio of $\delta T/\delta x$ to $\delta T/\delta z$ taken over the samples shows that the mean value of dz/dx is 1.12×10^{-2}.

In an independent investigation (also using thermistor chain data) of the thermal structure around the tip of Baja California (LaFond and LaFond, 1966),[18] two isotherms were selected for analysis, one in the main thermocline and one below it. The location of the data sections is shown in figure 7. The depth differences from point to point along the isotherms were determined from the equation

$$Y_k = X_i - X_{i+1} \tag{3}$$

where $1 \leq k \leq N$; X_i and X_{i+1} are depths in feet of a given isotherm at the beginning and end of the i^{th} distance interval along the track; and Y_k is the computed depth difference in feet for the k^{th} interval. The ship's speed was 6 knots and the sampling interval was 30 seconds, corresponding to a distance interval of 304 feet.

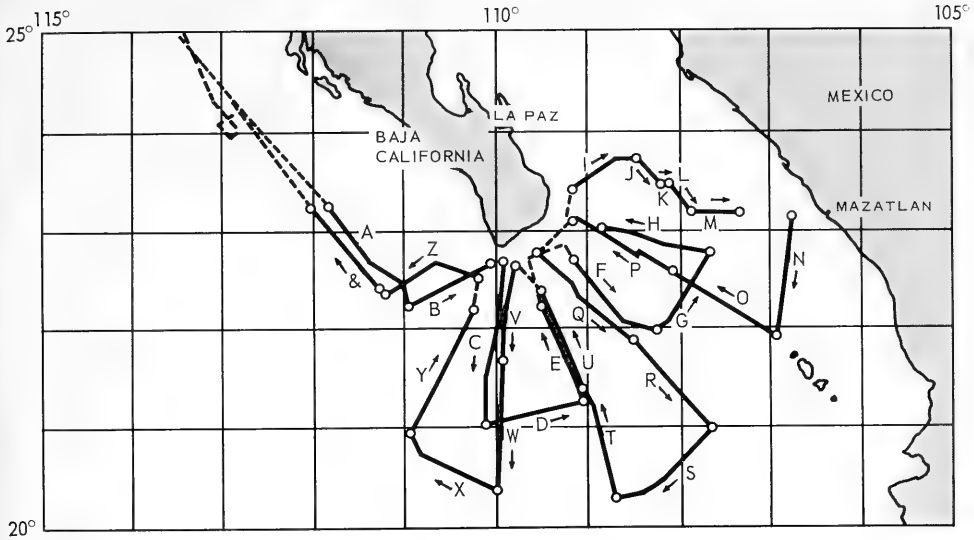

Figure 7. Track of USS MARYSVILLE showing where temperature data were collected off the southern tip of Baja California during NEL Thermistor Chain Cruise 8.

Dividing Y_k by 304 gave the isotherm slope in the direction of the ship's motion.

Using more than 65,000 data samplings, LaFond and LaFond found the median of the absolute slope values to be 0°25' and the 70th percentile of the absolute values to be 0°51' south of Baja California. On the Pacific side of the peninsula, LaFond found the mean slope to be 0°16' and the 70th percentile to be 0°30'.

The 70th percentile value for the Pacific slopes is 0.9×10^{-2}, and south of Baja California the 70th percentile value is 1.5×10^{-2}. These values agree with the previously given mean value for dz/dx. Therefore it is concluded that slopes of isothermal surfaces are of the order 10^{-2}.

For a closer examination of the horizontal- and vertical-gradient proportionality, the logarithm of the horizontal gradient was plotted as the ordinate and the logarithm of the corresponding vertical gradient was plotted as the abscissa (fig. 8). The method

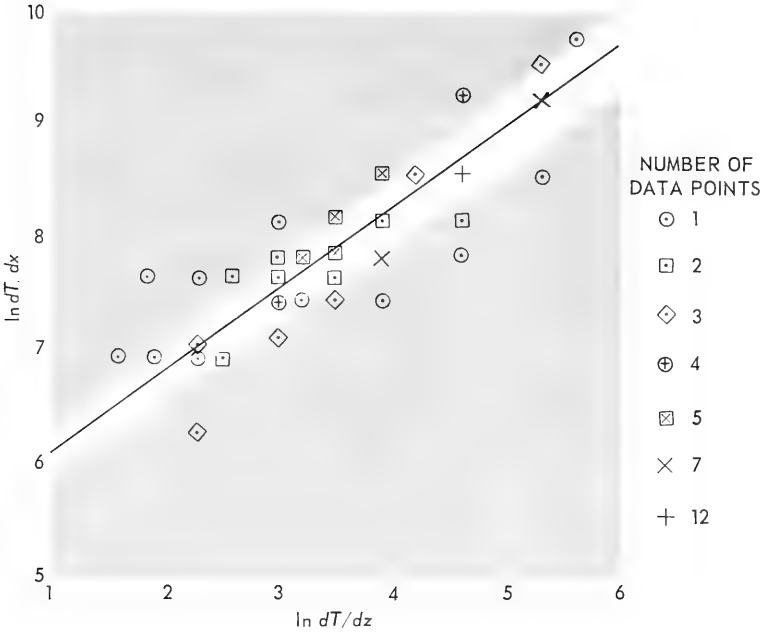

Figure 8. Least-squares fit of a straight line to the logarithms of the vertical- and horizontal-temperature gradients from 17 sample areas (black line) and the envelope of the standard error of estimate.

of least-squares fit to a straight line was applied, and the equation of the fitted straight line, standard deviation of the slope, and standard deviation of the intercept were determined. From the logarithmic relationship it was found

$$dT/dx = 0.0047\ (dT/dz)^{0.71} \tag{4}$$

Written in a more common form, equation 4 becomes

$$\ln (dT/dx) = -5.37 + 0.71\ \ln (dT/dz) \tag{5}$$

where, on a linear plot of the logarithms, -5.37 is the intercept with a standard deviation of 0.35 and the slope is 0.71 with a

standard deviation of 0.04. The black line in figure 8 is the fitted straight line and the envelope shows the standard error of estimate.

Although equation 5 displays a proportionality constant between the vertical and horizontal gradients, the use of this constant is not felt justified at this time because of the necessary averaging of the analog temperature data. We are presently studying this interrelationship further, using the digital temperature data, and we hope to be able to substantiate the proportionality constant. However, from the results here it is clear that (1) the vertical-temperature gradient is generally of the order 10^{-2} but can range between 10^{-1} and 10^{-3} °C/ft; (2) the horizontal-temperature gradient is generally of the order 10^{-4} but can range between 10^{-3} and 10^{-5} °C/ft; and (3) the two gradients normally differ by two orders of magnitude.

WAVELENGTHS

Inspection of the contoured horizontal-temperature-gradient fields reveals a regularity with which the gradient changes sign, strongly suggesting a periodic motion indicative of internal waves or convection cells. Although all information indicates the presence of a broad spectrum of frequencies in the ocean, the simplified interpretation of these data implies that there is a dominant oscillation at an intermediate frequency.

The power spectrum is a statistical method for gaining spectral information from a data sample of finite length and fluctuating values. The power spectrum $U(h)$ can be shown to be the Fourier transform of the autocorrelation $R(\lambda)$, and is proportional to the energy per unit band width. Consequently, any dominant frequency will appear as a peak in the spectrum.

The power spectrum method of analysis was first applied to NEL Thermistor Chain data of Cruise 4, which took place between San Diego and Hawaii in 1961. Cross sections (data strips) of 8-1/2- and 12-hour durations of depths of an isotherm were subjected to spectral analysis. Figure 9 shows the location of the analyzed data sections (LaFond and Moore, 1964).[19] The

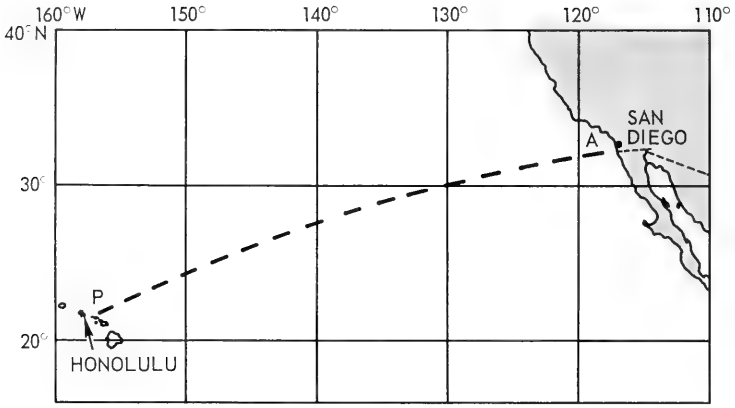

Figure 9. Track of USS MARYSVILLE showing locations where temperature data were collected between San Diego and Honolulu during NEL Thermistor Chain Cruise 4.

smoothed spectral ordinates for two isotherms, one in the main thermocline and one below, for each of the 16 data sections A through P, were obtained as follows:

$$U(h) = \frac{1}{n}\left[R(0) + \sum_{\lambda=1}^{\lambda=n-1} R(\lambda)\left(1 + \cos\frac{\pi\lambda}{n}\right)\cos\frac{\pi\lambda h}{n}\right] \qquad (6)$$

where $h = 0, 1, 2, 3 \ldots n$, index number of frequency (actual frequencies are given by $h/(2\Delta t)$ cycles/minute, $\Delta t = 1/2$ minute),

and $\lambda = 0, 1, 2, 3 \ldots n$, lag number.

The individual spectrum for the 32 computations showed no single dominant frequency but, instead, showed many peaks in the spectral curves within the range of 0 to 0.35 cycle per minute. The resolution into narrow frequency bands was prevented by the short duration of the sample sections. The frequency band resolved was 0.007 cycle per minute for 144 lags. However,

dividing each of the 32 spectra into bandwidths (Δf) of 0.025 cycle per minute and then averaging the energy per bandwidth does reveal some dominance in the spectrum. Figure 10 shows the average power spectrum for the two isotherms of the 16 data sections between San Diego and Hawaii. If no frequency band in the spectrum is dominant then the ensemble average would not show any peak. This is not the case, as shown by the two peaks clearly retained in the ensemble average spectrum (fig. 10). One peak is at 0.15 cycle per minute (λ = 0.67 mile) and the second at 0.25 cycle per minute (λ = 0.4 mile).

The thermistor chain data of Cruise 8, from around the tip of Baja California, were also synthesized into spectral ordinates (LaFond and LaFond, 1966).[18] Cross sections of up to 12-hour duration of depths of isotherms were analyzed in the same manner as described for the Cruise 4 data. Figure 7 shows the location

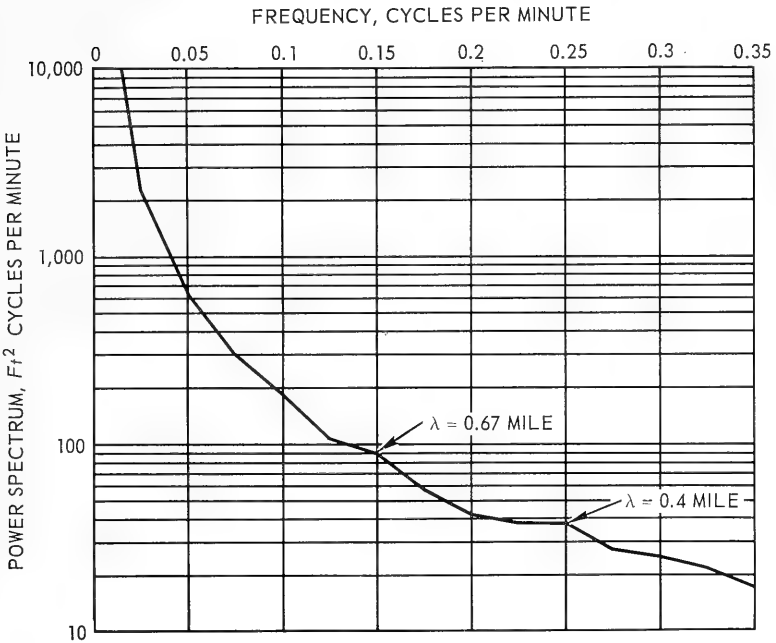

Figure 10. Ensemble average spectrum for NEL Thermistor Chain Cruise 4.

of the data sections. The smoothed power spectrum values for two isotherms, one in the main thermocline and one below, for each of the 27 data sections A through Z plus & were computed. In this case (as in Cruise 4) no single frequency or frequency bandwidth appeared to be dominant within the range of 0 to 0.35 cycle per minute in the individual spectra.

Averaging the energy per bandwidth (Δf = 0.025 cycle per minute) for the 54 computed spectra of Cruise 8 in the same manner as for Cruise 4 again revealed a peak in the emsemble average (fig. 11) at 0.15 cycle per minute (λ = 0.67 mile).

Reexamination of the spectra, individually, shows peaks at many wavelengths but also shows a peak at λ = 0.67 mile for 28 out of 32 cases and 48 out of 54 cases for Cruises 4 and 8, respectively. Hence, 88 percent of the spectra thus far computed show a peak at a wavelength of 0.67 mile.

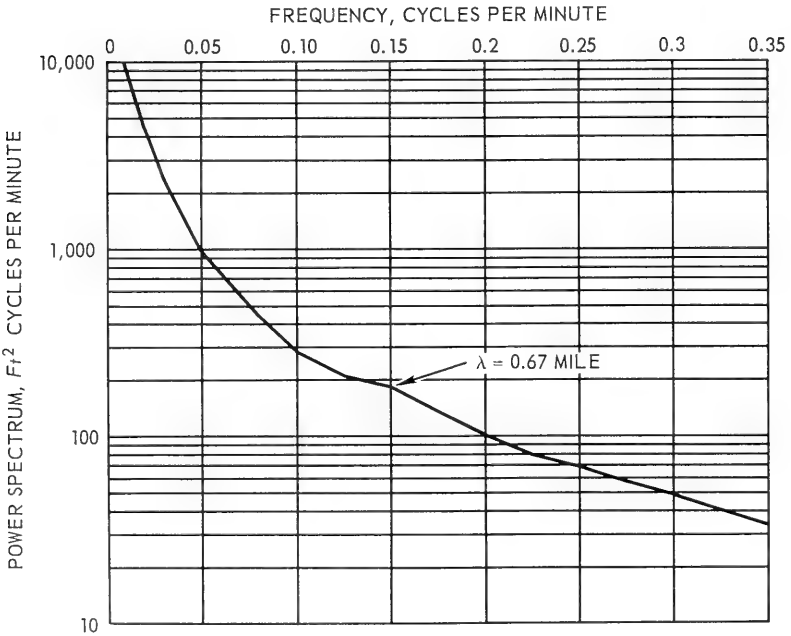

Figure 11. Ensemble average spectrum for NEL Thermistor Chain Cruise 8.

Further analysis of the 17 horizontal-temperature-gradient fields (obtained from the smoothed temperature structures) provides added support for the existence of a dominant frequency of oscillation. More than 600 wavelength measurements at two depths throughout the 17 horizontal gradient fields were made and the mean wavelength was found to be 0.72 mile (f = 0.14 cycle per minute) with a standard deviation of 0.07 mile. The horizontal bars in the histogram of figure 12 display the mean wavelength for each of the 17 sample areas, and the vertical lines show the mean wavelength and the standard deviation as derived from the ensemble averages. It should be observed that the mean wavelength (0.72 mile) for all the sample areas is in good agreement with the results of the spectral analysis (0.67 mile) for Cruises 4 and 8. However, the histogram gives no indication of the shorter wavelengths (0.4 and 0.3 mile) as shown in the average spectral curves for Cruises 4 and 8.

These results indicate that there is a dominant frequency of oscillation in the thermal structure of the ocean with a wavelength of about 0.7 mile. The frequency spectrum under investigation here indicates that this result combined with the relation of the magnitudes of the vertical and horizontal gradients could be utilized as the foundation for a simplified predictive model of the horizontal-temperature gradients of the sea. The consistency of these results over widely separated geographic areas leads to the speculation that they are characteristic of the world ocean.

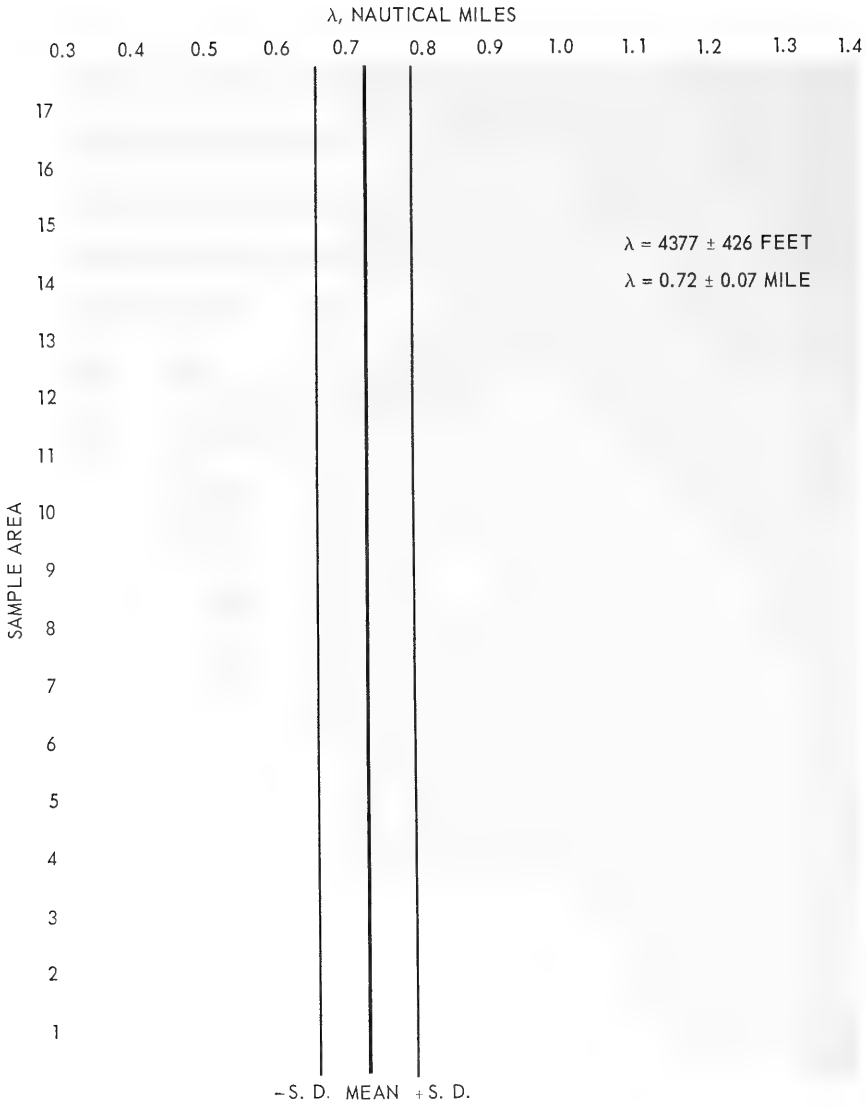

Figure 12. Wavelength histogram for 17 sample areas. Horizontal bars are mean wavelength for each sample area. Vertical lines are the mean wavelength, and standard deviation as derived from the ensemble averages.

PREDICTIVE MODEL OF HORIZONTAL-TEMPERATURE GRADIENTS

A predictive horizontal-temperature-gradient model can be constructed in two steps: first, use half the mean wavelength, 0.35 mile, as the distance for the periodic sign changes of the horizontal-gradient field;* second, from the results of a single bathythermograph lowering, compute the vertical-gradient strengths in °C/ft for selected depth ranges and assign the horizontal-gradient field with strength two orders of magnitude smaller than that of the vertical field for corresponding depth ranges.

As an example of the construction of such a model, consider the bathythermograph of figure 13. The change in the order of magnitude of the vertical-temperature-gradient strength determines the depth range interval as shown in table 2. The horizontal-temperature-gradient strengths for the corresponding depth ranges are also entered in the table.

The resulting horizontal-temperature-gradient field model is shown in figure 14. The gradient field changes sign each one-half wavelength as shown by the alternating shaded and unshaded areas. The orders of magnitude of the horizontal-gradient strength in °C/ft are contoured at the depths specified by the matching vertical gradients computed from the bathythermograph.

In the construction of such a model, obviously the larger the number of bathythermographs taken, the more reliable the depth ranges will be for establishing the order-of-magnitude contours in the model. The bathythermograph used here was made 0815, 7 August 1962, during Cruise 14 with the NEL Thermistor Chain. The simplified model results (fig. 14) may be compared with the more detailed computed horizontal-gradient field for Sample Area 1 in figure 15. The model is in reasonably good agreement with the more detailed horizontal-gradient field for the same time, place, and depth. There is a slight disagreement

---

* When a single BT is used, the initial gradient sign of the model has to be arbitrarily assigned. However, when two closely spaced BT's are used, the actual gradient sign can be determined.

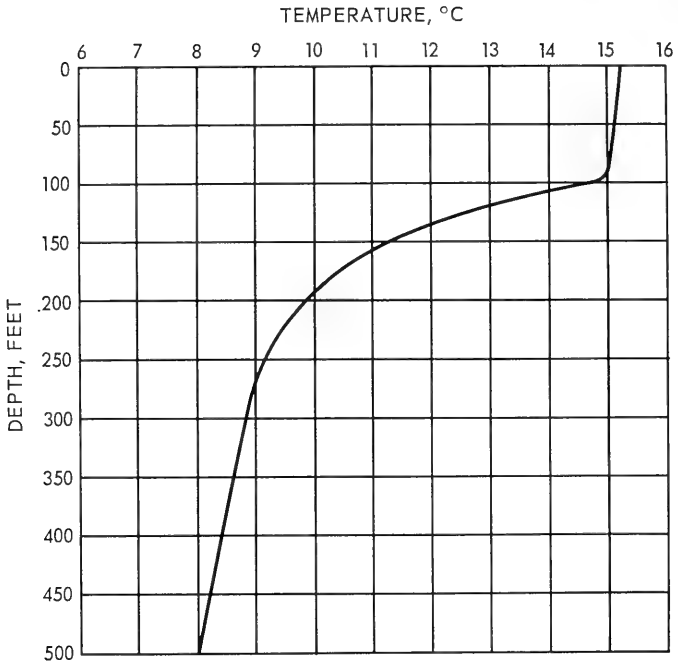

Figure 13. Bathythermograph taken 0815, 7 August 1962, during Cruise 14 of the NEL Thermistor Chain.

TABLE 2. TEMPERATURE-GRADIENT MAGNITUDES FOR SPECIFIC DEPTH RANGES FROM A SINGLE BATHYTHERMOGRAM

Depth Range (ft)	Magnitude of Vertical Gradient dT/dz (°C/ft)	Magnitude of Horizontal Gradient dT/dx (°C/ft)
0 - 95	10^{-3}	10^{-5}
95 - 100	10^{-2}	10^{-4}
100 - 110	10^{-1}	10^{-3}
110 - 275	10^{-2}	10^{-4}
275 - 500	10^{-3}	10^{-5}

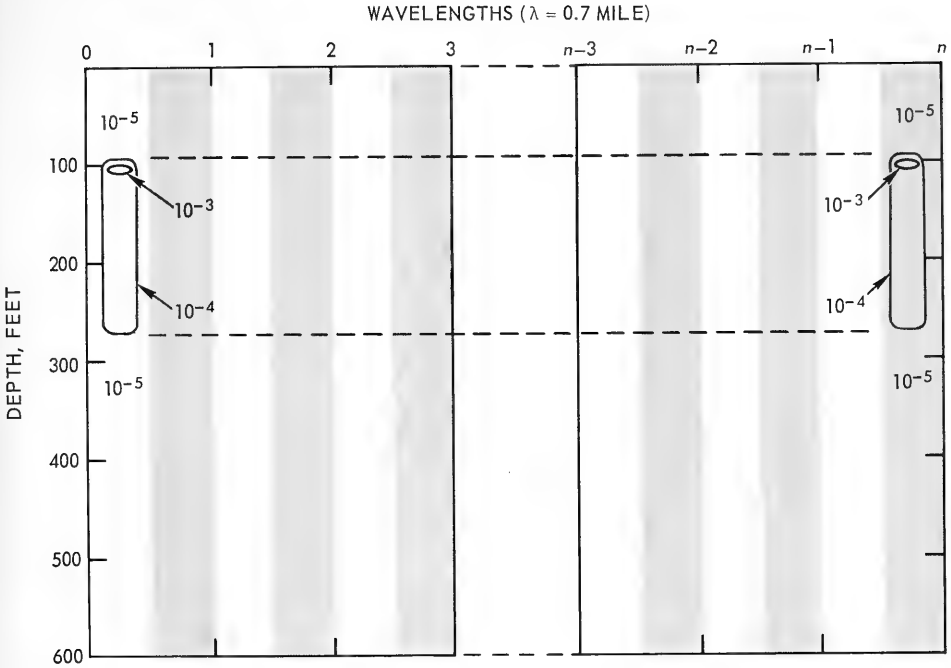

Figure 14. Predicted horizontal-temperature-gradient field model. Horizontal-temperature-gradient contour values are in °C/ft. Horizontal-temperature-gradient contours repeat every $\lambda/2$ from zero to n wavelengths throughout the model.

in the wavelength, probably because of the modal distribution of the internal waves. In general, the simplified model provides a valid description of the horizontal-temperature gradients.

Although the simplified model offers only the order of magnitude of the temperature gradients and the wavelength is restricted to a specified frequency spectrum, it must be noted that this is the first presentation of a formulated horizontal model accounting for first-order changes in the temperature structure in the sea. With further refinement in data-gathering-and-reduction processes, this model should reveal more detail and, possibly, a constant numerical relationship between vertical- and horizontal-temperature gradients in the sea.

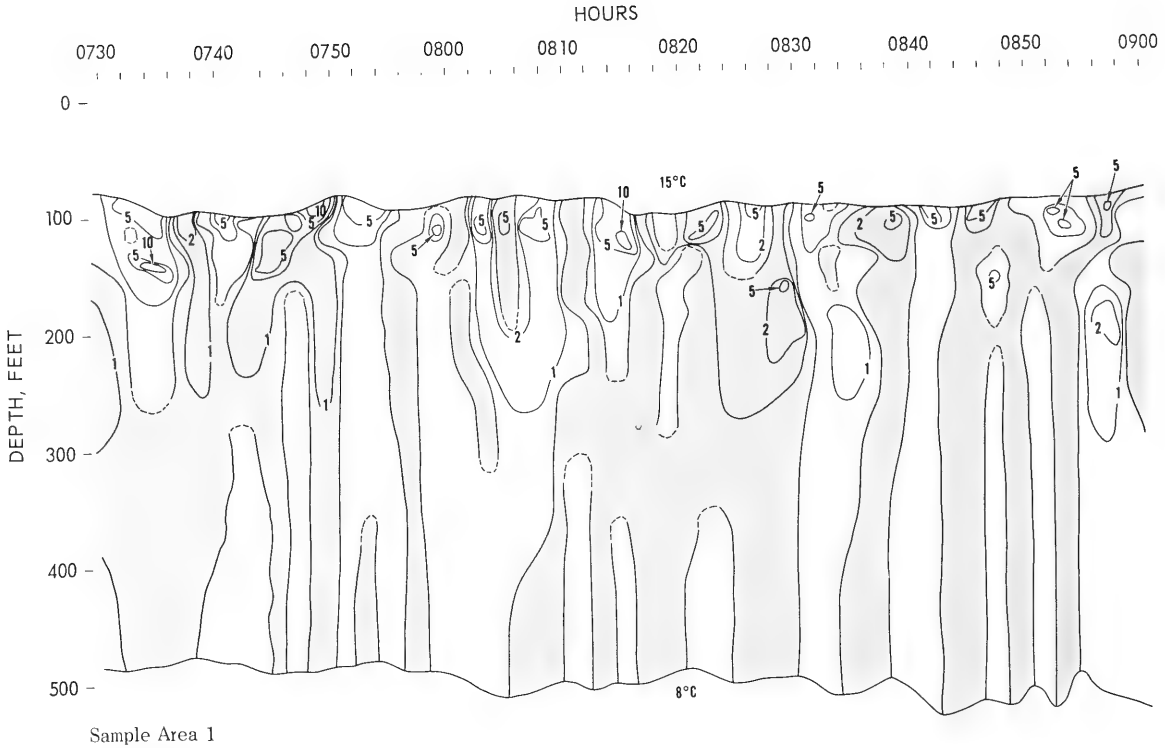

Sample Area 1

Figure 15. Example from Sample Area 1 of the horizontal-temperature-gradient field in °C/ft × 10^{-4}. Shaded areas denote negative gradient.

SUMMARY AND CONCLUSIONS

Time-dependent horizontal-temperature gradients were computed from low-pass-filtered, continuous, temperature cross sections of the upper 750 feet of the ocean in 17 widely separated geographic areas. The selected areas range north to the Bering Sea, south to the coastal waters of the Mexican mainland including the Gulf of California, and west to the Hawaiian Islands.

The horizontal-gradient fields, computed from smoothed temperature structures, alternate in sign with a regularity that implies a dominant frequency of internal waves or convection cells. The wavelength is 0.72 nautical mile with a standard deviation of 0.16 mile.

The vertical- and horizontal-temperature-gradient fields contain zones of diverse intensity gradient. The vertical-temperature gradient in the thermocline is generally of the order 10^{-2} °C/ft, but ranges between 10^{-1} and 10^{-3} °C/ft. The corresponding horizontal-temperature gradient is generally of the order 10^{-4} °C/ft, but ranges between 10^{-3} and 10^{-5} °C/ft. The slopes of isothermal surfaces are of the order 10^{-2}. A statistical analysis of the ratio of the horizontal to the vertical temperature gradient shows that the horizontal gradient in the thermocline can be predicted within useful limits from the measured vertical-temperature gradient by means of the equation

$$dT/dx = 0.0047\ (dT/dz)^{0.71}$$

The combined interrelationship of the vertical- and horizontal-temperature gradients and the wavelength of the dominant frequency of oscillation of the temperature structure were used as the foundation for a simplified predictive model of the horizontal-temperature gradients of the sea. The consistency of the results over widely separated geographic areas leads to the speculation that they are characteristic of the world ocean.

REFERENCES

1. Oceanic Observations of the Pacific: 1955, The NORPAC Atlas, University of California Press, 1960

2. U.S. Navy Radio and Sound Laboratory Report S-17, Measurements of the Horizontal Thermal Structure of the Ocean, by N.J. Holter, 18 August 1944

3A. Naval Research Laboratory Report S-3392, The Microthermal Structure of the Ocean Near Key West, Florida, Part I: Description, R.J. Urick and C.W. Searfoss, 1 December 1948

3B. Naval Research Laboratory Report S-3444, The Microthermal Structure of the Ocean Near Key West, Florida, Part II: Analysis, by R.J. Urick and C.W. Searfoss, 12 April 1949

4. Sheehy, M.J., "Transmission of 24-kc Underwater Sound From a Deep Source," Acoustical Society of America. Journal, v. 22, p.24-28, January 1950

5. Lieberman, L.N., "The Effect of Temperature Inhomogeneities in the Ocean on the Propagation of Sound," Acoustical Society of America. Journal, v. 23, p. 563-570, September 1951

6A. Mintzer, D., "Wave Propagation in a Randomly Inhomogeneous Medium, I." Acoustical Society of America. Journal, v. 25, p. 922-927, September 1953

6B. Mintzer, D., "Wave Propagation in a Randomly Inhomogeneous Medium, II," Acoustical Society of America, Journal, v. 25, p. 1107-1111, November 1953

6C. Mintzer, D., "Wave Propagation in a Randomly Inhomogeneous Medium, III," Acoustical Society of America. Journal, v. 26, p. 186-190, March 1954

7. Priimak, G.I., "Certain Results of the Studies of the Statistical Microheterogeneity of a Sea Medium," Academy of Sciences, USSR. Bulletin. Geophysics Series, No. 8, p. 805-810, 1961

8. Sagar, F.H., "Acoustic Intensity Fluctuations and Temperature Microstructure in the Sea," Acoustical Society of America. Journal, v. 32, p. 112-121, January 1960

9. Helle, J.R., "Thermal Microstructure Measurements in the Pacific," p. 249-271 in Naval Oceanographic Office, First U.S. Navy Symposium on Military Oceanography, v.2, CONFIDENTIAL, 17-19 June 1964

10. Murphy, S.R. and Lord, G.E., "Thermal and Sound Velocity Microstructure Data Taken With an Unmanned Research Vehicle," p. 343-360 in Naval Ordnance Laboratory, Second U.S. Navy Symposium on Military Oceanography, 5-7 May 1965. The Proceedings of the Symposium, v. 1, 7 May 1965

11. Smith, E.L., "Magnitudes of Time-Dependent Horizontal Temperature Gradients in the Ocean," U.S. Navy Journal of Underwater Acoustics, v. 15, p. 637-640, CONFIDENTIAL, July 1965

12. Fisher, F.H. and others, "Convergent Zone Bearing Accuracy Measurements," U.S. Navy Journal of Underwater Acoustics, v. 15, p. 609-626, CONFIDENTIAL, July 1965

13. Sverdrup, J.U. and others, The Oceans, Prentice-Hall, 1942

14. LaFond, E.C. and LaFond, K.G., "Thermal Structure of Waters Adjacent to the Southern End of Baja California (Abstract)," American Geophysical Union. Transactions, v. 47, p. 432, June 1966

15. Griffiths, R.C., "Studies of Oceanic Fronts in the Mouth of the Gulf of California, An Area of Tuna Migrations," Experience Paper No. 34 presented at the World Scientific Meeting on the Biology of Tunas and Related Species, La Jolla, California, 2-14 July 1962

16. Hesselberg, T., "Über die Stabilitätsverhältnisse bei Vertikalen Verschiebungen in der Atmosphäre und im Meer," Annalen der Hydrographie und Maritimen Meteorologie, v. 46, p. 118-129, 1918

17. Lyamin, E.A. and others, "on the Use of a Towed Chain of Thermistors to Investigate the Thermal Structure of the Sea," Oceanology, v. 5, No. 3, p. 129-132, 1965

18. Navy Electronics Laboratory Report 1395, Vertical and Horizontal Thermal Structures in the Sea, by E.C. LaFond and K.G. LaFond, 29 July 1966

19. Navy Electronics Laboratory Report 1210, Measurements of Thermal Structure Between Southern California and Hawaii With the Thermistor Chain, by E.C. LaFond and A.T. Moore, 7 February 1964

APPENDIX A: SMOOTHED TEMPERATURE STRUCTURES

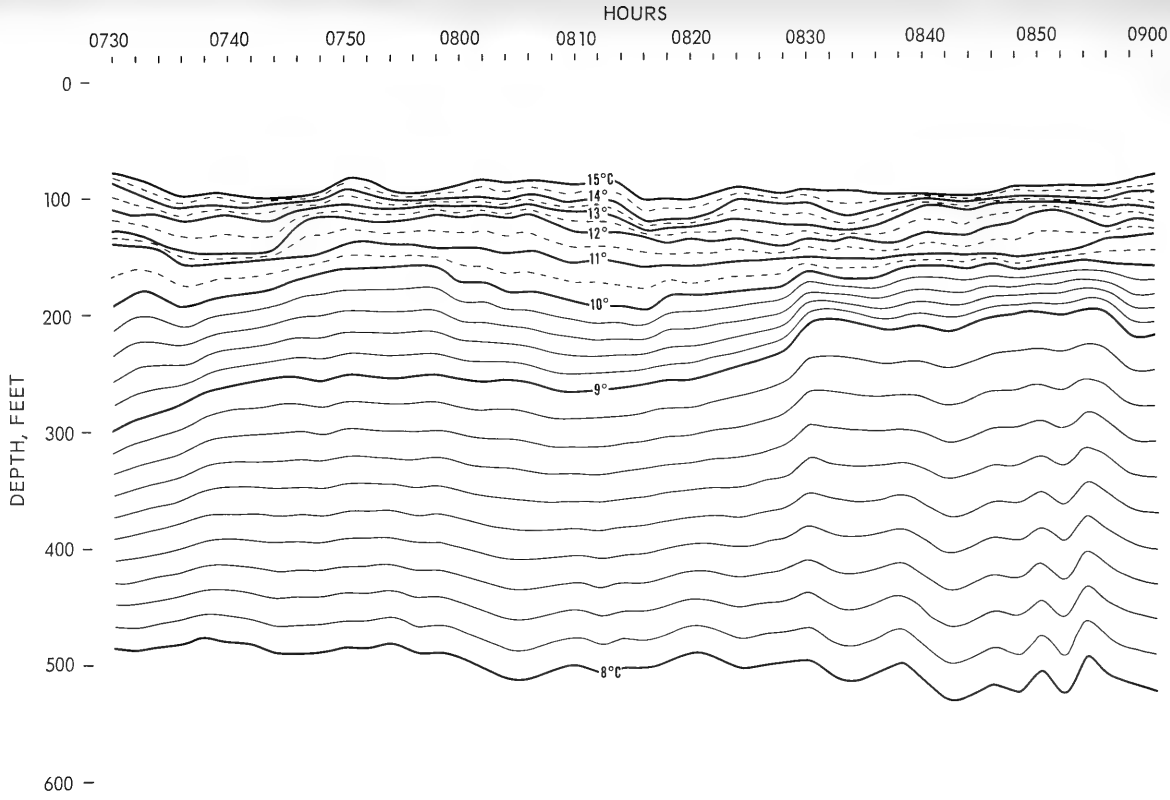

Sample Area 1

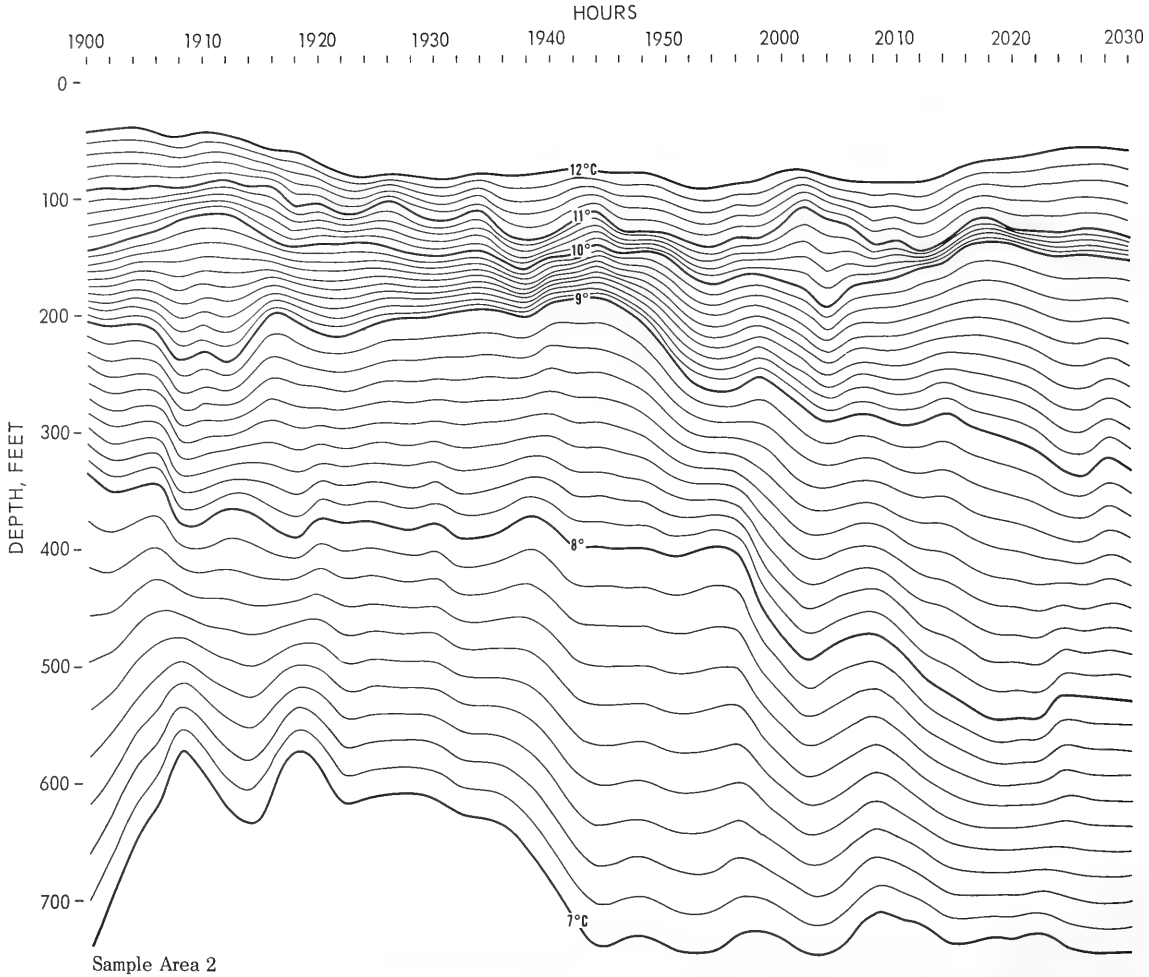

Sample Area 2

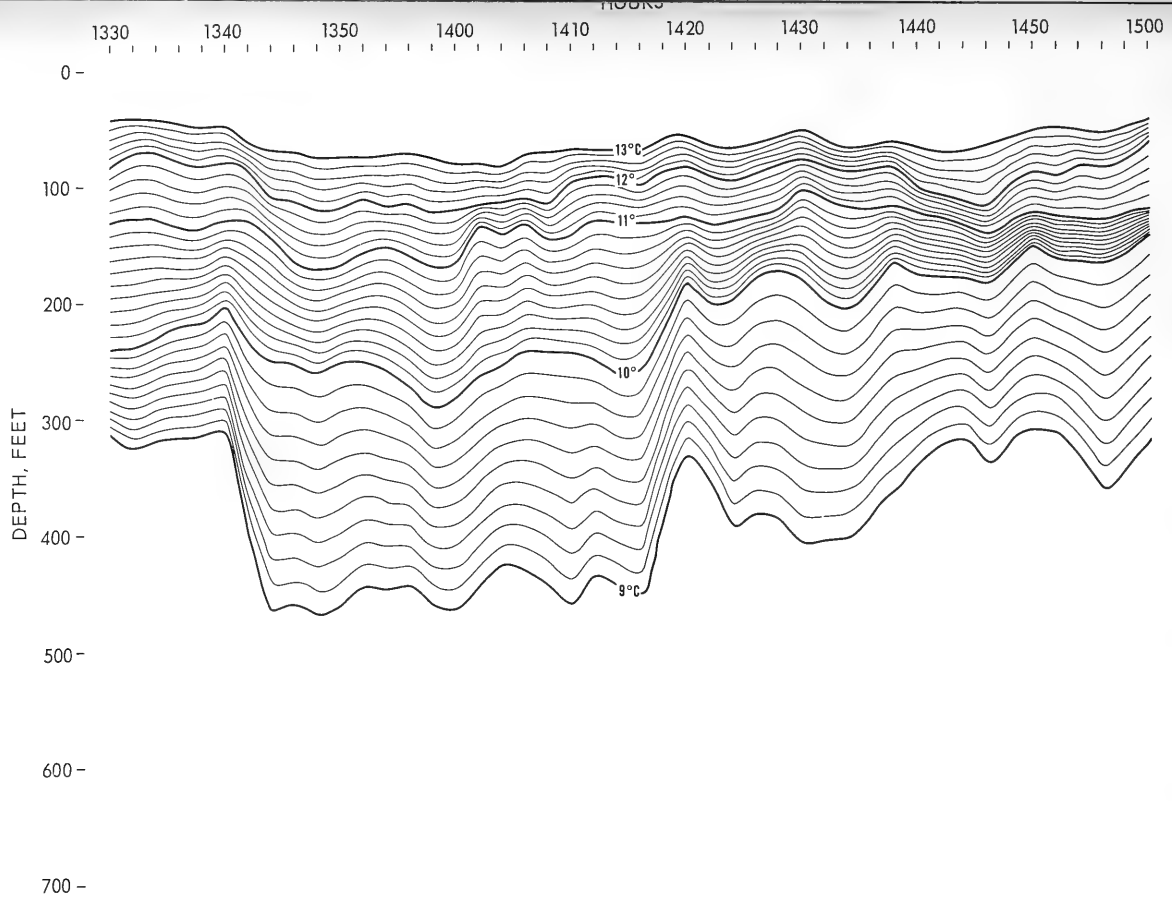

Sample Area 3

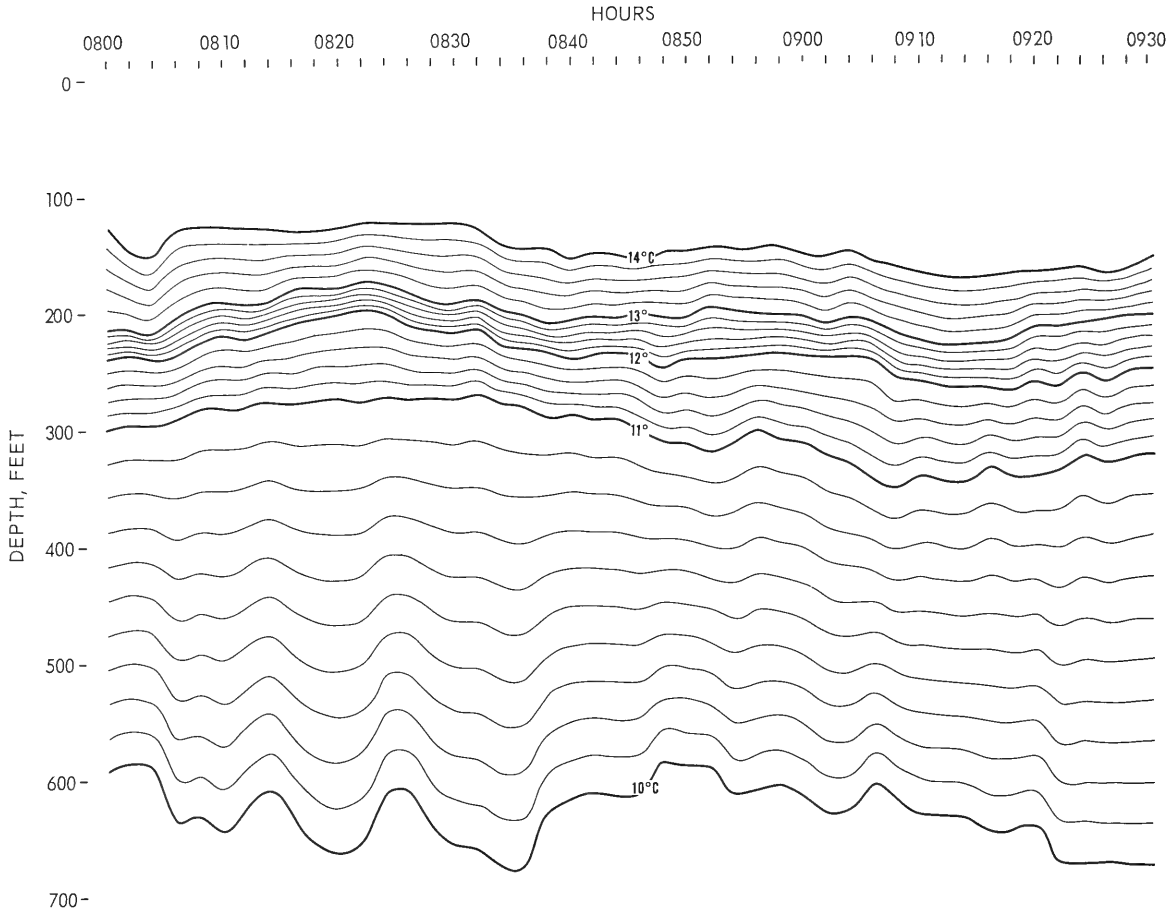

Sample Area 4

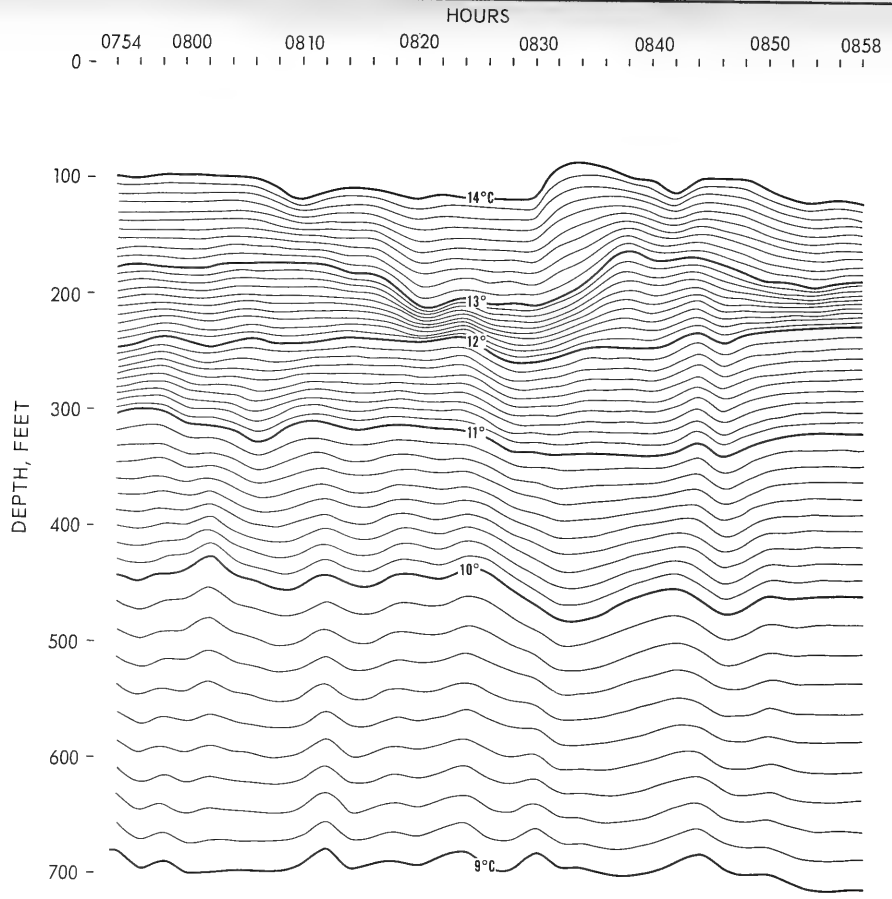

Sample Area 5

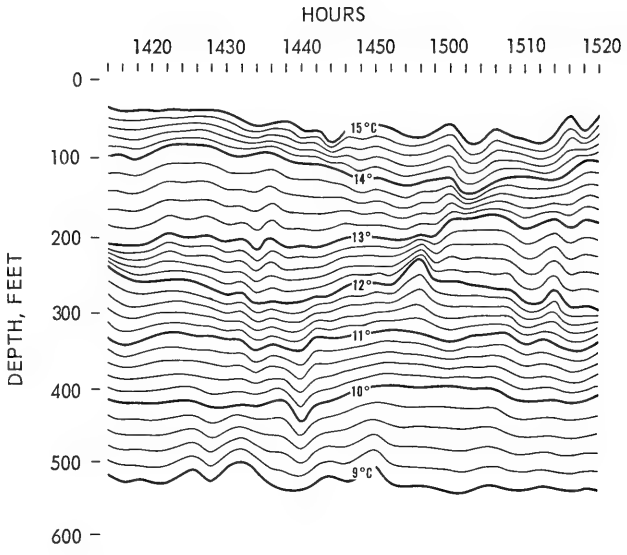

Sample Area 6

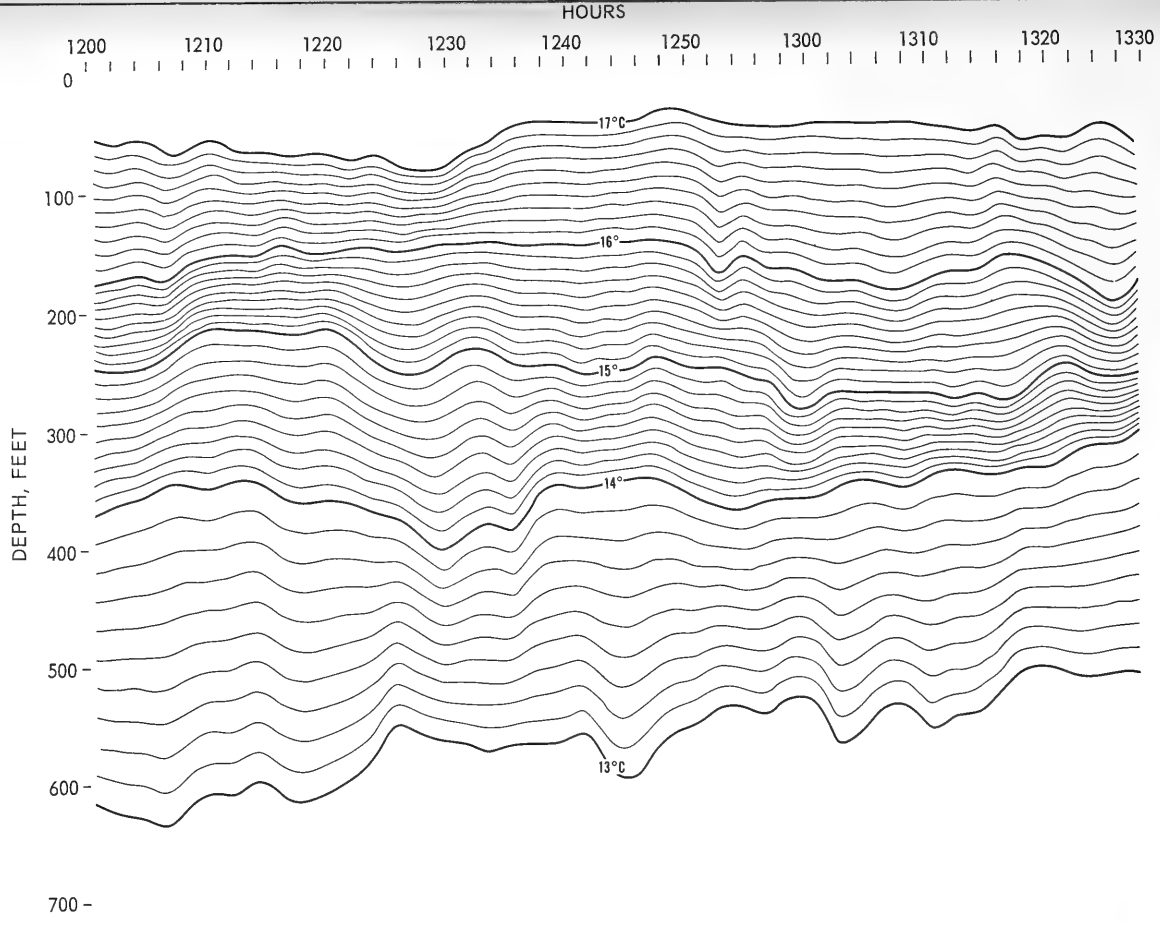

Sample Area 7

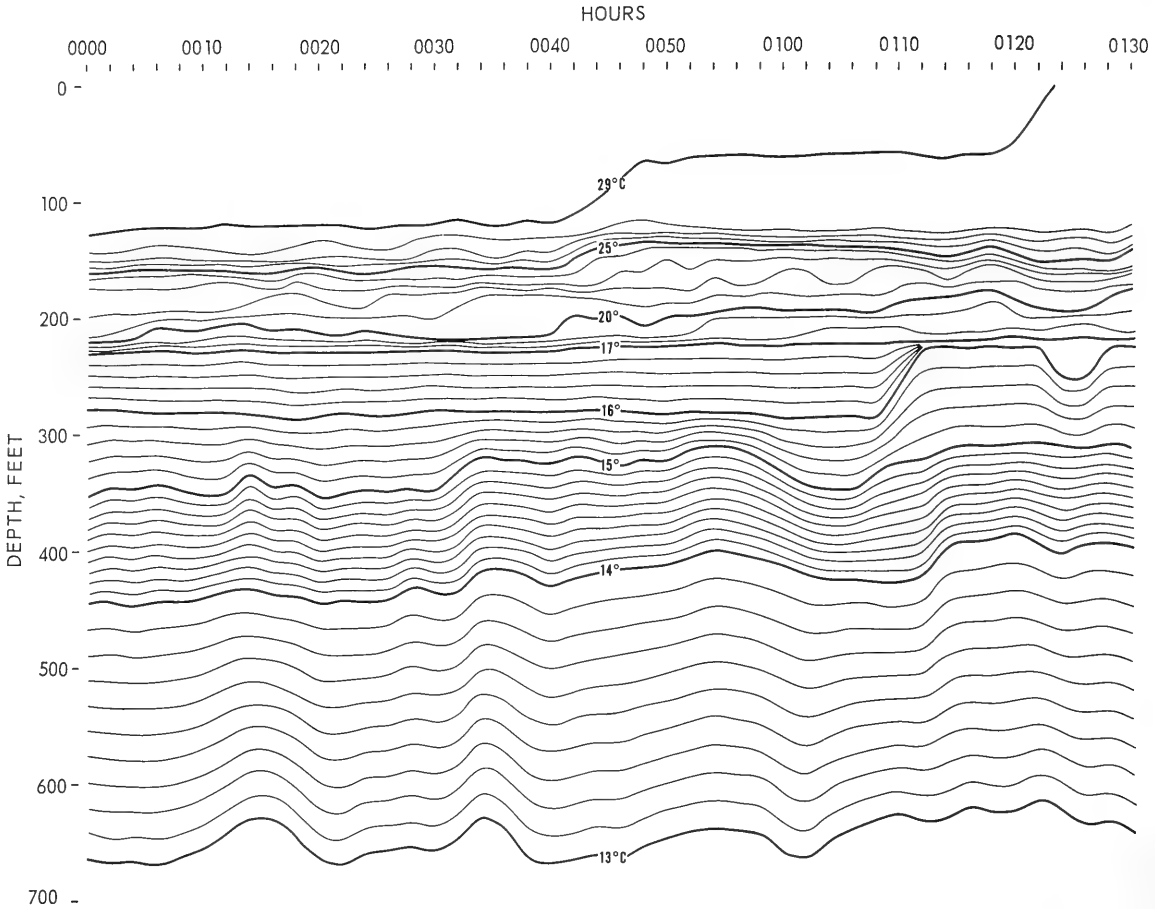

Sample Area 9

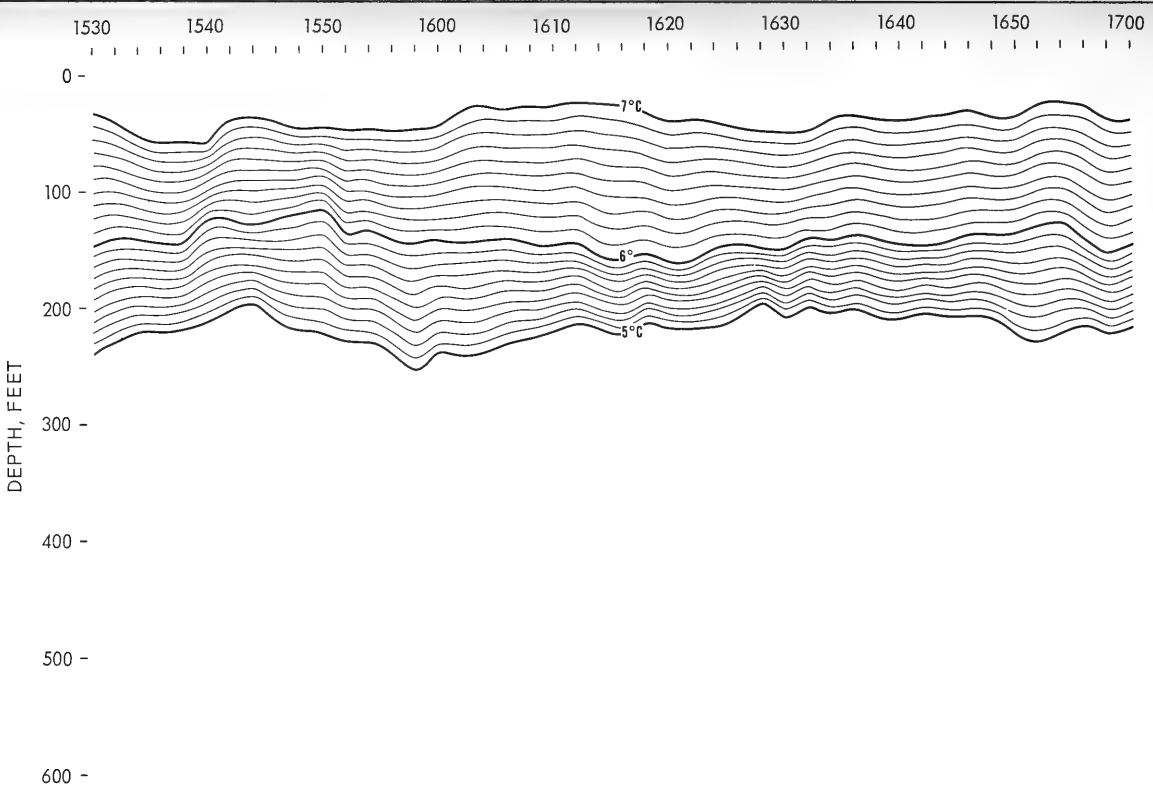

Sample Area 10

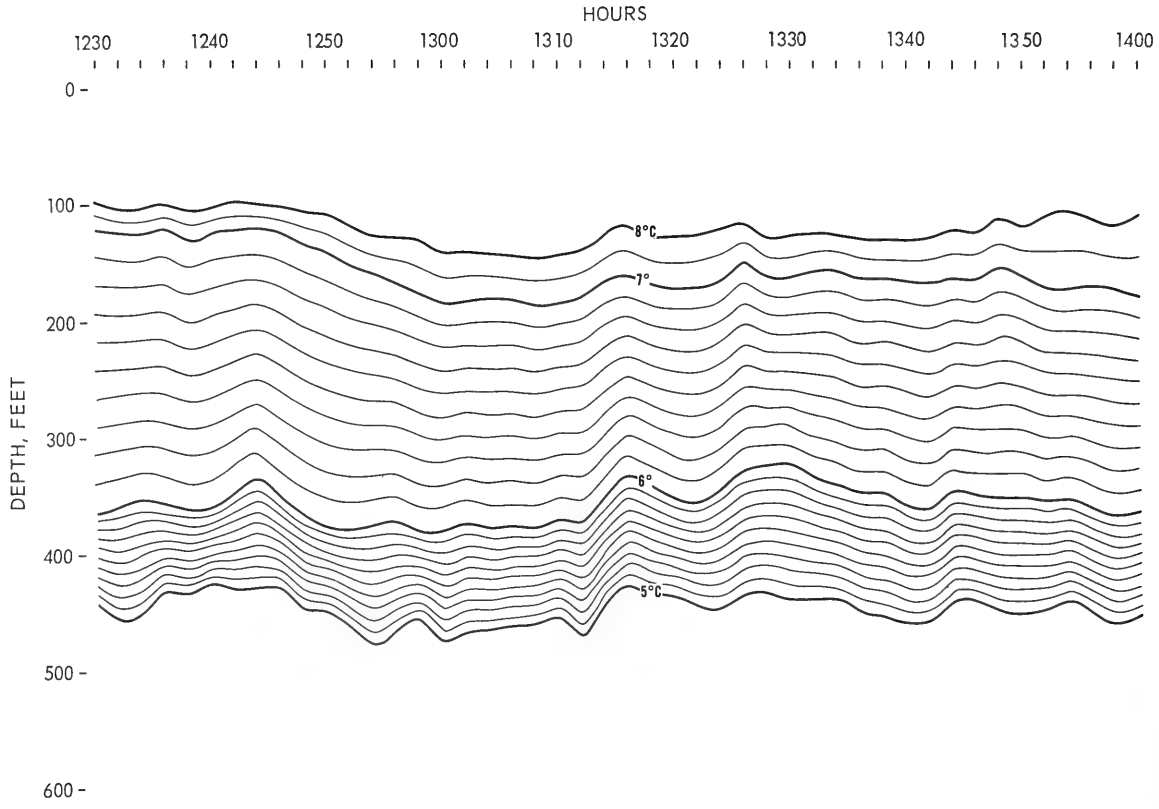

Sample Area 11

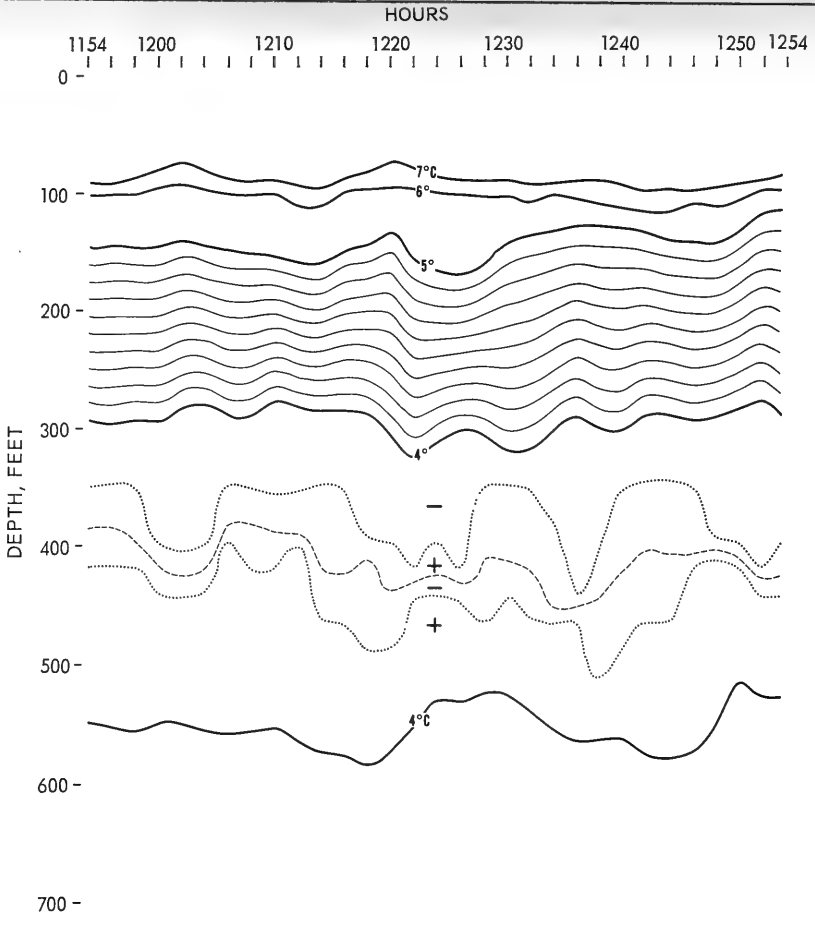

Sample Area 12

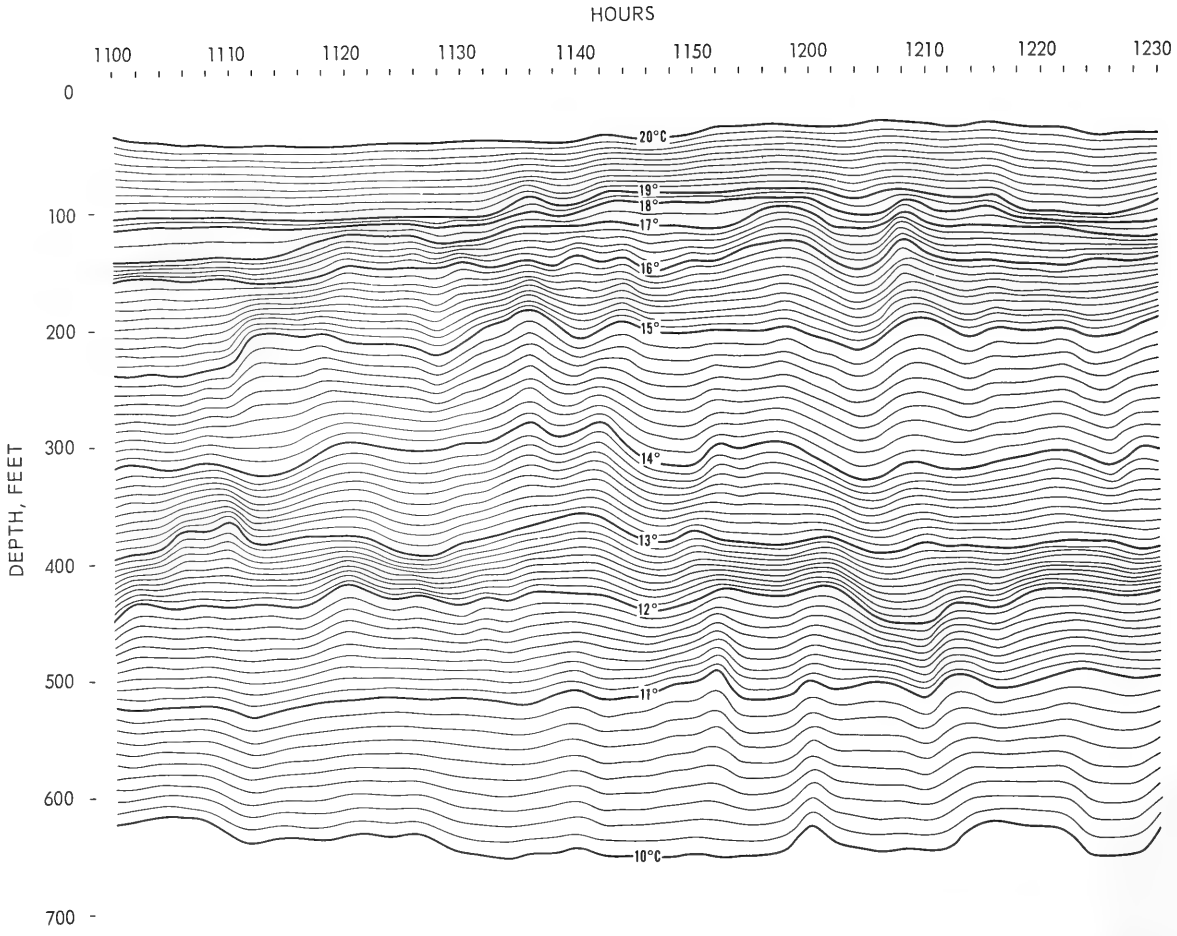

Sample Area 13

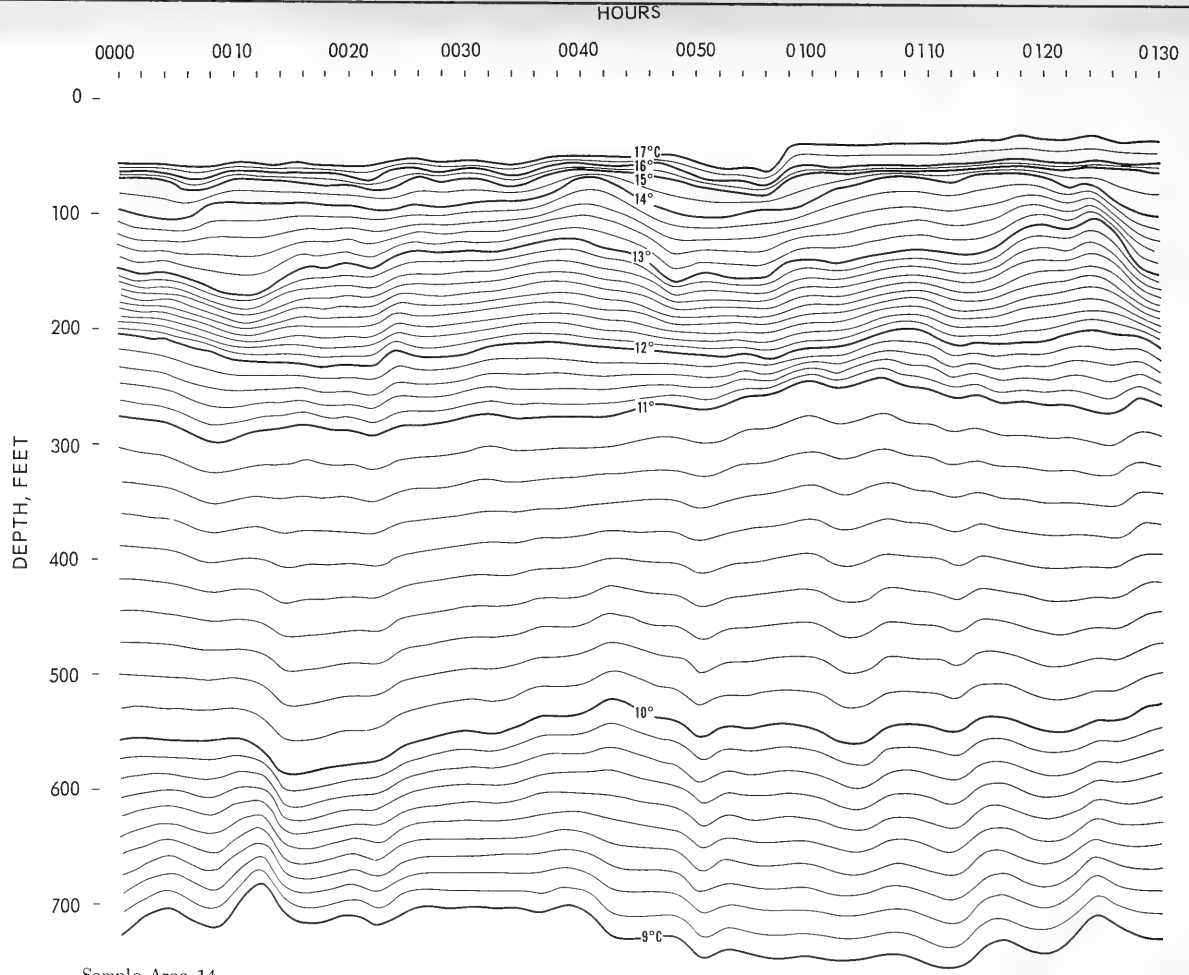

Sample Area 14

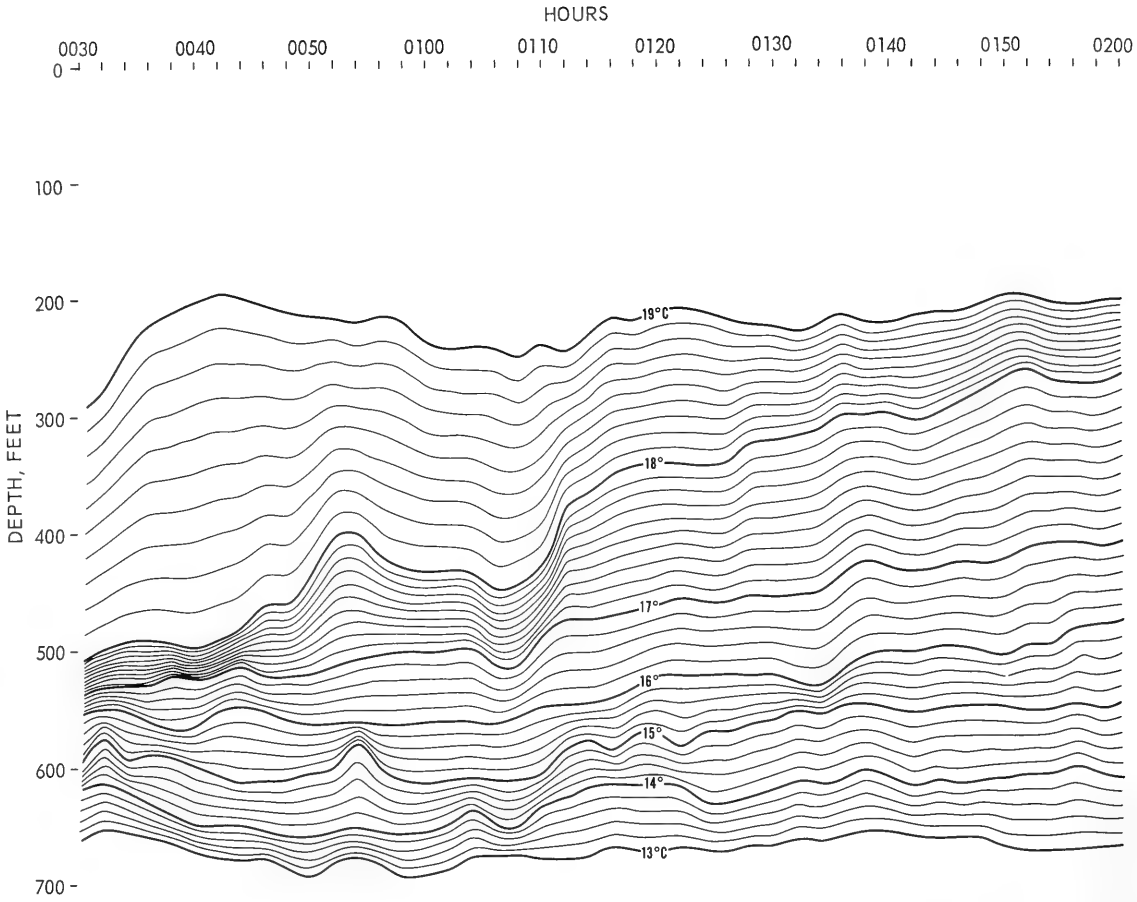

Sample Area 15

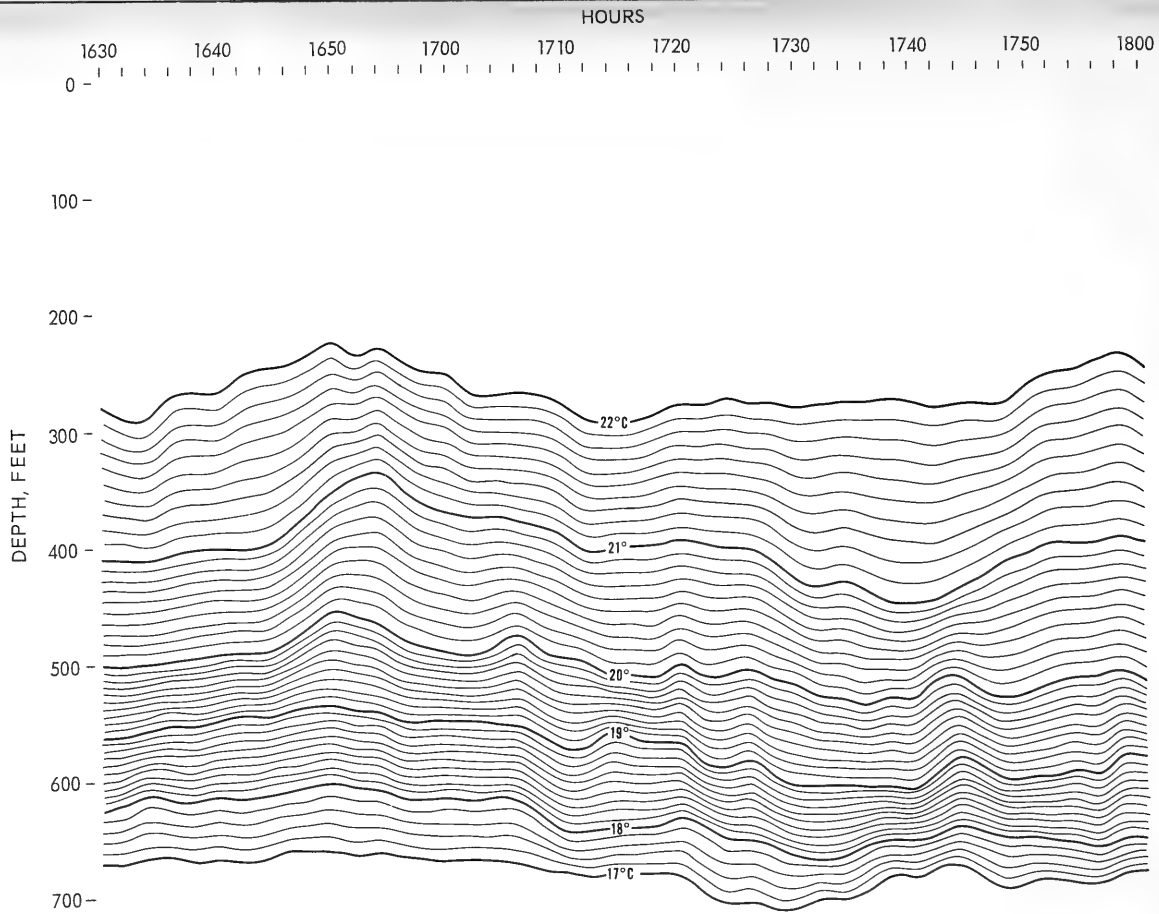

Sample Area 16

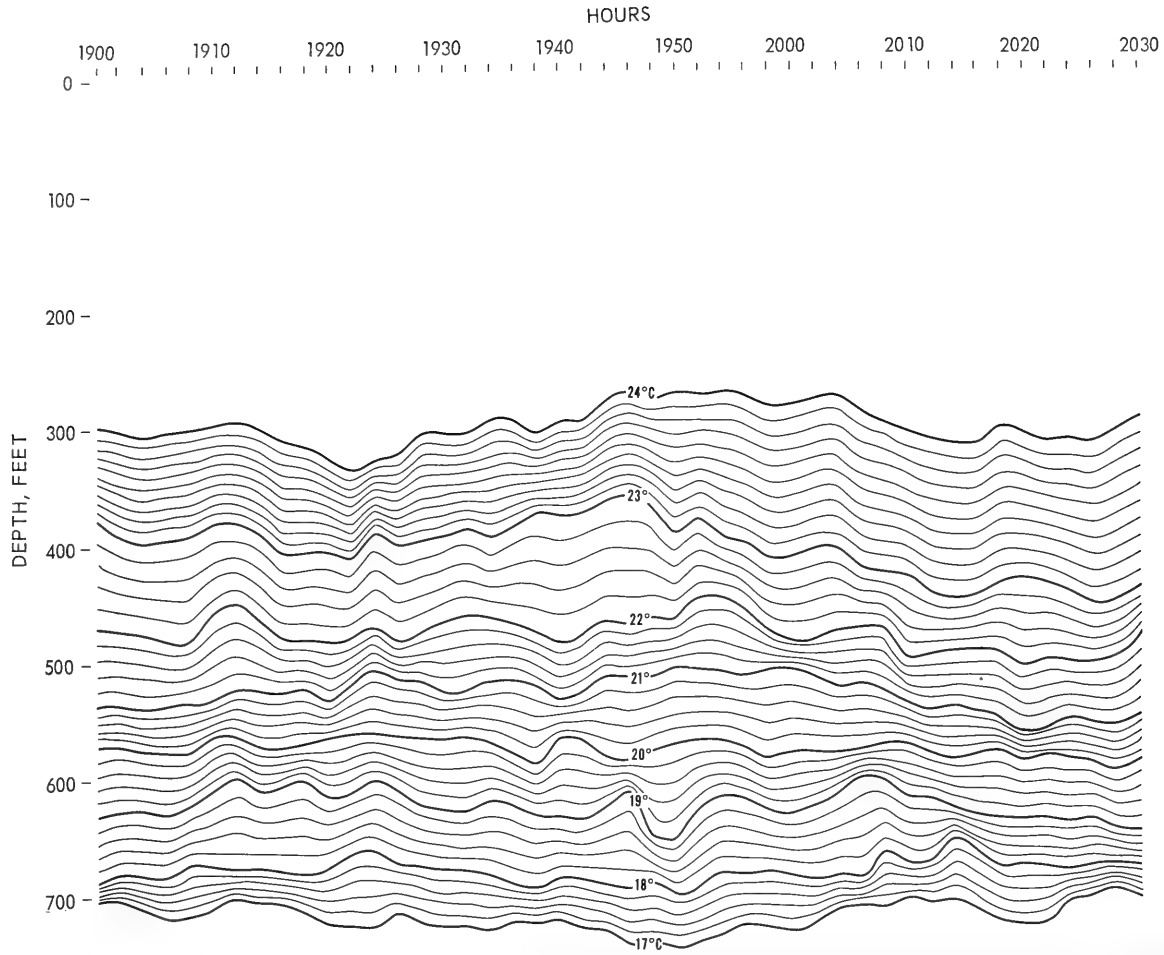

Sample Area 17

APPENDIX B: VERTICAL-TEMPERATURE-GRADIENT FIELDS

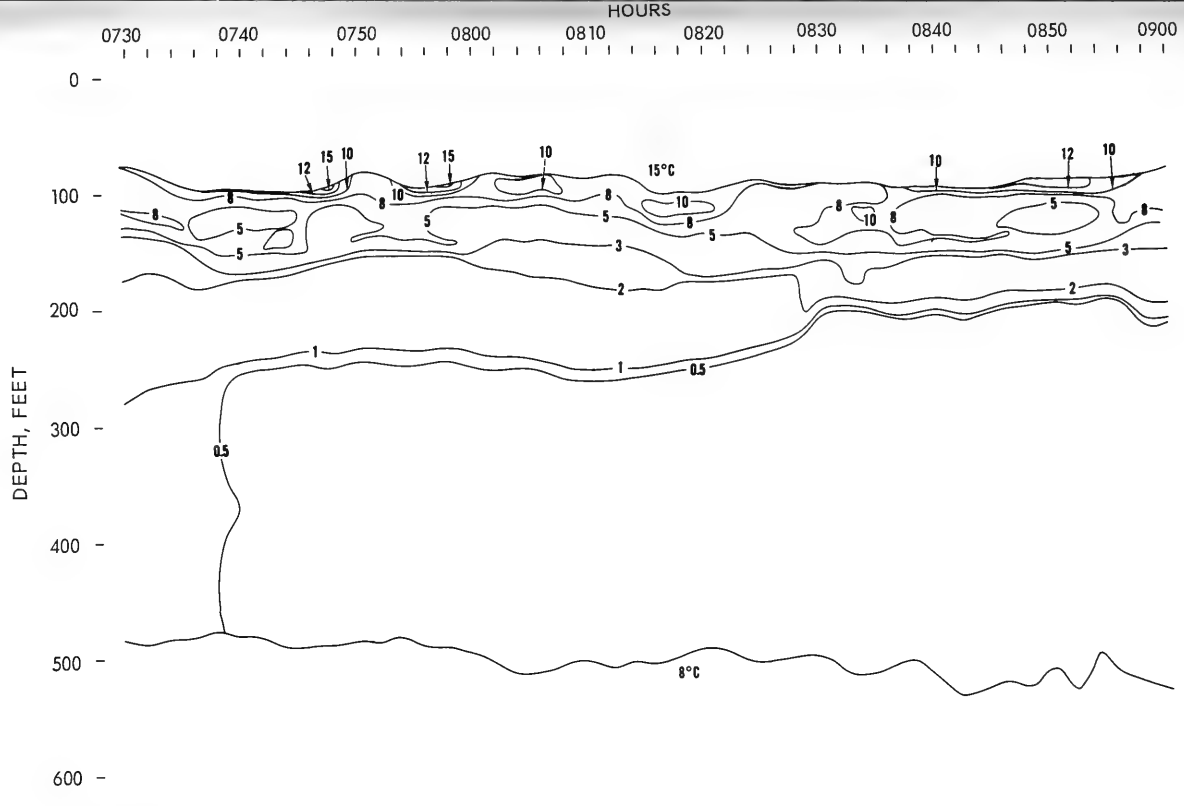

Sample Area 1

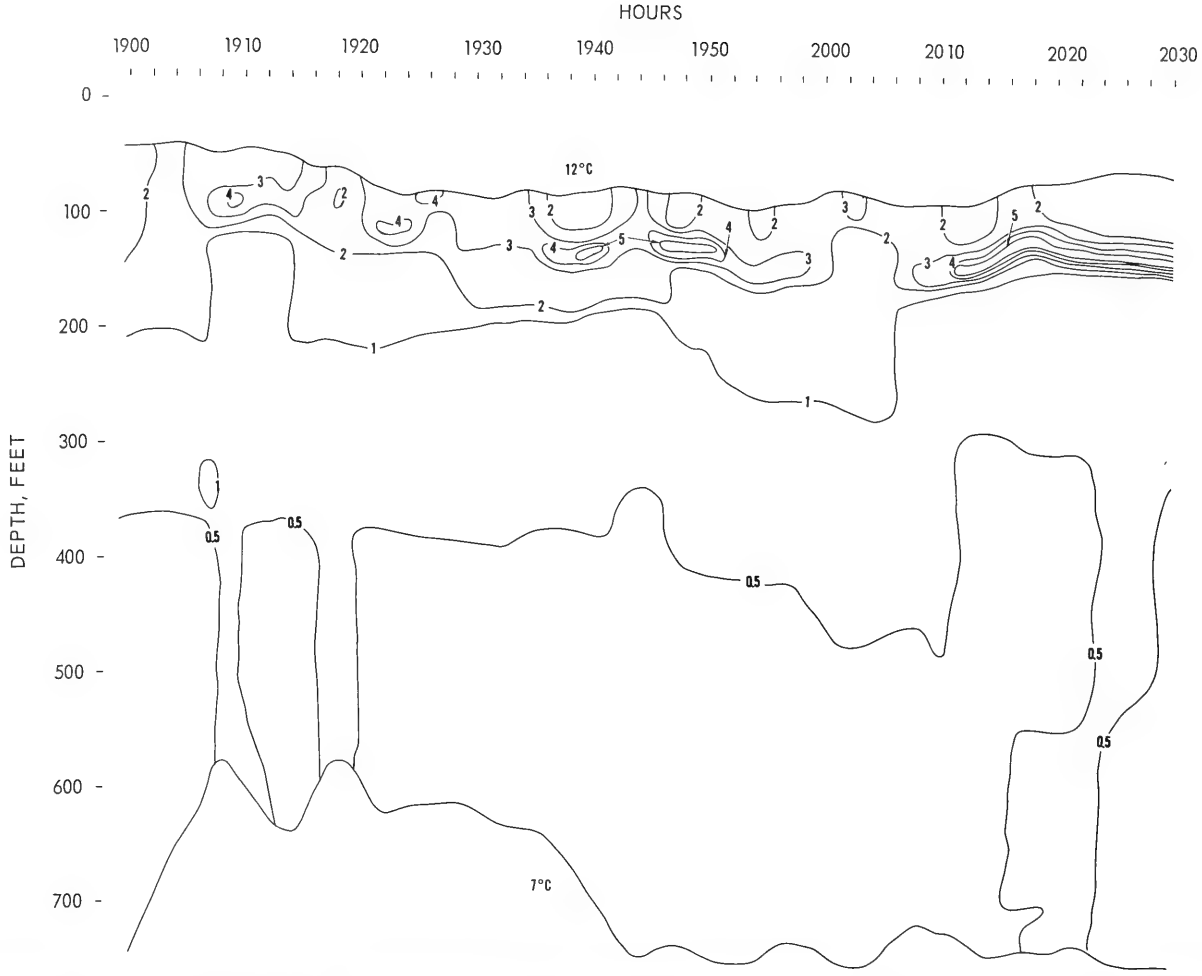

Sample Area 2

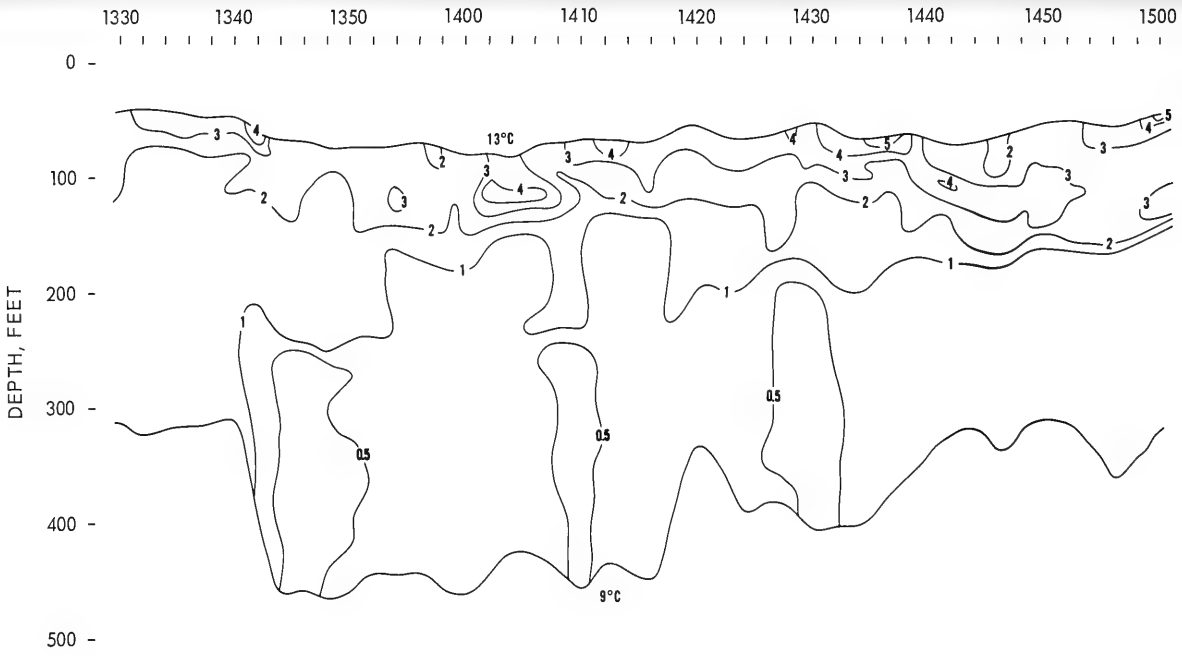

Sample Area 3

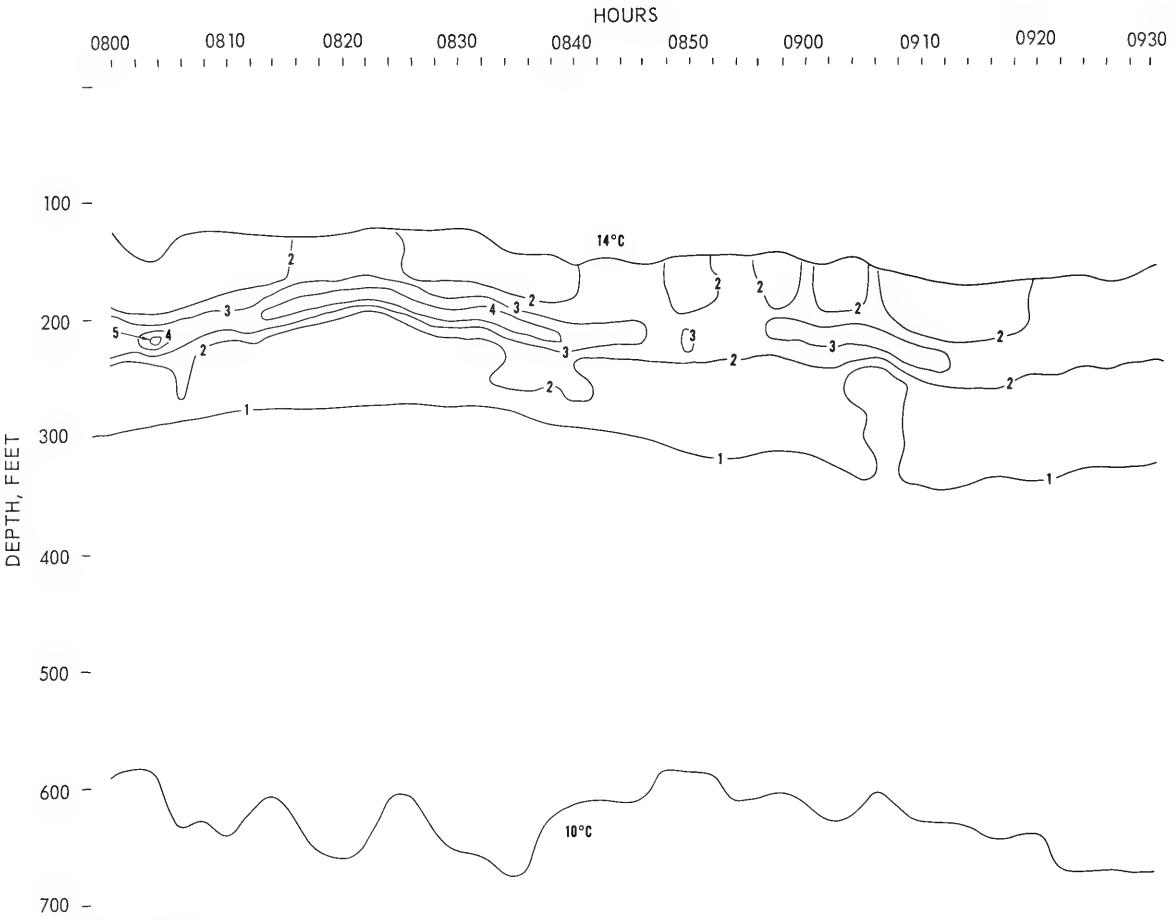

Sample Area 4

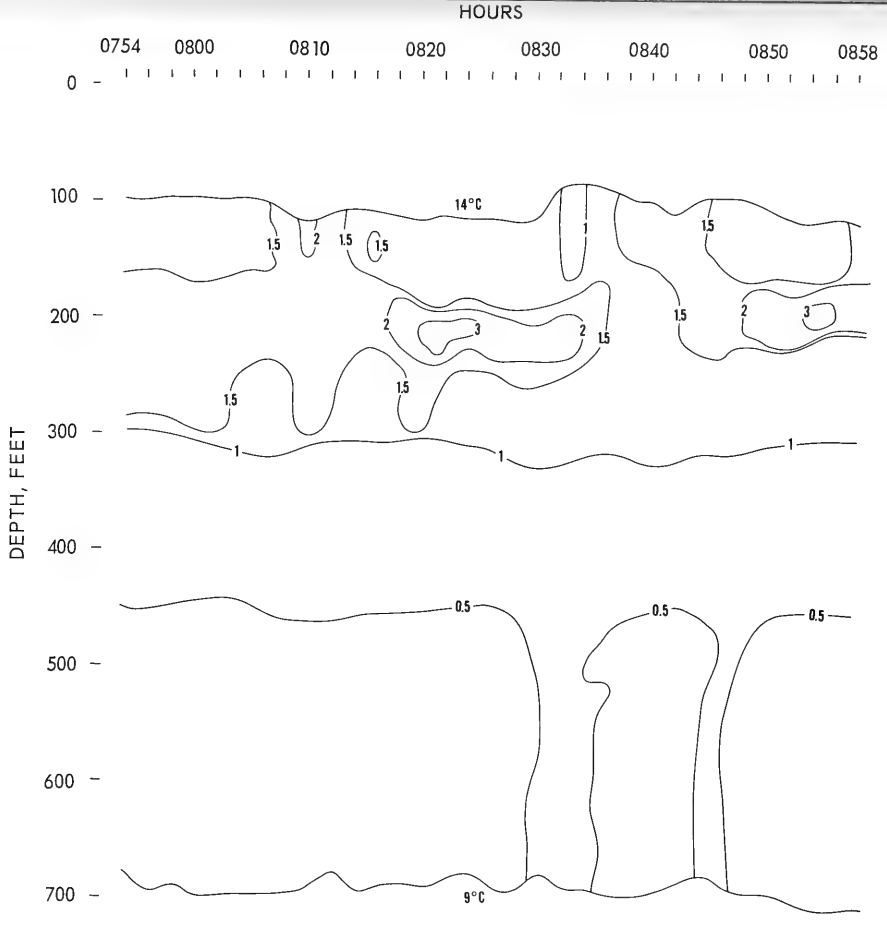

Sample Area 5

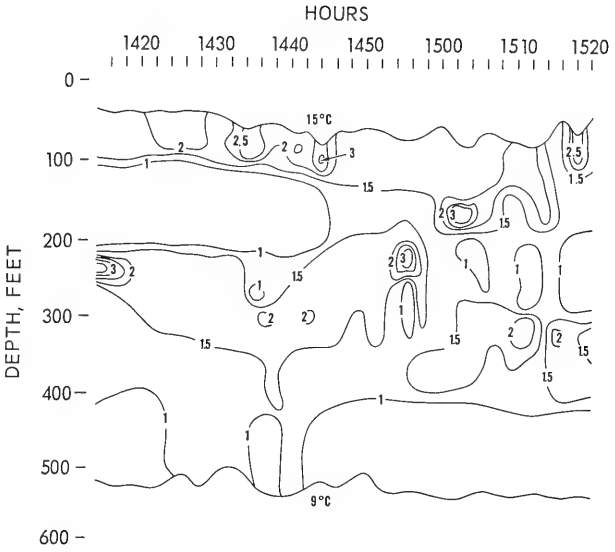

Sample Area 6

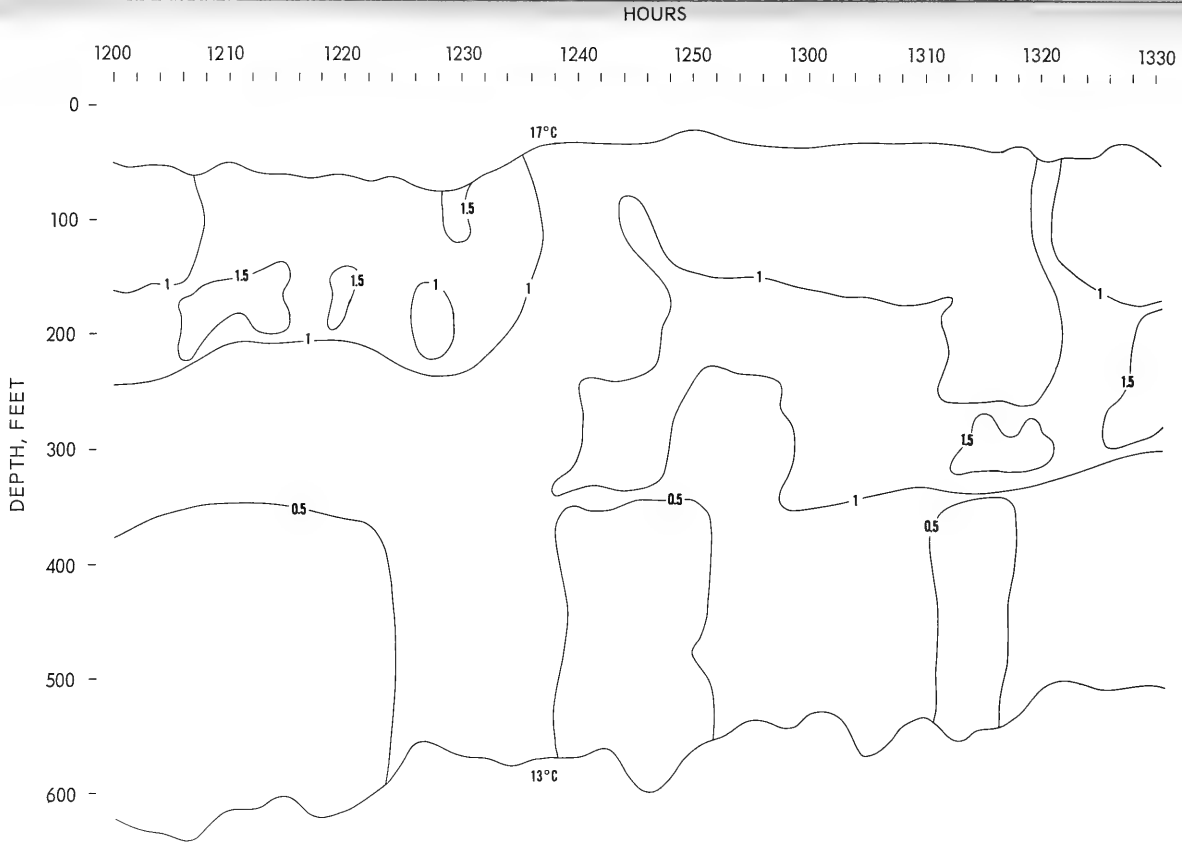

Sample Area 7

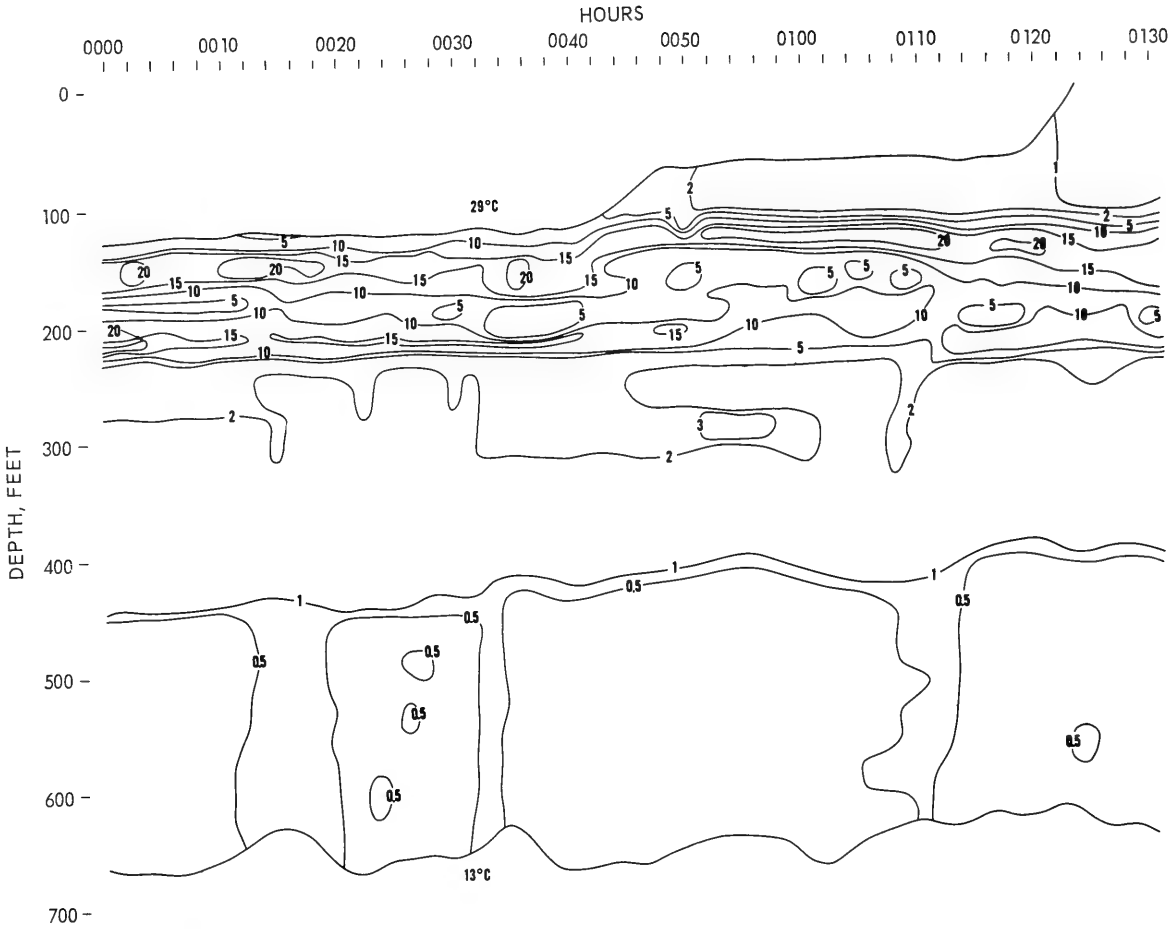

Sample Area 9

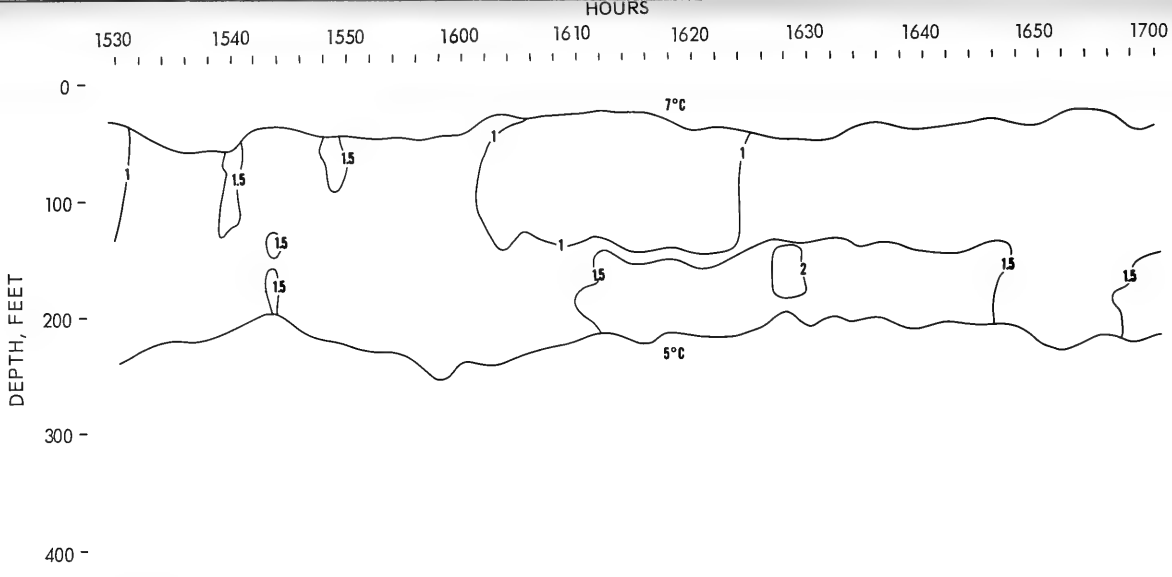

Sample Area 10

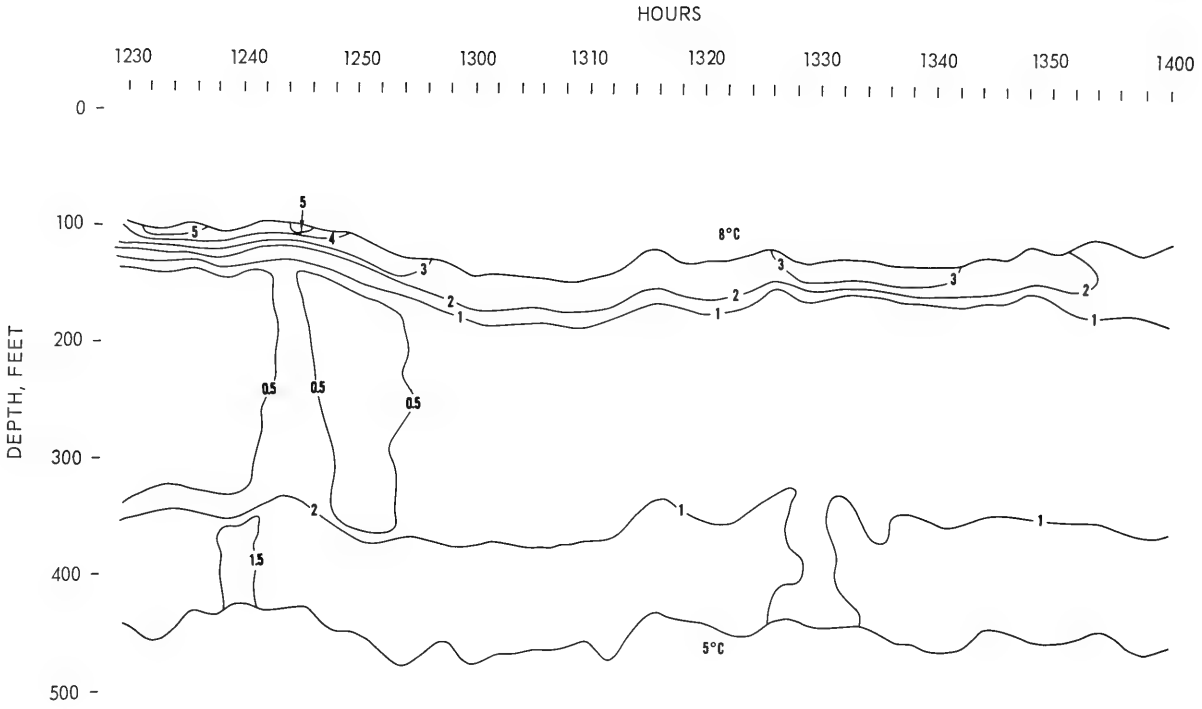

Sample Area 11

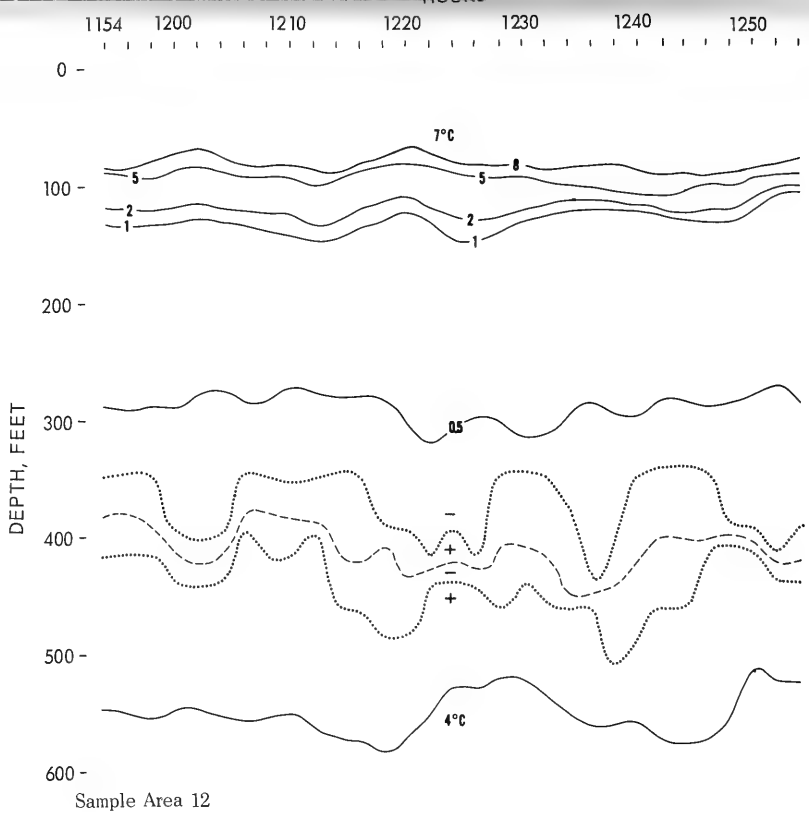

Sample Area 12

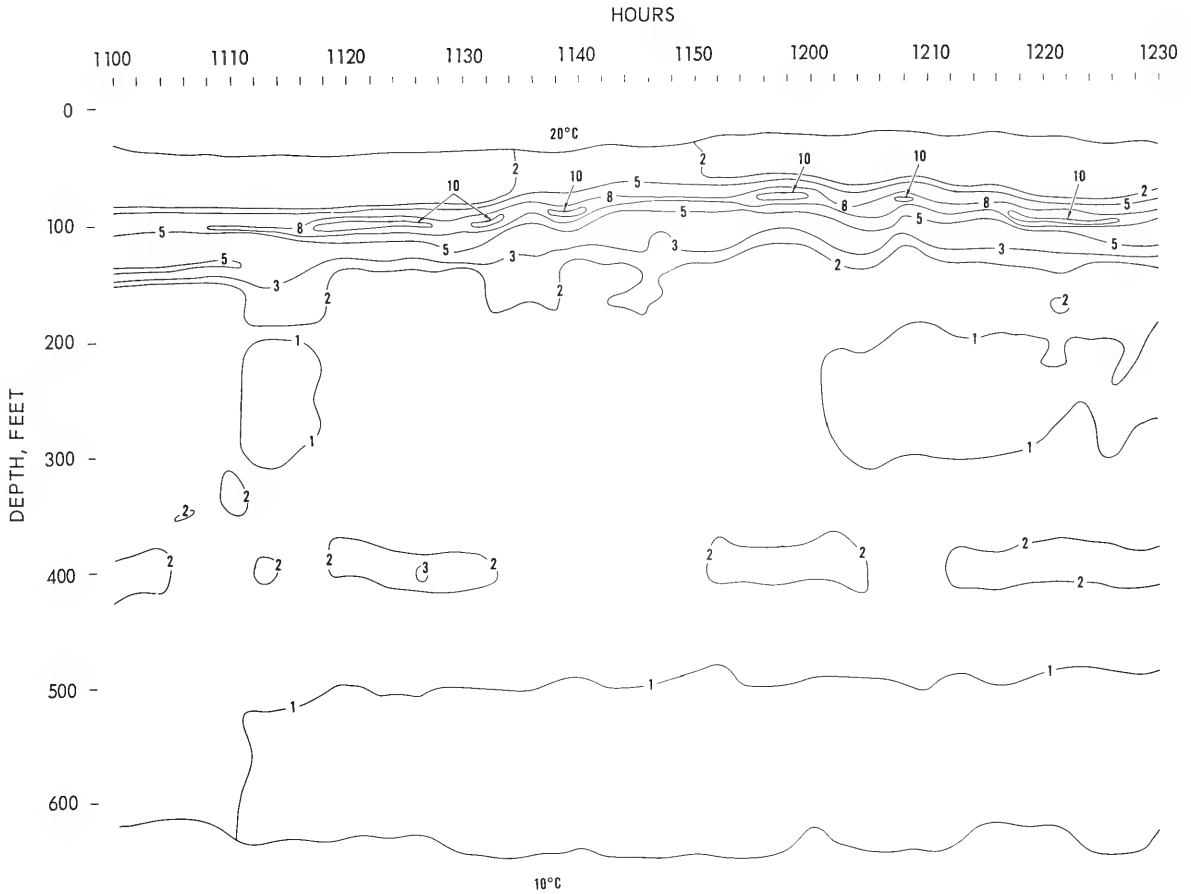

Sample Area 13

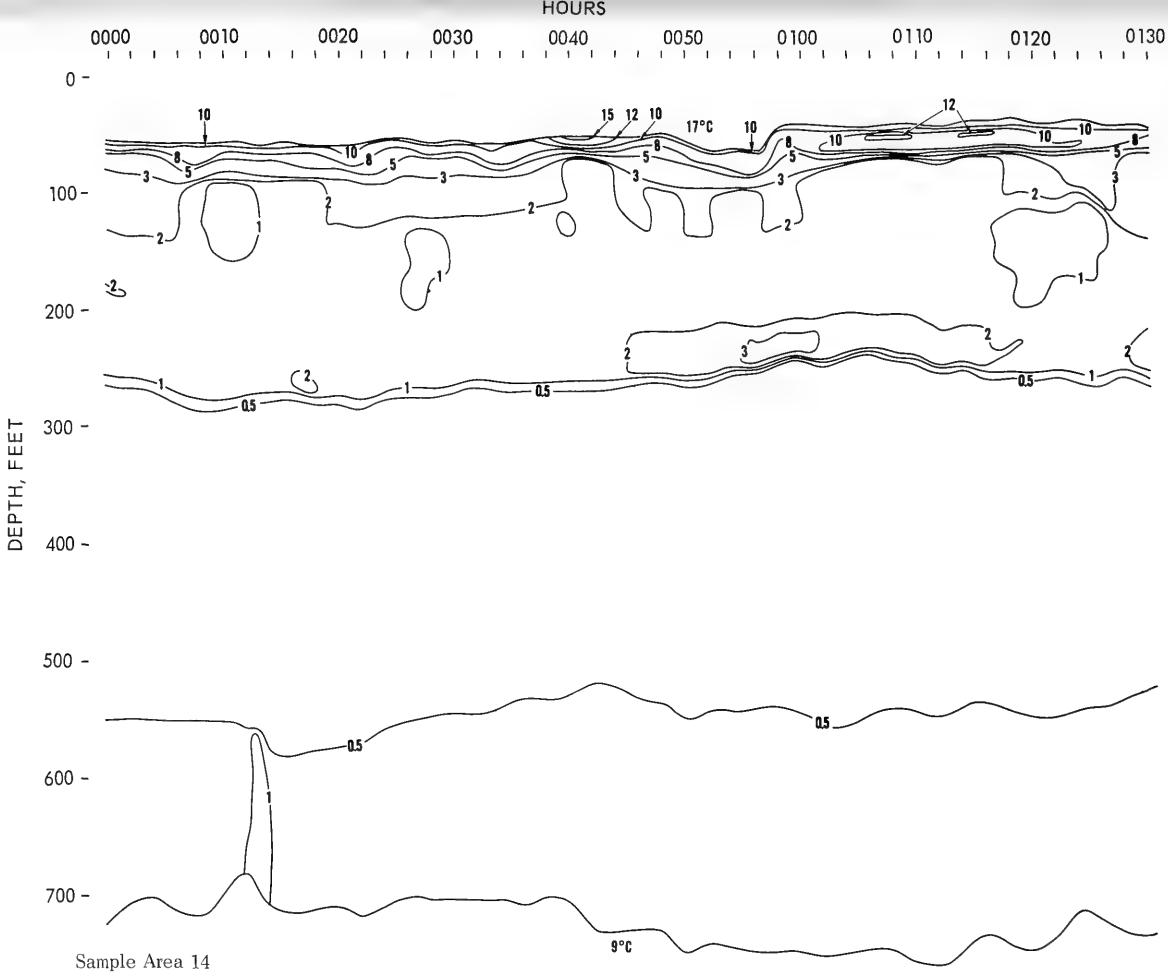

Sample Area 14

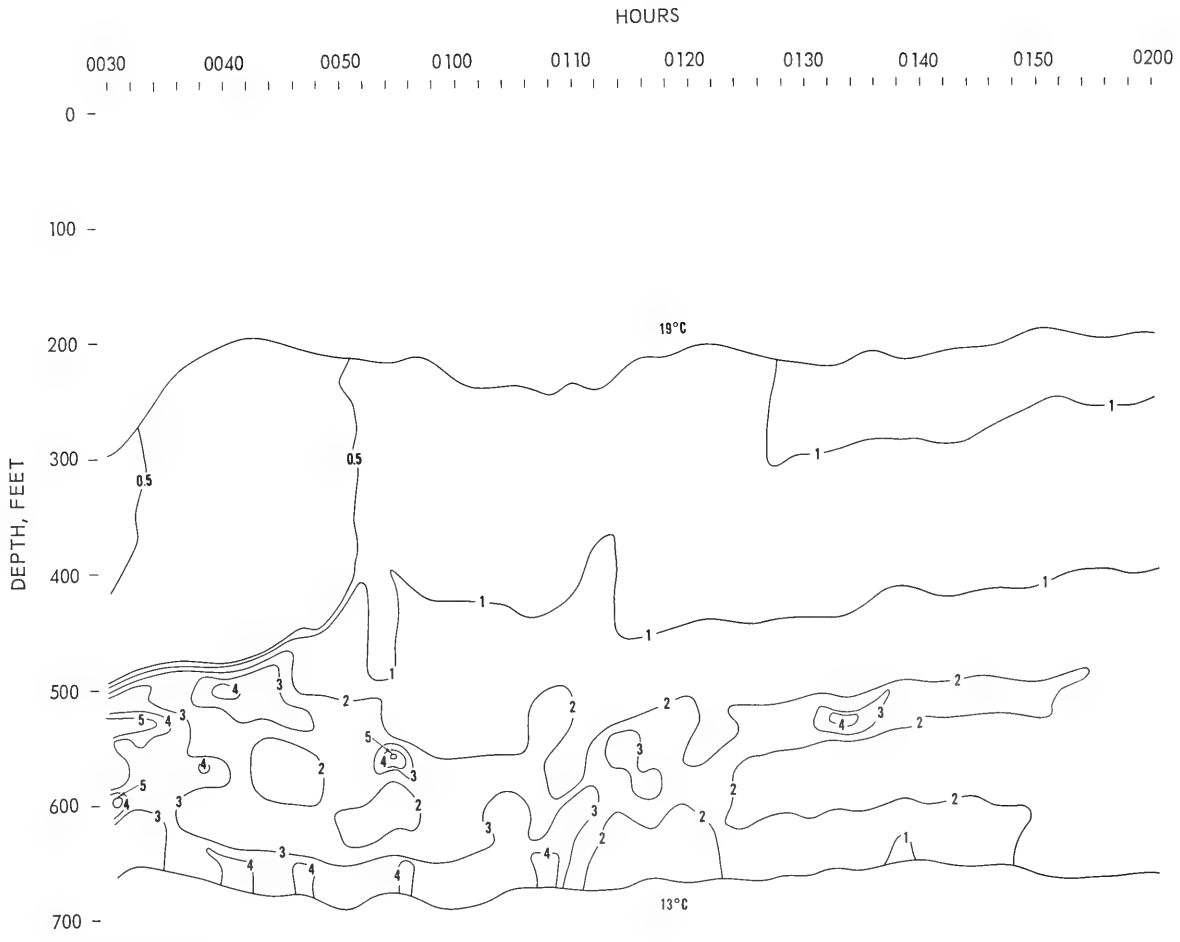

Sample Area 15

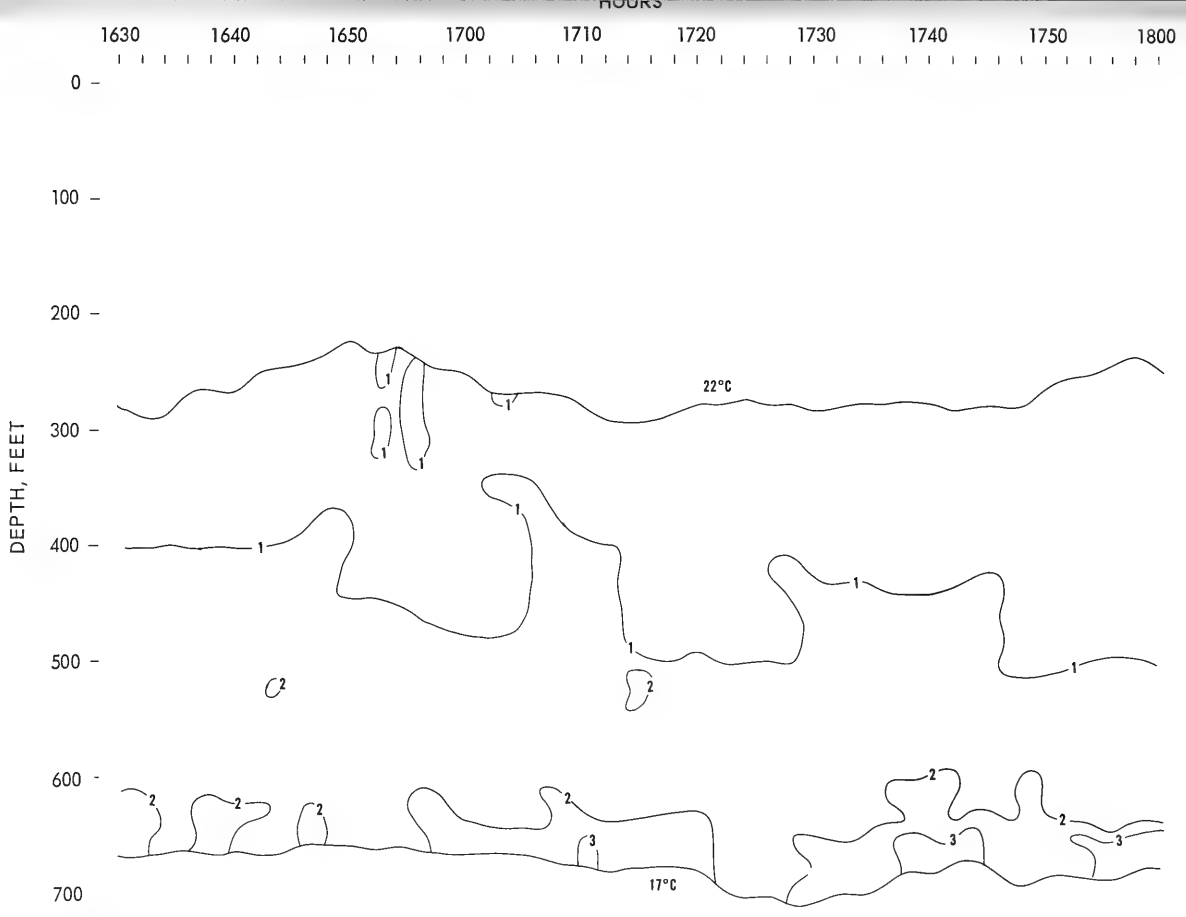

Sample Area 16

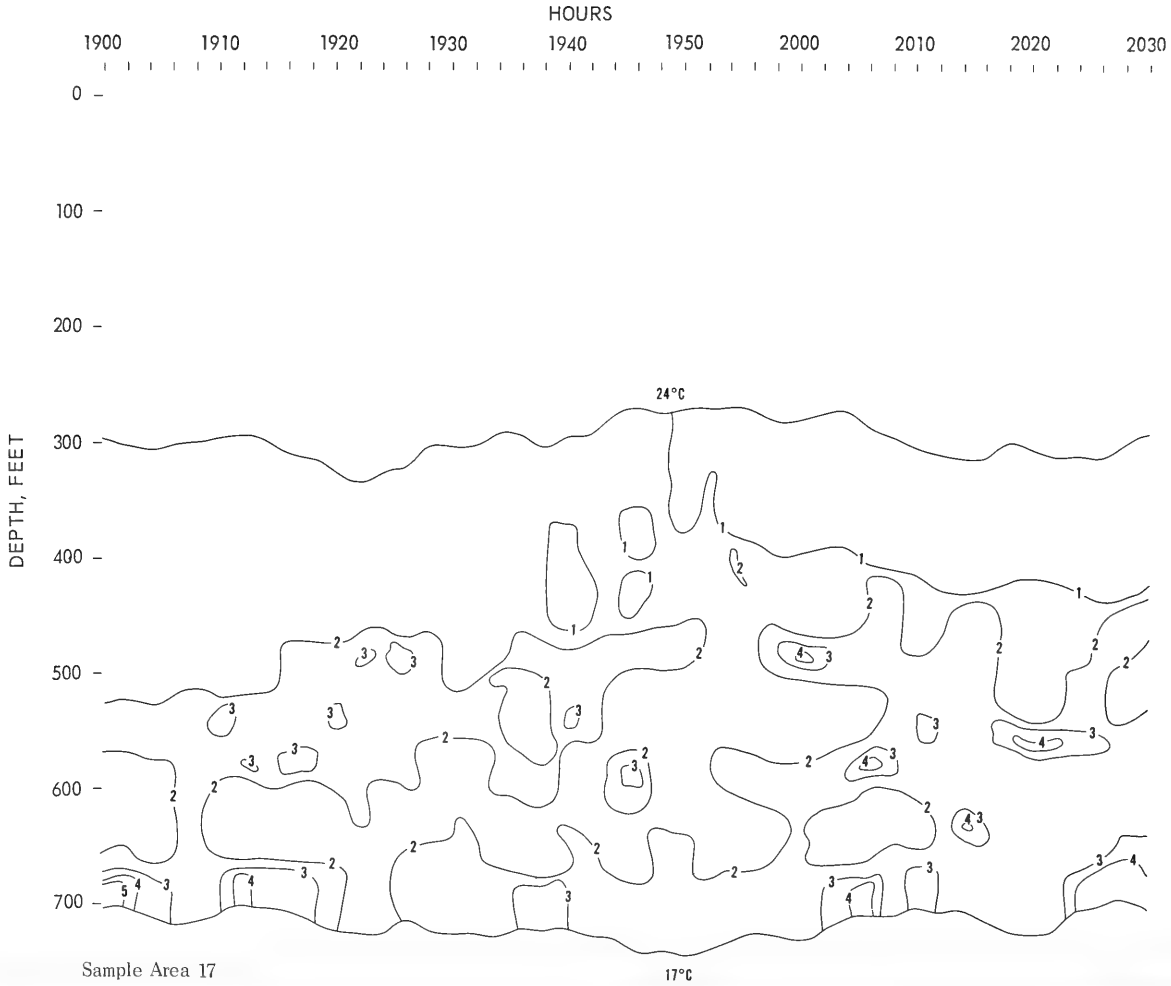

Sample Area 17

APPENDIX C: HORIZONTAL - TEMPERATURE - GRADIENT FIELDS

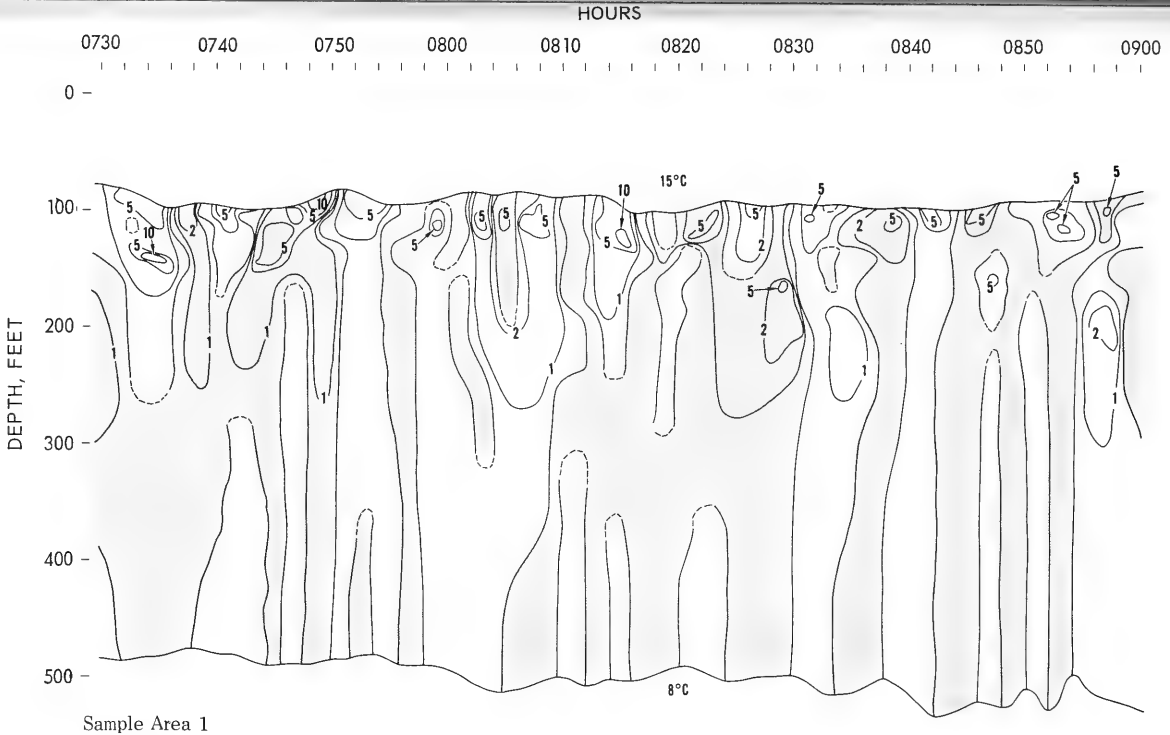

Sample Area 1

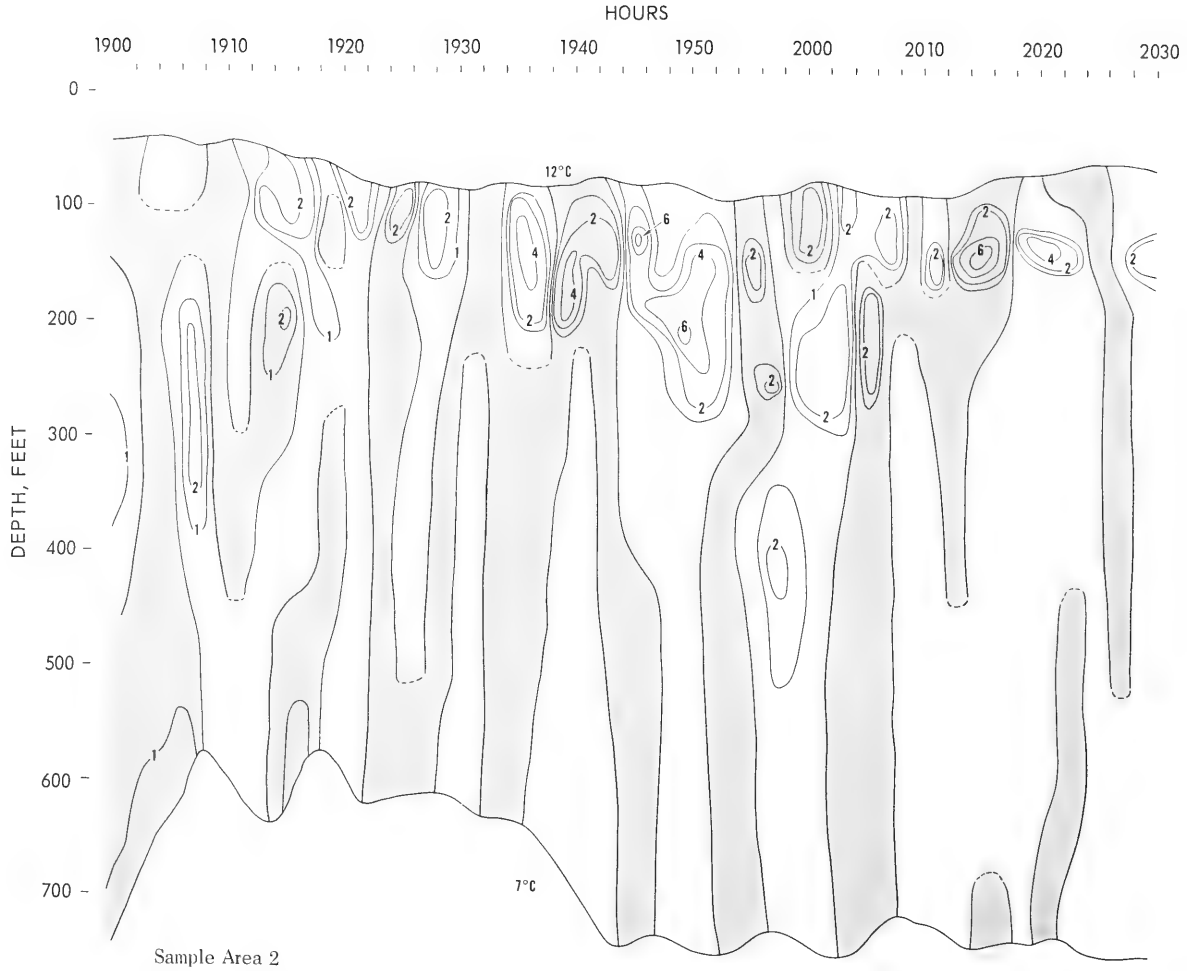

Sample Area 2

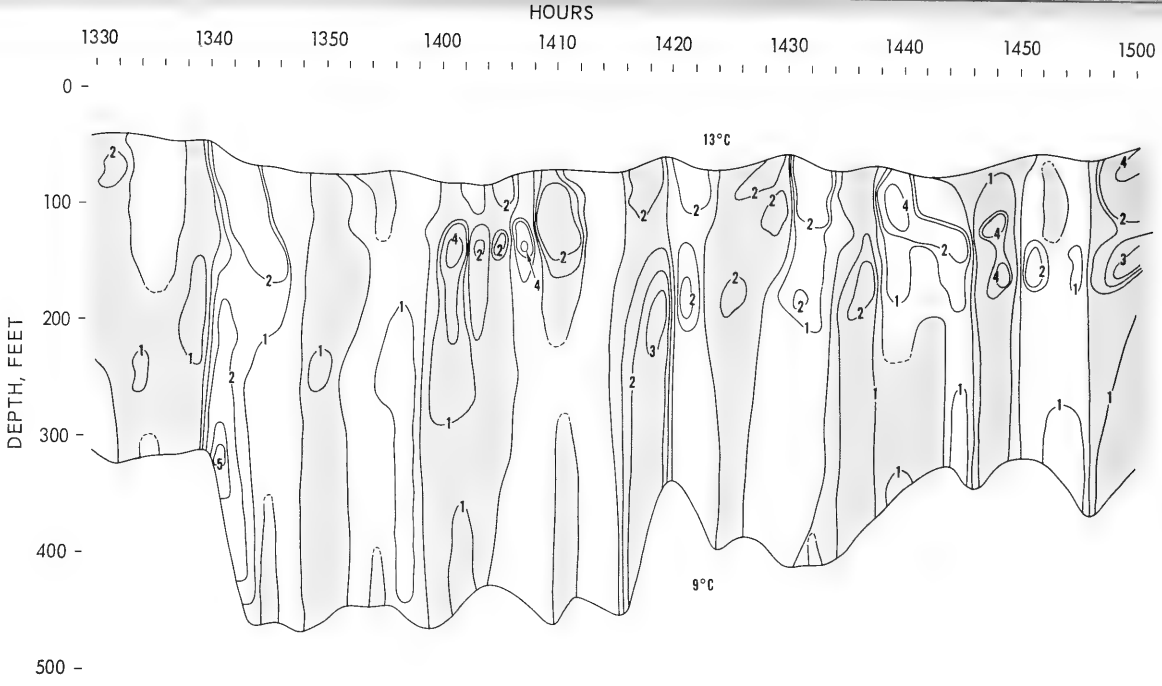

Sample Area 3

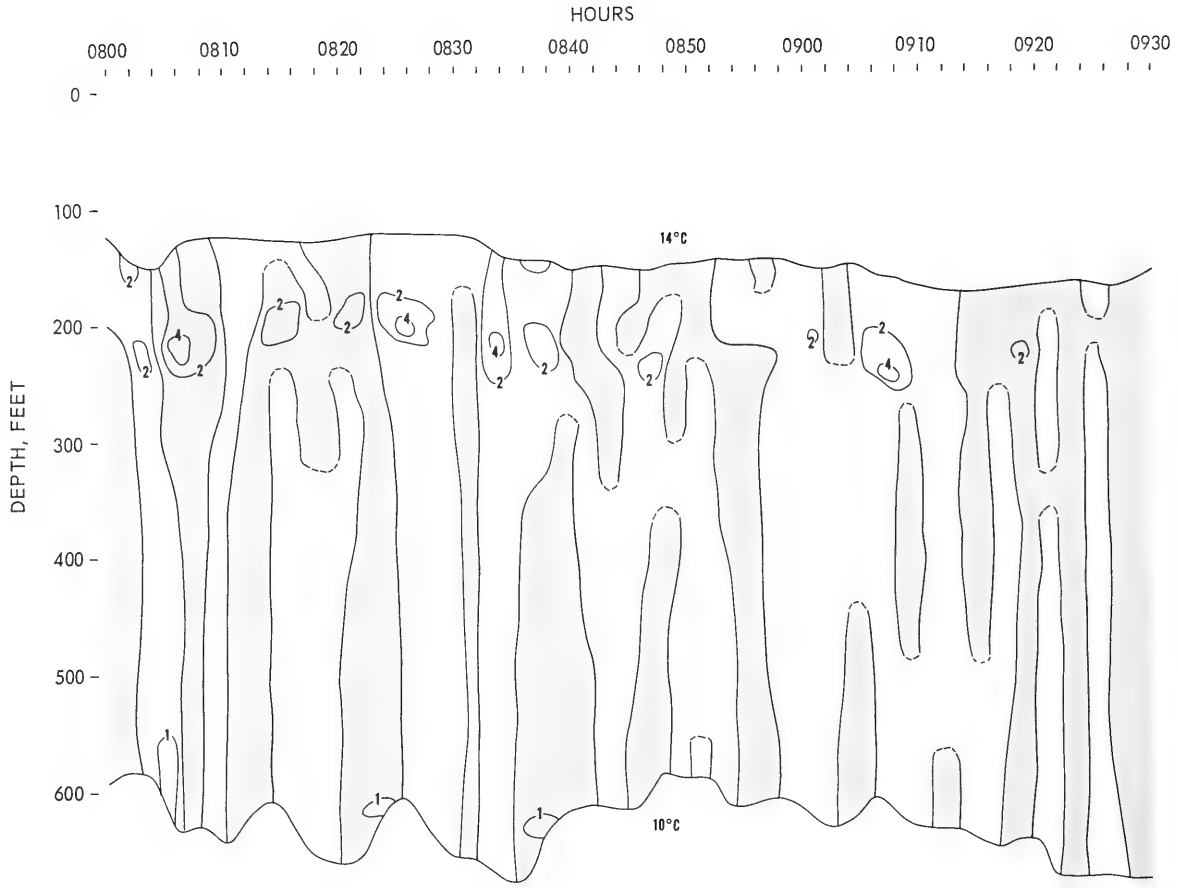

Sample Area 4

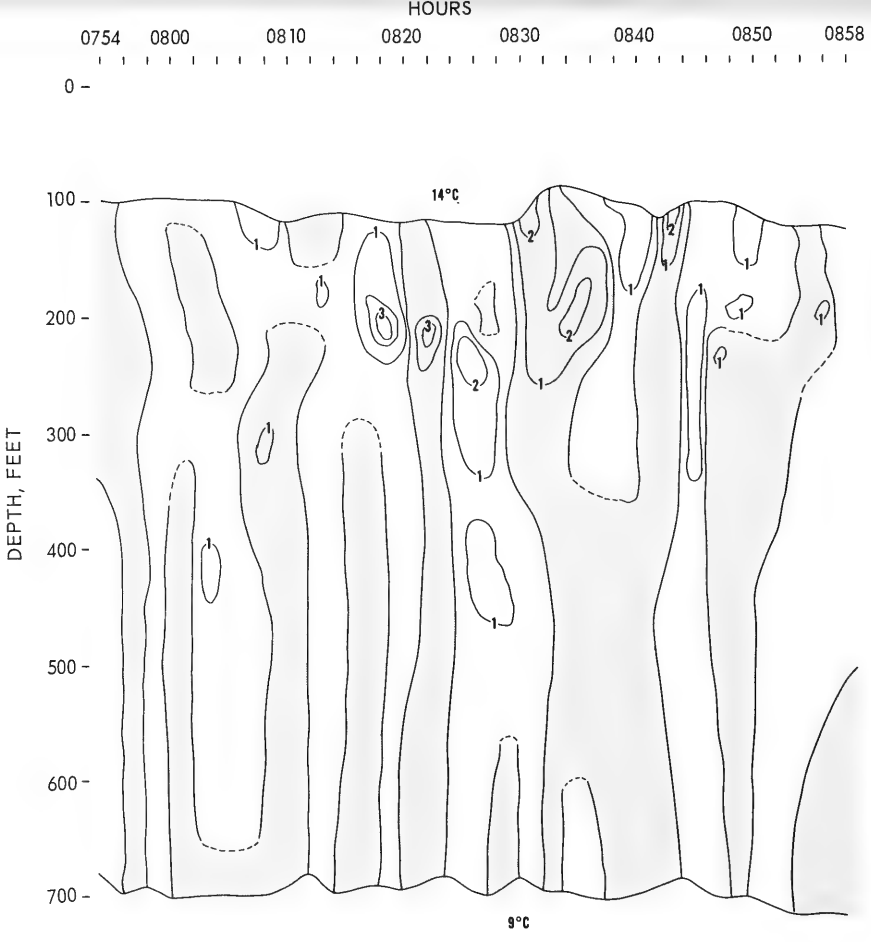

Sample Area 5

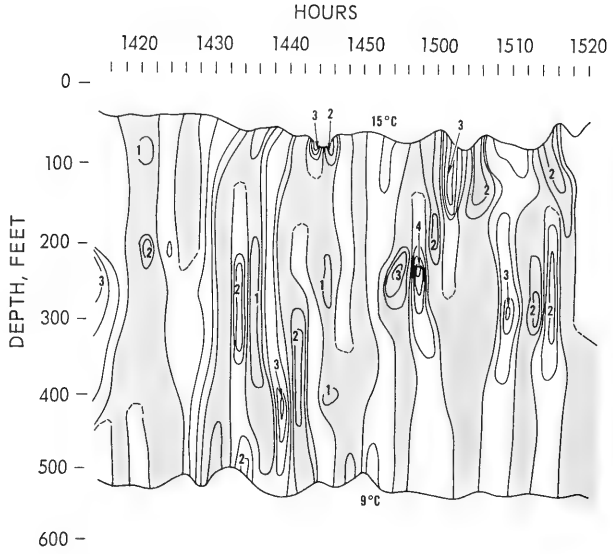

Sample Area 6

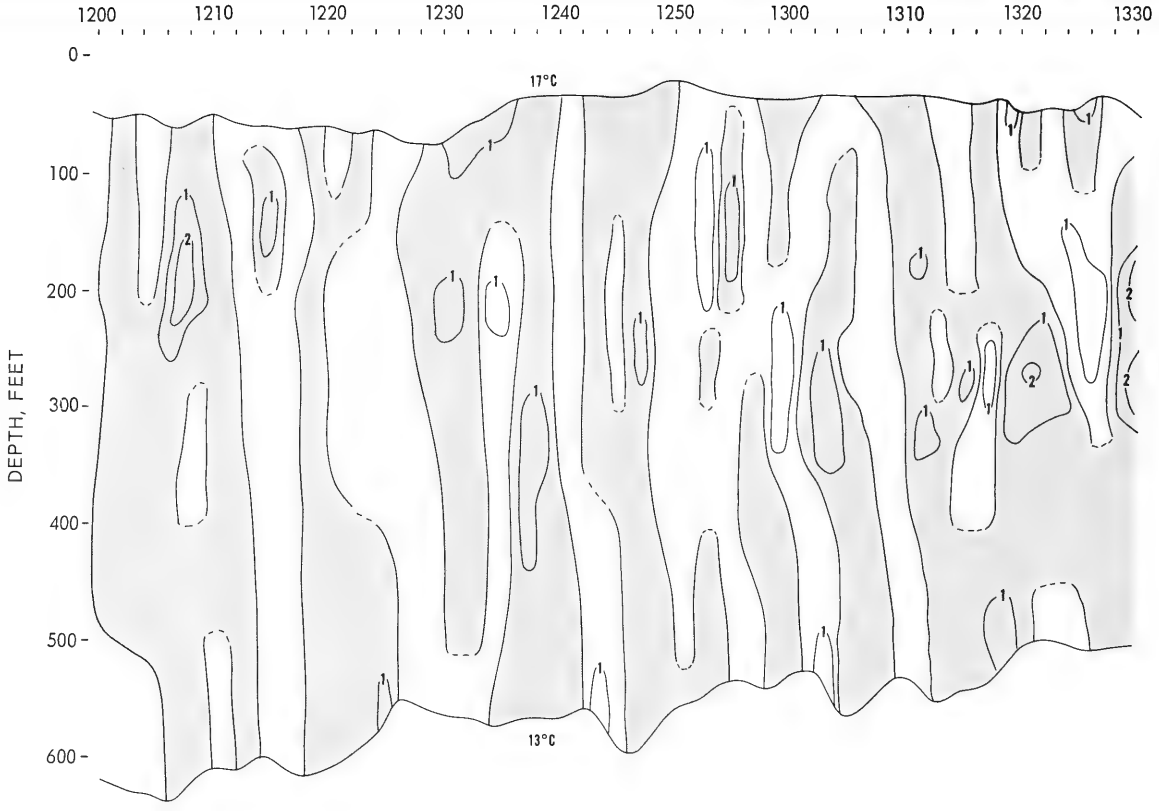

Sample Area 7

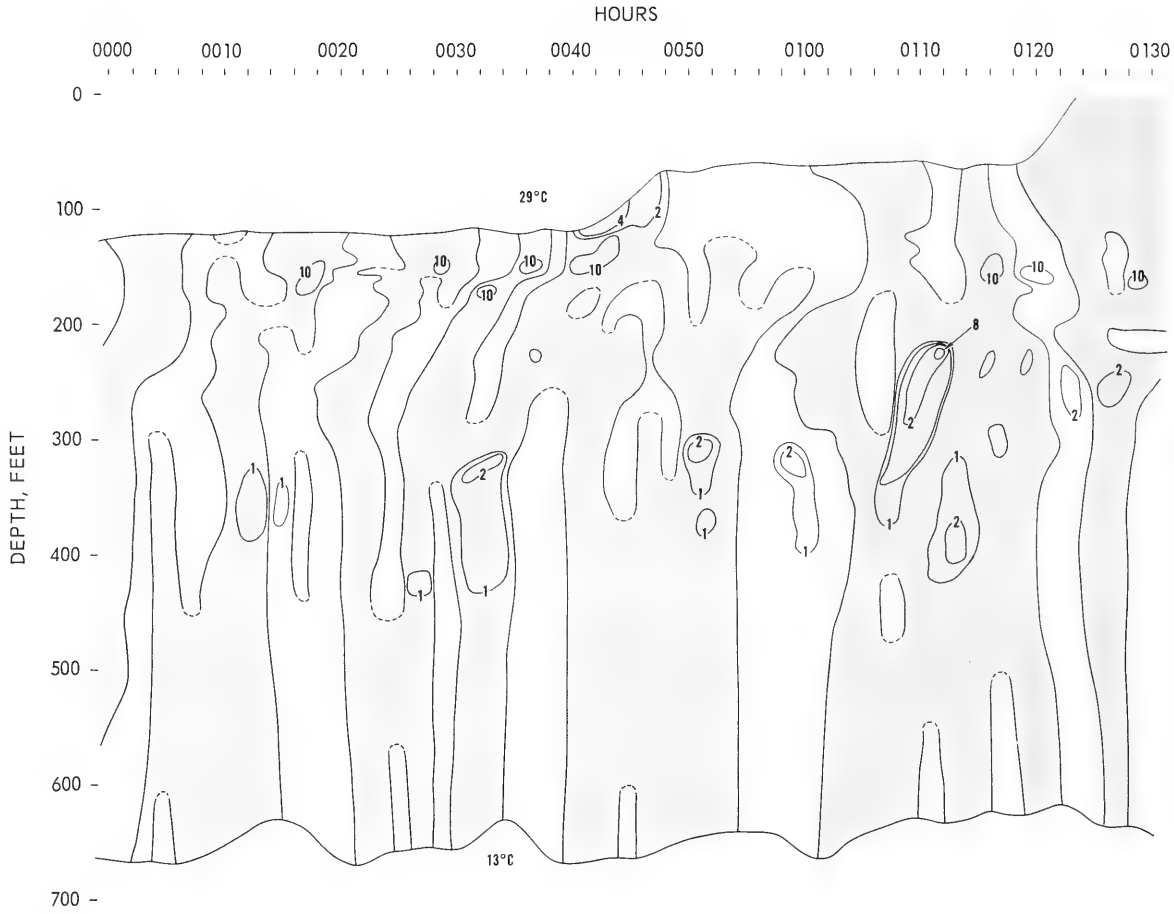

Sample Area 9

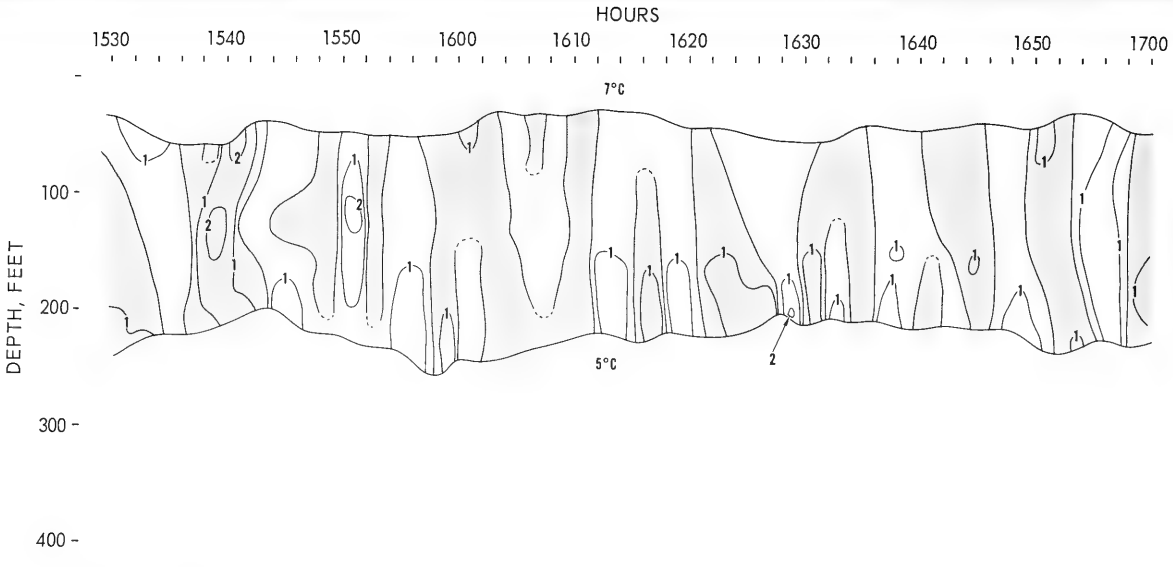

Sample Area 10

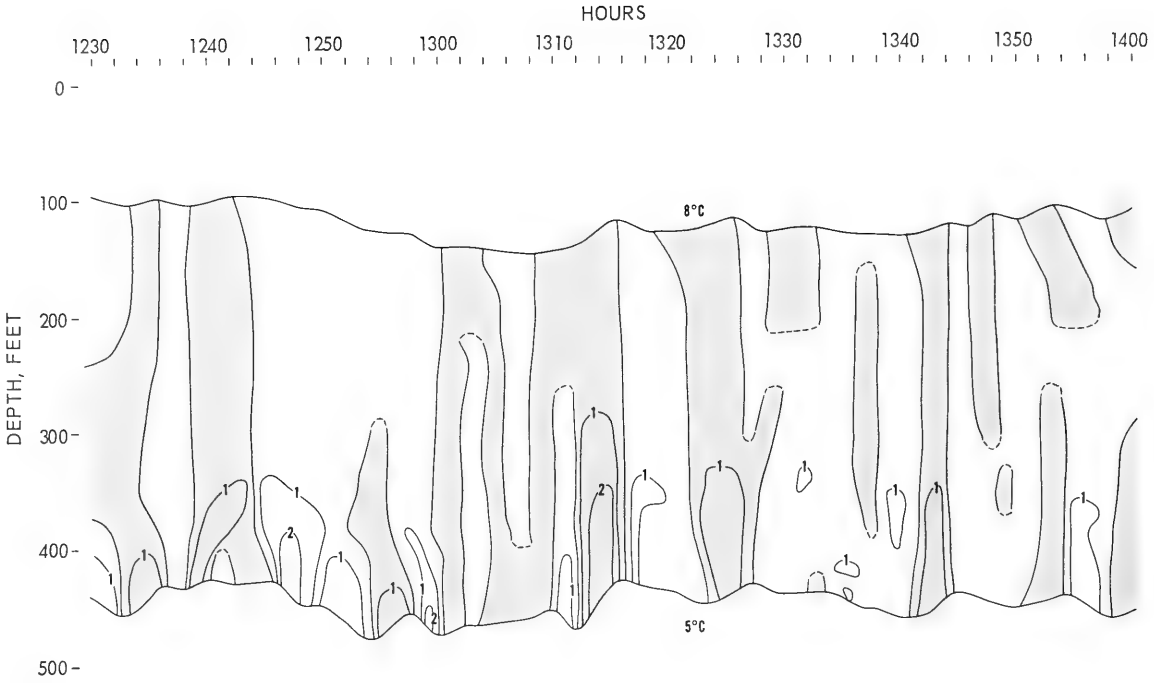

Sample Area 11

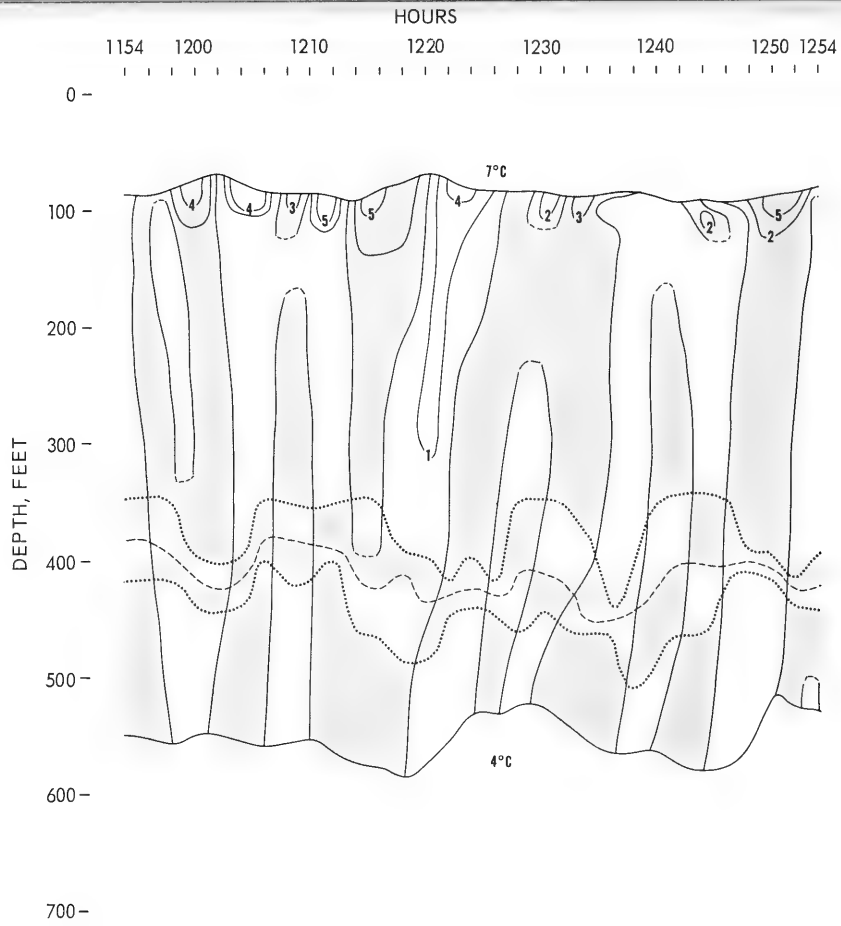

Sample Area 12

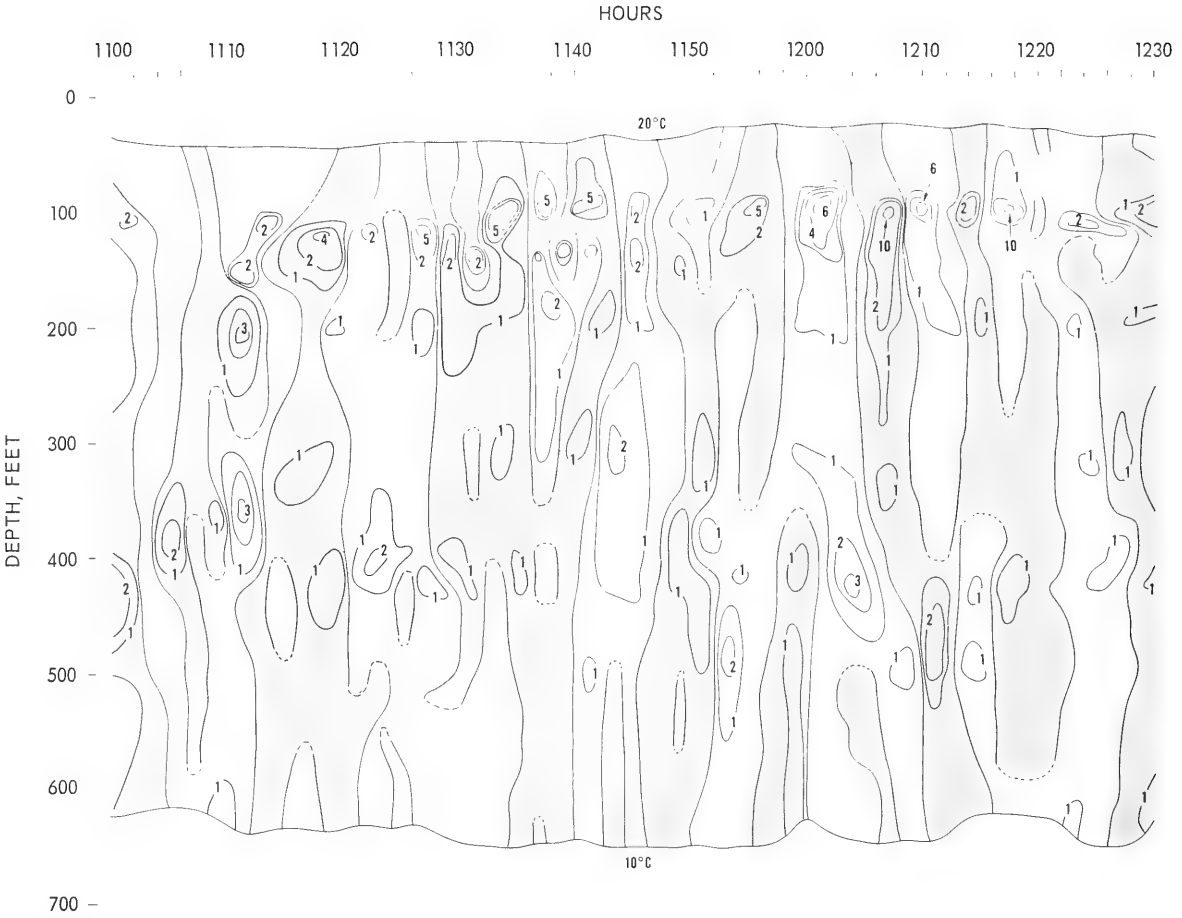

Sample Area 13

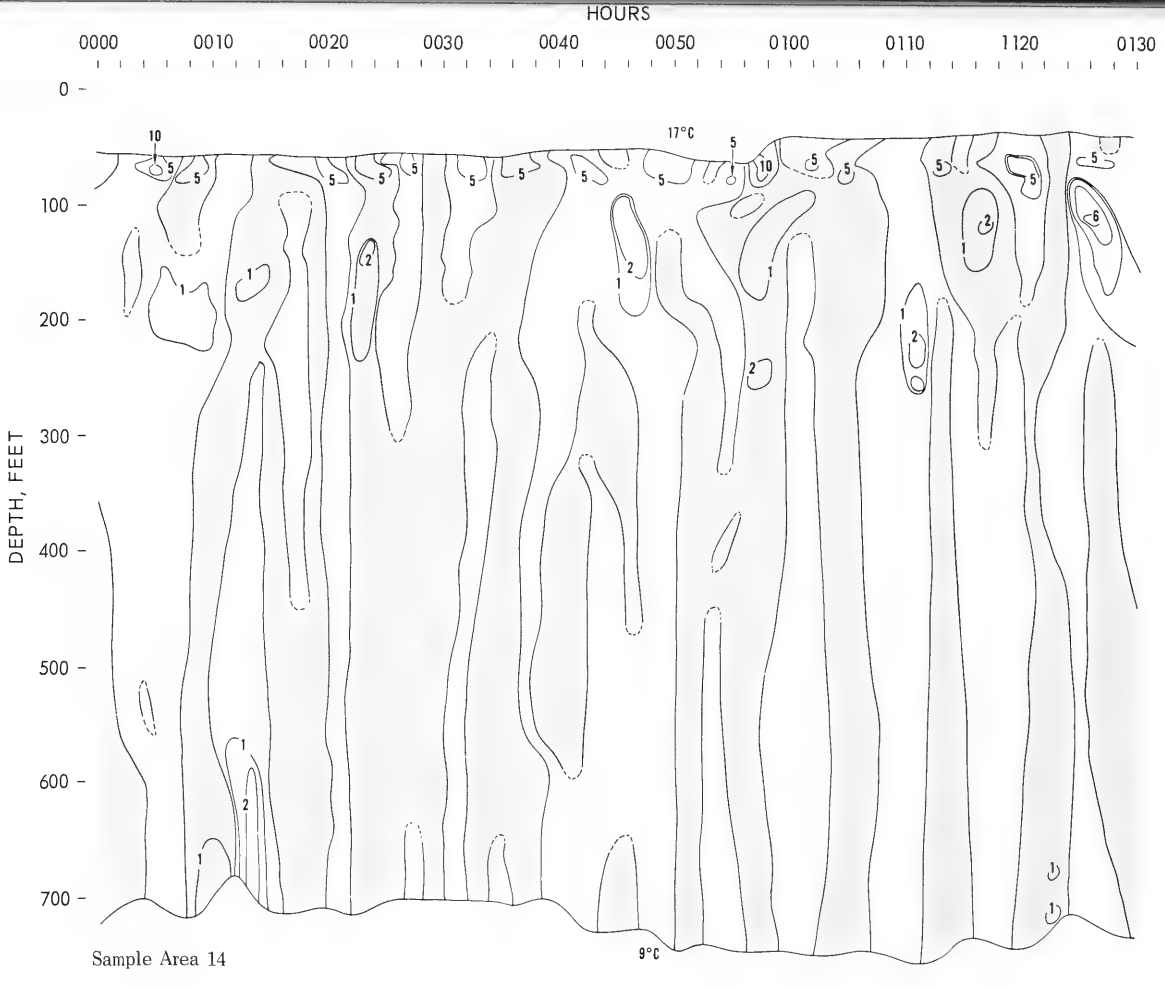
HOURS
0000
0010
0020
0030
0040
0050
0100
0110
1120
0130
0
100
200
300
400
500
600
700
DEPTH, FEET
17°C
9°C
Sample Area 14

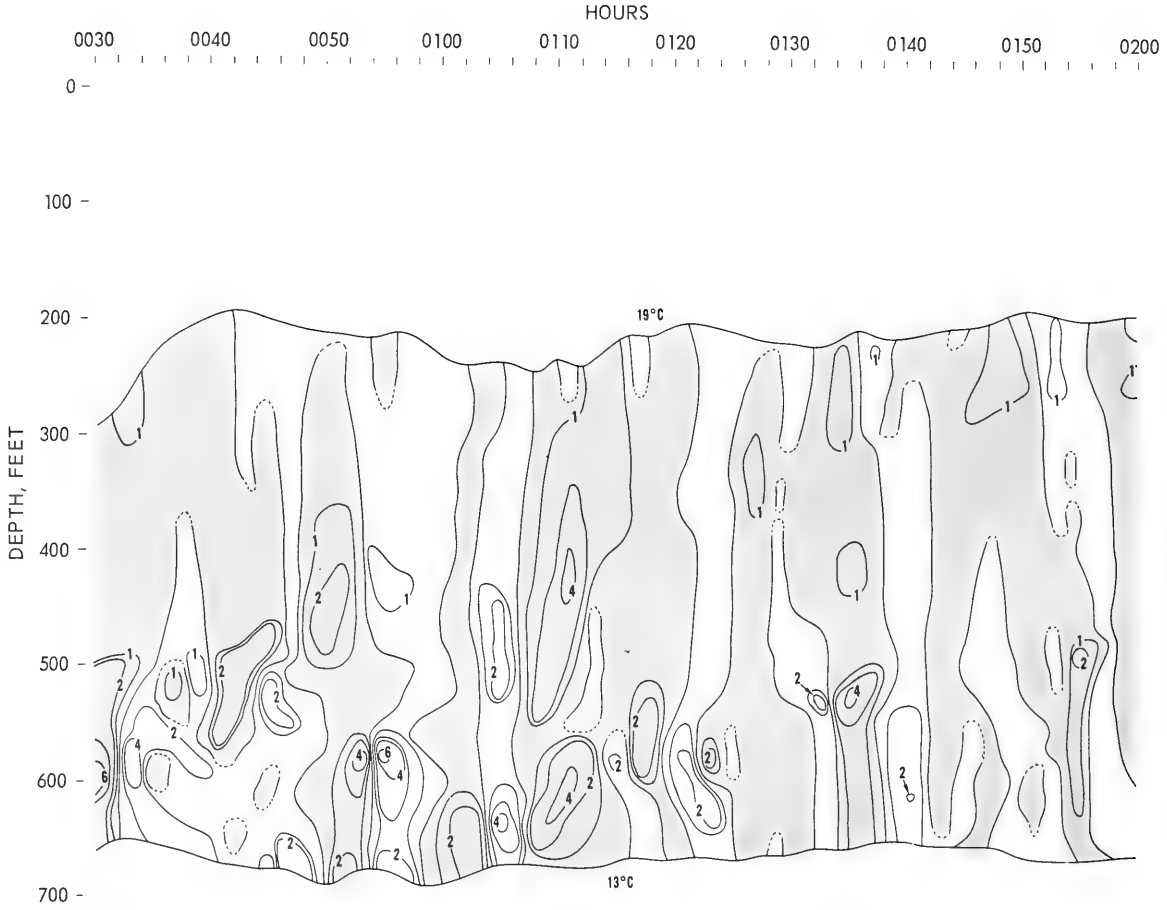

Sample Area 15

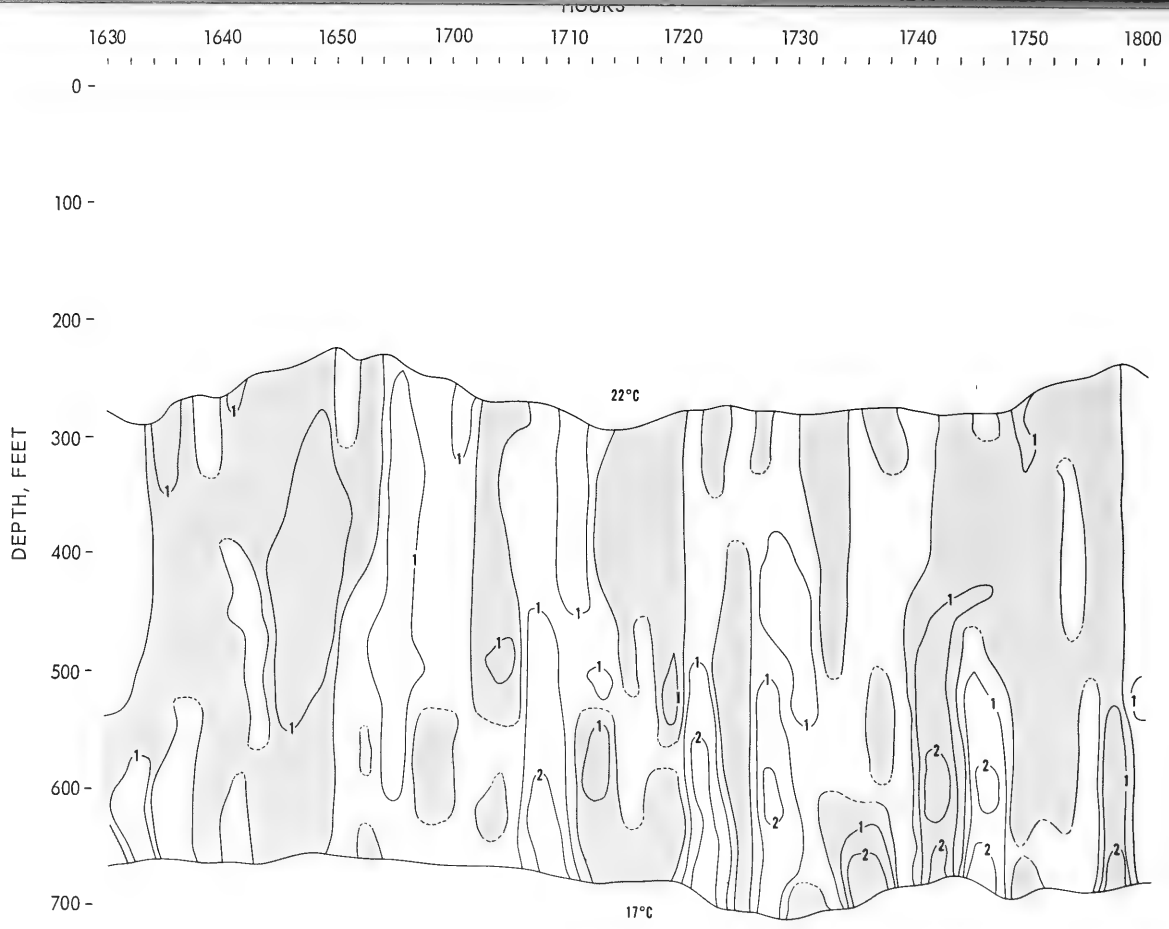

Sample Area 16

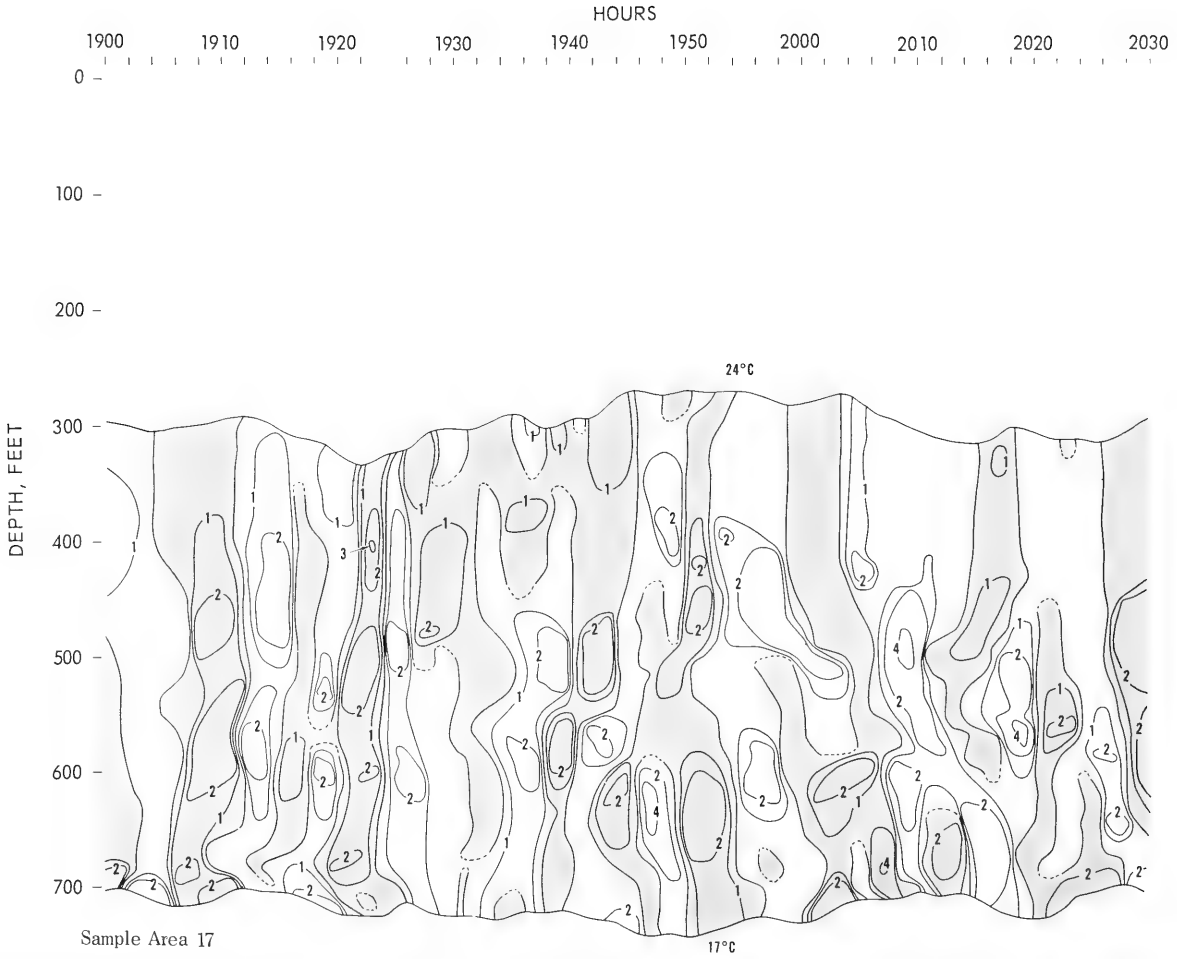

Sample Area 17

UNCLASSIFIED

Security Classification

DOCUMENT CONTROL DATA - R & D

(Security classification of title, body of abstract and indexing annotation must be entered when the overall report is classified)

1. ORIGINATING ACTIVITY *(Corporate author)*
Navy Electronics Laboratory
San Diego, California 92152

2a. REPORT SECURITY CLASSIFICATION
UNCLASSIFIED

2b. GROUP

3. REPORT TITLE

A PREDICTIVE HORIZONTAL-TEMPERATURE-GRADIENT MODEL OF THE UPPER 750 FEET OF THE OCEAN

4. DESCRIPTIVE NOTES *(Type of report and inclusive dates)*
Research Report July 1962 to July 1965

5. AUTHOR(S) *(First name, middle initial, last name)*

E. L. Smith

6. REPORT DATE	7a. TOTAL NO. OF PAGES	7b. NO. OF REFS
17 March 1967	90	19

8a. CONTRACT OR GRANT NO.	9a. ORIGINATOR'S REPORT NUMBER(S)
b. PROJECT NO. SR 004 03 01	1445
c. Task 580 NEL L40461	9b. OTHER REPORT NO(S) *(Any other numbers that may be assigned this report)*
d.	

10. DISTRIBUTION STATEMENT

Distribution of this document is unlimited.

11. SUPPLEMENTARY NOTES	12. SPONSORING MILITARY ACTIVITY
	Naval Ship Systems Command Department of the Navy

13. ABSTRACT

Time-dependent horizontal-temperature gradients were computed from vertical-temperature cross sections taken with the towed thermistor chain in 17 areas of the eastern North Pacific. The horizontal gradients were found to be generally smaller than the vertical gradients by two orders of magnitude. The horizontal-gradient field alternated regularly in sign, implying a dominant frequency of internal waves or convection cells (with a corresponding wavelength of 0.72 nautical mile). The horizontal gradient in the thermocline can be predicted from the measured vertical gradient by means of the equation:

$$\frac{dT}{dx} = 0.0047 \left(\frac{dT}{dz}\right)^{0.71}$$

On the basis of these results, plus a single bathythermograph lowering, a simplified predictive model of the horizontal-temperature gradients was constructed.

DD FORM 1 NOV 65 1473 (PAGE 1)

S/N 0101-807-6801

UNCLASSIFIED

Security Classification

14 KEY WORDS	LINK A		LINK B		LINK C	
	ROLE	WT	ROLE	WT	ROLE	WT
Oceans - Temperature - Prediction						

Navy Electronics Lab., San Diego, Calif.
Report 1445

A PREDICTIVE HORIZONTAL-TEMPERATURE GRADIENT MODEL OF THE UPPER 750 FEET OF THE OCEAN, by E. L. Smith, 90 p., 17 Mar 67.

UNCLASSIFIED

Time-dependent horizontal-temperature gradients were computed from vertical-temperature cross sections taken with the towed thermistor chain in 17 areas of the eastern North Pacific. The horizontal gradients were found to be generally smaller than the vertical gradients by two orders of magnitude. The horizontal-gradient field alternated regularly in sign, implying a dominant frequency of internal waves or convection cells (with a corresponding wavelength of 0.72 nautical mile). The horizontal gradient in the thermocline can be predicted from the measured vertical gradient by means of the equation:

1. Oceans - Temperature - Prediction

I. Smith, E. L.

SR 004 03 01, Task 580
(NEL L4046I)

This card is UNCLASSIFIED

Navy Electronics Lab., San Diego, Calif.
Report 1445

A PREDICTIVE HORIZONTAL-TEMPERATURE GRADIENT MODEL OF THE UPPER 750 FEET OF THE OCEAN, by E. L. Smith, 90 p., 17 Mar 67.

UNCLASSIFIED

Time-dependent horizontal-temperature gradients were computed from vertical-temperature cross sections taken with the towed thermistor chain in 17 areas of the eastern North Pacific. The horizontal gradients were found to be generally smaller than the vertical gradients by two orders of magnitude. The horizontal-gradient field alternated regularly in sign, implying a dominant frequency of internal waves or convection cells (with a corresponding wavelength of 0.72 nautical mile). The horizontal gradient in the thermocline can be predicted from the measured vertical gradient by means of the equation:

1. Oceans - Temperature - Prediction

I. Smith, E. L.

SR 004 03 01, Task 580
(NEL L4046I)

This card is UNCLASSIFIED

Navy Electronics Lab., San Diego, Calif.
Report 1445

A PREDICTIVE HORIZONTAL-TEMPERATURE GRADIENT MODEL OF THE UPPER 750 FEET OF THE OCEAN, by E. L. Smith, 90 p., 17 Mar 67.

UNCLASSIFIED

Time-dependent horizontal-temperature gradients were computed from vertical-temperature cross sections taken with the towed thermistor chain in 17 areas of the eastern North Pacific. The horizontal gradients were found to be generally smaller than the vertical gradients by two orders of magnitude. The horizontal-gradient field alternated regularly in sign, implying a dominant frequency of internal waves or convection cells (with a corresponding wavelength of 0.72 nautical mile). The horizontal gradient in the thermocline can be predicted from the measured vertical gradient by means of the equation:

1. Oceans - Temperature - Prediction

I. Smith, E. L.

SR 004 03 01, Task 580
(NEL L4046I)

This card is UNCLASSIFIED

Navy Electronics Lab., San Diego, Calif.
Report 1445

A PREDICTIVE HORIZONTAL-TEMPERATURE GRADIENT MODEL OF THE UPPER 750 FEET OF THE OCEAN, by E. L. Smith, 90 p., 17 Mar 67.

UNCLASSIFIED

Time-dependent horizontal-temperature gradients were computed from vertical-temperature cross sections taken with the towed thermistor chain in 17 areas of the eastern North Pacific. The horizontal gradients were found to be generally smaller than the vertical gradients by two orders of magnitude. The horizontal-gradient field alternated regularly in sign, implying a dominant frequency of internal waves or convection cells (with a corresponding wavelength of 0.72 nautical mile). The horizontal gradient in the thermocline can be predicted from the measured vertical gradient by means of the equation:

1. Oceans - Temperature - Prediction

I. Smith, E. L.

SR 004 03 01, Task 580
(NEL L4046I)

This card is UNCLASSIFIED

$$\frac{dT}{dx} = 0.0047 \left(\frac{dT}{dz}\right)^{0.71}$$

On the basis of these results, plus a single bathythermograph lowering, a simplified predictive model of the horizontal-temperature gradients was constructed.

$$\frac{dT}{dx} = 0.0047 \left(\frac{dT}{dz}\right)^{0.71}$$

On the basis of these results, plus a single bathythermograph lowering, a simplified predictive model of the horizontal-temperature gradients was constructed.

$$\frac{dT}{dx} = 0.0047 \left(\frac{dT}{dz}\right)^{0.71}$$

On the basis of these results, plus a single bathythermograph lowering, a simplified predictive model of the horizontal-temperature gradients was constructed.

$$\frac{dT}{dx} = 0.0047 \left(\frac{dT}{dz}\right)^{0.71}$$

On the basis of these results, plus a single bathythermograph lowering, a simplified predictive model of the horizontal-temperature gradients was constructed.

INITIAL DISTRIBUTION LIST

CHIEF OF NAVAL MATERIAL
MAT 0331
COMMANDER, NAVAL SHIP SYSTEMS COMMAND
SHIPS 1610
SHIPS 1631
SHIPS 2021 (2)
SHIPS 204113
COMMANDER, NAVAL AIR SYSTEMS COMMAND
AIR 5330
AIR 5401
AIR 604
COMMANDER, NAVAL ORDNANCE SYSTEMS COMMAND
ORD 03C
ORD 0322
ORD 9132
COMMANDER, NAVAL FACILITIES ENGINEERING COMMAND
FAC 42310
COMMANDER, NAVAL ELECTRONIC SYSTEMS COMMAND
TECHNICAL LIBRARY
COMMANDER, NAVAL SHIP ENGINEERING CENTER
CODE 6120
CODE 6179B
CODE 6179C03
CODE 6360
CHIEF OF NAVAL PERSONNEL
PERS 11B
CHIEF OF NAVAL OPERATIONS
OP-03EG
OP-311
OP-312F
OP-322C
OP-07T
OP-702C
OP-71
OP-716
OP-098S
OP-922Y4C1
CHIEF OF NAVAL RESEARCH
CODE 416
CODE 418
CODE 427
CODE 466
CODE 468
COMMANDER IN CHIEF
US PACIFIC FLEET
CODE 93
US ATLANTIC FLEET
COMMANDER OPERATIONAL TEST AND EVALUATION FORCE
KEY WEST TEST AND EVALUATION DETACHMENT
DEPUTY COMMANDER OPERATIONAL TEST AND EVALUATION FORCE, PACIFIC
COMMANDER SUBMARINE FORCE
US PACIFIC FLEET
CODE 21
US ATLANTIC FLEET
COMMANDER ANTISUBMARINE WARFARE FORCE
US PACIFIC FLEET
COMMANDER FIRST FLEET
COMMANDER SECOND FLEET
COMMANDER TRAINING COMMAND
US ATLANTIC FLEET
OFFICE OF THE OCEANOGRAPHER OF THE NAVY
COMMANDER OCEANOGRAPHIC SYSTEM PACIFIC
COMMANDER SUBMARINE DEVELOPMENT GROUP TWO
COMMANDER, DESTROYER DEVELOPMENT GROUP, PACIFIC
COMMANDER FLEET AIR WINGS, ATLANTIC FLEET
NAVAL AIR DEVELOPMENT CENTER
LIBRARY
NAVAL MISSILE CENTER
TECHNICAL LIBRARY
PACIFIC MISSILE RANGE
CODE 3250
NAVAL ORDNANCE TEST STATION
CHINA LAKE
CODE 753
PASADENA ANNEX
LIBRARY
NAVAL WEAPONS LABORATORY
KXL
LIBRARY
PEARL HARBOR NAVAL SHIPYARD
CODE 246P
PORTSMOUTH NAVAL SHIPYARD
CODE 242L
PUGET SOUND NAVAL SHIPYARD
CODE 246
SAN FRANCISCO NAVAL SHIPYARD
HUNTERS POINT DIVISION
NAVAL RADIOLOGICAL DEFENSE LABORATORY
CODE 222A
OCEANOGRAPHIC OFFICE PACIFIC SUPPORT GROUP, SAN DIEGO
NAVAL SHIP RESEARCH & DEVELOPMENT CENTER
CARDEROCK DIVISION
LIBRARY
ANAPOLIS DIVISION
CODE 257

NAVY MINE DEFENSE LABORATORY
CODE 716
NAVAL TRAINING DEVICE CENTER
TECHNICAL LIBRARY
NAVY UNDERWATER SOUND LABORATORY
LIBRARY
CODE 905
ATLANTIC FLEET ASW TACTICAL SCHOOL
LIBRARY
NAVAL CIVIL ENGINEERING LABORATORY
L54
NAVAL RESEARCH LABORATORY
CODE 2027
CODE 4320
CODE 5440
NAVAL ORDNANCE LABORATORY
CORONA
TECHNICAL LIBRARY
SILVER SPRING, MD.
DIVISION 221
DIVISION 730
NAVY UNDERWATER SOUND REFERENCE LABRATORY
LIBRARY
FLEET ASW SCHOOL
TACTICAL LIBRARY
FLEET SONAR SCHOOL
NAVAL UNDERWATER WEAPONS RESEARCH AND ENGINEERING STATION
LIBRARY
OFFICE OF NAVAL RESEARCH BRANCH OFFICE
PASADENA
CHIEF SCIENTIST
BOSTON
CHICAGO
SAN FRANCISCO
LONDON
NAVAL SHIP MISSILE SYSTEMS ENGINEERING STATION
CODE 903
CHIEF OF NAVAL AIR TRAINING
TRAINING RESEARCH DEPARTMENT
NAVY WEATHER RESEARCH FACILITY
NAVAL OCEANOGRAPHIC OFFICE
CODE 1640
SUPERVISOR OF SHIPBUILDING, US NAVY
GROTON, CONN.
CODE 249
NAVAL POSTGRADUATE SCHOOL
DEPT. OF ENVIRONMENTAL SCIENCES
LIBRARY
FLEET NUMERICAL WEATHER FACILITY
NAVAL APPLIED SCIENCE LABORATORY
CODE 9200
CODE 9832
NAVAL ACADEMY
ASSISTANT SECRETARY OF THE NAVY (RESEARCH AND DEVELOPMENT)
NAVAL SECURITY GROUP
G43
AIR DEVELOPMENT SQUADRON ONE
VX-1
SUBMARINE FLOTILLA ONE, US PACIFIC FLEET
DEFENSE DOCUMENTATION CENTER (20)
DEPARTMENT OF DEFENSE RESEARCH AND ENGINEERING
WEAPONS SYSTEMS EVALUATION GROUP
DEFENSE ATOMIC SUPPORT AGENCY
DOCUMENT LIBRARY SECTION
NATIONAL OCEANOGRAPHIC DATA CENTER
CODE 2400
COAST GUARD OCEANOGRAPHIC UNIT
NATIONAL ACADEMY OF SCIENCES/ NATIONAL RESEARCH COUNCIL
COMMITTEE ON UNDERSEA WARFARE
COAST GUARD HEADQUARTERS
OSR-2
ARCTIC RESEARCH LABORATORY
WOODS HOLE OCEANOGRAPHIC INSTITUTION
DOCUMENT LIBRARY LO-206
ENVIRONMENTAL SCIENCE SERVICE ADM.
COAST AND GEODETIC SURVEY
ROCKVILLE, MD.
WASHINGTON SCIENCE CENTER - 23
WASHINGTON, D. C.
US WEATHER BUREAU
DIRECTOR, METEOROLOGICAL RESEARCH
LIBRARY
GEOLOGICAL SURVEY LIBRARY
DENVER SECTION
ESSA/INSTITUTE FOR TELECOMMUNICATION SCIENCES AND AERONOMY
BOULDER, COLO.
FEDERAL COMMUNICATIONS COMMISSION
RESEARCH DIVISION
NATIONAL SEVERE STORMS LABORATORY
CENTRAL INTELLIGENCY AGENCY
OCR/DD-STANDARD DISTRIBUTION
NATIONAL BUREAU OF STANDARDS
BOULDER, COLO.

BUREAU OF COMMERCIAL FISHERIES
LA JOLLA, CALIF.
TUNA RESOURCES LABORATORY LA JOLLA
WASHINGTON, D. C.
BRANCH OF MARINE FISHERIES
WOODS HOLE, MASS.
BIOLOGICAL LABORATORY LIBRARY
HONOLULU, HAWAII
FISH AND WILDLIFE SERVICE LIBRARY
STANFORD, CALIF.
BIOLOGICAL LABORATORY
ABERDEEN PROVING GROUND
TECHNICAL LIBRARY
ARMY MISSILE CENTER
REDSTONE SCIENTIFIC INFORMATION CENTER
DOCUMENT SECTION
ARMY ELECTRONICS RESEARCH AND DEVELOPMENT LABORATORY
ARMY ELECTRONICS COMMAND
MANAGEMENT & ADMINISTRATIVE SERVICES DEPT
AMSEL-RD-MAT
COASTAL ENGINEERING RESEARCH CENTER
ARMY CORPS OF ENGINEERS
AIR FORCE HEADQUARTERS
DIRECTOR OF SCIENCE AND TECHNOLOGY
AFRSTA
AIR UNIVERSITY LIBRARY
AUL3T-5028
AIR FORCE EASTERN TEST RANGE
AFMTC TECHNICAL LIBRARY - MU-135
AIR PROVING GROUND CENTER
PGBPS-12
HEADQUARTERS AIR WEATHER SERVICE
AWSSS/SIPD
WRIGHT-PATTERSON AIR FORCE BASE (1)
SYSTEMS ENGINEERING GROUP (RTD)
SEPIR
UNIVERSITY OF MICHIGAN
OFFICE OF RESEARCH ADMINISTRATION
NORTH CAMPUS
COOLEY ELECTRONICS LABORATORY
UNIVERSITY OF CALIFORNIA-SAN DIEGO
MARINE PHYSICAL LABORATORY
SCRIPPS INSTITUTION OF OCEANOGRAPHY
LIBRARY
UNIVERSITY OF MIAMI
THE MARINE LABORATORY LIBRARY
MICHIGAN STATE UNIVERSITY
LIBRARY-DOCUMENTS DEPARTMENT
COLUMBIA UNIVERSITY
LAMONT GEOLOGICAL OBSERVATORY
DARTMOUTH COLLEGE
RADIOPHYSICS LABORATORY
CALIFORNIA INSTITUTE OF TECHNOLOGY
JET PROPULSION LABORATORY
HARVARD COLLEGE OBSERVATORY
HARVARD UNIVERSITY
GORDON MCKAY LIBRARY
LYMAN LABORATORY
OREGON STATE UNIVERSITY
DEPARTMENT OF OCEANOGRAPHY
UNIVERSITY OF WASHINGTON
DEPARTMENT OF OCEANOGRAPHY
FISHERIES-OCEANOGRAPHY LIBRARY
APPLIED PHYSICS LABORATORY
NEW YORK UNIVERSITY
DEPARTMENT OF METEOROLOGY AND OCEANOGRAPHY
UNIVERSITY OF ALASKA
GEOPHYSICAL INSTITUTE
UNIVERSITY OF RHODE ISLAND
NARRAGANSETT MARINE LABORATORY
LIBRARY
YALE UNIVERSITY
BINGHAM OCEANOGRAPHIC LABORATORY
FLORIDA STATE UNIVERSITY
OCEANOGRAPHIC INSTITUTE
UNIVERSITY OF HAWAII
HAWAII INSTITUTE OF GEOPHYSICS
ELECTRICAL ENGINEERING DEPARTMENT
A&M COLLEGE OF TEXAS
DEPARTMENT OF OCEANOGRAPHY
THE UNIVERSITY OF TEXAS
DEFENSE RESEARCH LABORATORY
ELECTRICAL ENGINEERING RESEARCH LABORATORY
PENNSYLVANIA STATE UNIVERSITY
ORDNANCE RESEARCH LABORATORY
STANFORD RESEARCH INSTITUTE
NAVAL WARFARE RESEARCH CENTER
MASSACHUSETTS INSTITUTE OF TECHNOLOGY
ENGINEERING LIBRARY
LINCOLN LABORATORY
RADIO PHYSICS DIVISION
FLORIDA ATLANTIC UNIVERSITY
DEPARTMENT OF OCEAN ENGINEERING
THE JOHNS HOPKINS UNIVERSITY
APPLIED PHYSICS LABORATORY
DOCUMENT LIBRARY
INSTITUTE FOR DEFENSE ANALYSES
DOCUMENT LIBRARY